Applications of Many Body Dynamics of Solid State Systems to Quantum Metrology and Computation

Dissertation Advisor: Claudio Chamon Author: Garry Goldstein

Applications of Many Body Dynamics of Solid State Systems to Quantum Metrology and Computation

Abstract

This thesis describes aspects of dynamics of solid state systems which are relevant to quantum metrology and computation. It may be divided into three research directions (parts). For the first part, a new method to enhance precision measurements that makes use of a sensor's environment to amplify its response to weak external perturbations is described. In this method a "central" spin is used to sense the dynamics of surrounding spins, which are affected by the external perturbations that are being measured. The enhancement in precision is determined by the number of spins that are coupled strongly to the central spin and is resilient to various forms of decoherence. For polarized environments, nearly Heisenberg-limited precision measurements can be achieved.

The second part of the thesis focuses on the decoherence of Majorana fermions. Specializing to the experimentally relevant case where each mode interacts with its own bath we present a method to study the effect of external perturbations on these modes. We analyze a generic gapped fermionic environment (bath) interacting via tunneling with individual Majorana modes - components of a qubit. We present examples with both static and dynamic perturbations (noise), and derive a rate of information loss for Majorana memories, that depends on the spectral density of both the noise and the fermionic bath.

For the third part of the thesis we discuss vortices in topological superconductors which we model as closed finite systems, each with an odd number of real fermionic modes. We show that even in the presence of many-body interactions, there are always

at least two fermionic operators that commute with the Hamiltonian. There is a zero mode corresponding to the total Majorana operator [1] as well as additional linearly independent zero modes, one of which is continuously connected to the Majorana mode in the non-interacting limit. We also show that in the situation where there are two or more well separated vortices their zero modes have non-Abelian Ising statistics under braiding.

Contents

References to previously published works

Most of the chapters and appendices of this thesis have appeared in print elsewhere. Below is a list by appendix and chapter number of the relevant works.

Chapter 2: "Environment assisted precision measurement", G. Goldstein, P. Cappellaro, J. R. Maze, J. S. Hodges, L. Jiang, A. S. Sorensen, and M. D. Lukin, Phys. Rev. Lett. **106**, 140502, (2011).

Chapter 3: "Decay rates for topological memories encoded with Majorana fermions", G. Goldstein and C. Chamon, Phys. Rev. B **84**, 205109, (2011).

Chapter 4: "Exact zero modes in closed systems of interacting fermions", G. Goldstein and C. Chamon, arXiv 1108.1734

Appendix B: "Decay rates for topological memories encoded with Majorana fermions", G. Goldstein and C. Chamon, Phys. Rev. B 84, 205109, (2011).

Acknowledgments

With my PhD finally at completion I have the luxury and pleasure to thank the many people who have helped me along the way. While it would be virtually impossible to thank everyone involved, from my fellow graduate students who have spent many a sleepless nights working on problem sets with me; the professors who taught me many wonderful courses imparting the knowledge I needed for my research and the support staff who made my stay at Harvard possible; several people have had a particularly positive impact on me during my stay at Harvard and I shall endeavor to thank them below.

First and foremost I would like to thank Claudio, my thesis advisor, without whom my PhD would be impossible. Claudio is an exceptional academic and research advisor. He consented to take me in as a graduate student at the end of my fourth year - after I suddenly switched research directions - and allowed me to graduate in two short years. During this time he spent innumerate hours teaching me basics of "many body quantum dynamics", mainly Keldysh formalism, and working with me on the research that makes up the majority of my thesis.

I'm particularly indebted to him for the amount of time he spent on our research on the decay rates of Majorana fermions, which was his pet project for several months. Together we performed the numerous calculations needed for this project and painstakingly polished the paper into presentable form. I'm sure that the project would not have been successful without his guidance, advice and labor.

I also greatly enjoyed the various brainstorming sessions we have with Claudio. His

great physical insight and perseverance with intricate mathematical and physical problems were inspirational. His patience with my, at times bungling, reasoning and research is greatly appreciated. I also benefited from the fact that he introduced me to various research collaborators: Dima Feldman, Patrick Lee and Andrew Potter. Overall Claudio provided me an extremely positive and kind research experience.

I would also like to thank many people for insightful and inspirational research discussions. The meetings with Patrick Lee and Andrew Potter were particularly useful in interpreting the results on decay rates of Majorana modes. I'm also grateful for discussions with Subir Sachdev, Bert Halperin, Christopher Mudry, Luiz Santos, Ivar Martin, Mikhail Lukin, Dima Feldman, Liang Jiang, Paolla Cappellaro, Jonathan Hodges, Jaro Maze, Carlos Meriles and Anders Sorensen.

As always I would like to thank my family, in particular my mother, for love and support during these trying times.

List of Figures

1 Introduction

1.1 Overview

Recently advances in nanofabircation have made it possible to manipulate matter at the nanoscale. Current experimental resolution allows the experimentalist to change the quantum state of single atoms and electrons (spins). Multiple new technologies in trapped ions [2, 3, 4, 5, 6, 7, 8, 9], Microcavity QED [10, 11, 12, 13, 14, 15], electrons in Quantum dots [16, 17, 18, 19, 20, 21, 22, 23], Josephson junctions [24, 25, 26, 27] and cold atoms [28, 29, 30] have recently been experimentally demonstrated. This new ability to manipulate on the nanoscale individual qubits has a wide range of applicability. Novel devices for quantum enhanced metrology have been both designed and implemented [31, 32, 33, 34]. A range of quantum simulators have been proposed and recently implemented [35, 36]. Proposals exist to use various qubits (ions, spins, cooper pairs) as components of quantum computers. This, if experimentally realized, would lead to improved cryptography, quantum (putatively absolutely secure) communication, improved sorting algorithms, better quantum clocks and sensors and through quantum simulation a better understanding of various states of matter. Many of the leading platforms for these devices come from solid state implementations. Understanding the dynamics of certain types solid state systems, when combined with, currently technologically feasible, manipulation of single two level "qubits" can lead to great advances in quantum metrology and computation. The study of the dynamics of two such systems: Majorana fermions and central spins is the subject of this thesis.

1.2 Organization of this thesis

Below we give an outline of the rest of the thesis. In Section 1.3 we discuss in general terms some of the types of possible practical applications of the theoretical work presented in this thesis. In particular in Section 1.3.1 we give a discussion of entanglement enhanced "quantum" metrology. We also connect the discussion to the work presented in Chapter 2. In Section 1.3.2 we give a brief overview of quantum computation. We then specialize in Section 1.3.2 to topological quantum computation, which is directly related to the work presented in Chapters 3 and 4. The rest of the thesis describes work done by the author which can be applied to the fields discussed in Section 1.3.

In Chapter 2 we study a pulse sequence which uses the environment of a quantum sensor to amplify its response to external perturbations. This is an application of solid state dynamics to quantum metrology. We show that for a polarized environment nearly Heisenberg limited metrology is possible with this pulse sequence. We present some examples of applications with NV (Nitrogen Vacancy) centers and cold ions. In Section 2.5 we also present some numerical simulations to confirm our results.

The material presented in Chapter 3 is relevant to topological quantum computation. We study the decay rates of qubits composed of Majorana fermions. After summarizing our main ideas in Section 3.3; in Section 3.4 we present generic factorization formulas for two time correlation function for these qubits. In Section 3.5 we derive some Keldysh based formalism to compute these correlators. We study examples of classical and quantum noise that effect qubits composed of Majorana fermions. We find that for zero temperature equilibrium quantum environments there is no long term decay of such a qubit, while for non-equilibrium or classical noise there is an exponential decay of the fidelity of the information stored in a Qubit composed of Majorana fermions with the decay rate being related to the spectral function of the environment evaluated at or above the superconducting gap. We present explicit formulas for the decay rates in Section 3.6.

In Chapter 4 we study finite systems composed of odd numbers of real fermionic modes.

This is a model relevant to vortices in topological superconductors. We find that even in the presence of many body interactions there are always multiple zero modes inside the vortex core, see Section 4.3. We find that for weak interactions there is a zero mode that is adiabatically connected to the mean field zero mode solution, as discussed in Section 4.4. In Section 4.7 we show that well separated zero modes have Ising statistics under braiding.

The appendices present some technical details and derivations. In Appendix A we present technical details relevant to the numerical simulations needed for Chapter 2. In particular we describe the linked cluster expansion, see Section A.4, and derive some formulas for the signal from multipulse sequence which generalize those given in the main text (A.3). In Appendix B we present some technical details relevant for our work on decay rates of Majorana fermions presented in Chapter 3. In particular in Section B.1 we give alternate derivations of some formulas; we generalize some of our results for decay rates to include quantum fluctuating noise (B.2) and give derivations of various formulas used in the main text (B.3).

1.3 Motivation

The work presented in this thesis has applications to quantum metrology and computation. To motivate it, below we present some of the challenges and prospects of these fields.

1.3.1 Quantum metrology

Any measurement can be divided into three stages: preparation of the probe system; evolution of the probe system under interaction with an external perturbation and readout of the probe to extract the effects of the interaction. This process is generically fraught with noise. The most fundamental being shot noise which comes from quantum mechanical uncertainties in the measurement outcome, although noises like imperfect

readout, signal fluctuation and systematic errors are of great importance too. The uncertainty due to the noise may be reduced by repetitive readout. For N uncorrelated measurements the improvement in sensitivity, as described by the central limit theorem scales $\propto \sqrt{N}$ as compared to a single readout. By exploiting entanglement as a resource for quantum metrology it is possible to improve the precision of measurement with N resources by a factor of N as compared to the precision of measurement with a single resource. Such applications of quantum entanglement are amongst the most important technological uses of quantum mechanical properties of matter currently know [37]. For example quantum control of isolated atomic systems in particular single ions forms the physical basis of the world's best clocks. It has been recently demonstrated that quantum entanglement can enhance precision measurements with trapped cold ions [31, 38]. At the same time, many solid-state quantum systems have been recently developed with the purpose of producing novel realizations of solid-state qubits. It is likely that such systems can be used for realizations of new quantum sensors and precision measurement devices. For example it was shown recently that optically and magnetically controlled spin impurities in diamond (NV centers) can be used to create novel magnetic sensors with unique combination of sensitivity and spatial resolution [32, 33, 39]. In Chapter 2 we describe a novel application of quantum entanglement to enhance quantum metrology. We describe a technique that makes use of the entanglement between a sensor spin and its local environment as a resource to amplify its response to external perturbations. The study of the dynamics of such a solid state system forms the core of the design of this sensor and is described in great detail in this thesis.

1.3.2 Quantum computation

Quantum computation is one of the great technological and intellectual challenges of the twenty first century. Unlike regular computers which can only process one classical input at a time quantum computers can accept coherent superpositions of many different

initial states (inputs) and produce coherent superpositions of these states as their output. The act of computing can be described as a unitary evolution of the input into a final output during which, simultaneously, each term of the coherent superposition of inputs can be effected. This generates massive parallelism as the outcome of the computation is potentially dependent on all of the states of the system. This parallelism can lead to dramatic speed up of various computing algorithms. Two of the most prominent examples of such speed up are the Shor factorization algorithm [40] and the Grover search algorithm [41]. The Shor search algorithm offers the possibility to factorize a number N in $\sim \log^3(N)$ steps (which is opposed to the classical limit of $N^{1/3}$) while the Grover search algorithm allows sorting through N options in $\sim N^{1/2}$ time. There are many technical difficulties (requirements) for a quantum computer [42]. They include a physical platform with multiple qubits, the ability to initialize the state of this platform, the ability to perform arbitrary evolution on the qubits (quantum gates) and efficient readout. The most difficult criteria though is low decoherence. For a quantum computer to be practical it is necessary that the error rate for any single computation be $\sim 10^{-4}$ or less. A potential method to overcome this difficulty is discussed below.

Topological quantum computation

One of the most promising routes towards overcoming the issue of decoherence in quantum computation is topological quantum computation. The concept is based on two dimensional systems, whose fundamental excitations (quasiparticles) are neither bosons nor fermions but are non-Abelian anyons. The ground states of such systems with a number of fixed quasiparticles, anyons, posses a high level of degeneracy and undergo non-Abelian (non-trivial, non-commuting) transformations when two or more of these quasiparticles exchange position (a process commonly referred to as braiding). Quantum information is stored in the degenerate ground states of these two dimensional materials. Because of the exact degeneracy of these ground states (in the thermodynamic

limit) putatively the information stored in the state of these two dimensional systems is protected from decoherence. Furthermore quantum "gates" may be enacted on these systems through braiding. Virtually all know experimentally viable realizations of this idea are based on Majorana fermions. These are half of a regular complex fermion and have non-Abelian "Ising" statistics under braiding (as such they are anyons). One of the goals of this thesis is a study of the dynamics of these quasiparticles in particular their protection from decoherence and many-body interactions.

2 Environment enhanced imaging

2.1 Introduction

In this chapter we describe a new method to enhance the sensitivity of precision measurements that makes use of the quantum sensor's environment to amplify its response to weak external perturbations. In our method an individual spin qubit ("central" spin) is used to sense the dynamics of surrounding spins, which are in turn affected by the external perturbations that are being measured. The resulting enhancement is determined by the number of spins that are coupled strongly to the central spin and does not depend on the exact values of the coupling strengths and is highly resilient to various forms of decoherence. For a polarized environment and sufficiently large coupling constants, the sensitivity of the proposed pulse sequence scales linearly with the number of environment spins or in other words nearly Heisenberg-limited precision measurements can be achieved using a novel class of entangled spin states. We discuss specific applications to improve clock sensitivity using trapped ions and magnetic field sensing based on spins in diamond crystals.

2.2 Overview

Precision measurements are among the most important applications of resonance methods in physics. For example quantum control of isolated atomic systems forms the physical basis of the world's best clocks. Ideas from quantum information science, in which

these systems have emerged as promising qubit candidates, have been recently used to demonstrate that quantum entanglement can enhance such precision measurements [31, 38]. At the same time, a wide range of solid-state quantum systems have been recently developed aimed at novel realizations of solid-state qubits. Potentially such systems can be used for realization of novel quantum sensors and measurement devices. For example it was shown recently that optically detected spin impurities in diamond can be used to create a novel nonsecular magnetic sensor with a unique combination of sensitivity and spatial resolution [32, 33, 39]. That work utilized coherent control of the sensor spin qubit to decouple it from the environment, which was composed of randomly positioned impurity spins. In this chapter we describe a novel technique that makes use of the sensor spin's local environment as a resource to amplify its response to weak perturbations. We shall use both solid state sensors and ion clocks as examples.

The purpose of quantum metrology is to detect a small external field, which is coupled to the sensor qubit by an effective Hamiltonian $H_{eff} = b(t)S_z$ (where S_z is the spin operator of the Quantum sensor). Here $b(t)$ may be an external magnetic field to be measured (in the case of nanomagnetometry) or the detuning of a laser from a clock transition (in the case of ion clocks). The working principle of almost any quantum metrology scheme is to read out the phase difference acquired between two states of a quantum sensor via a Ramsey experiment [43, 44]. In a typical Ramsey experiment the sensor spin is initialized, say by optical pumping, along the z-axis (say in the state $|0\rangle$); it is then flipped onto the x-axis by a $-\frac{\pi}{2}_y$ pulse (both of these processes are typically fast on the timescale of a single experiment [43, 44]). With this the spin is prepared in the state $\frac{1}{\sqrt{2}}(|0\rangle + |1\rangle)$ see Figure 2.1(a). The spin then precesses in the x-y plane under the action of H_{eff} and picks up a phase $\Delta\varphi$ ending up in the state $\frac{1}{\sqrt{2}}\left(e^{-i\Delta\varphi}|0\rangle + e^{i\Delta\varphi}|1\rangle\right)$. Then a final $-\frac{\pi}{2}_x$ pulse converts this phase into a population difference between the states $|0\rangle$ and $|1\rangle$ so that the final state of the spin is $\sim \sin\left(\frac{\pi}{4} + \Delta\varphi\right)|1\rangle + \sin\left(\frac{\pi}{4} - \Delta\varphi\right)|0\rangle$. The state of the spin, whether its in $|0\rangle$ or $|1\rangle$, is then readout. The signal from the pulse sequence

is then given by the change in probability of obtaining the state $|1\rangle$ due to the magnetic field. It is given by $\sin^2\left(\frac{\pi}{4}+\Delta\varphi\right)-\frac{1}{2}\cong\Delta\varphi$. The process is then repeated multiple times to improve statistics. The figure of merit for a quantum sensor is the smallest δb_{min} which may be read out during a total time T. If Ramsey experiment sensing time is limited to τ (say by environmental decoherence) the signal is $\Delta\varphi\sim b\tau$ so assuming perfect detection $\delta b_{min}\sim\frac{1}{\sqrt{T\tau}}$. As such it is advantageous to enhance the sensing time τ or equivalently decrease environmental decoherence to improve sensitivity. In particular, in order to measure an AC field, in many cases it is advantageous to replace a Ramsey sequence with a spin echo sequence, see Figure 2.1(b). The sequence is identical to a Ramsey sequence except the static component of the environment noise is echoed out by inserting and extra π_y pulse in the middle of the sequence. This can greatly prolong the coherence time of the sensor spin [46]. The signal, or the population difference between the states $|0\rangle$ and $|1\rangle$ is the difference of the phase picked up by the sensor spin during the two halves of the sensing sequence so generically only AC fields are detectable by this method.

In many cases the external field also acts on the sensor's environment. This effect can be used to enhance the sensitivity of the quantum sensor while still echoing out this external environment with a spin echo type measurement sequence and detecting both AC and DC external field (described below). For generality we will illustrate the key ideas using the so-called central spin model. In this model a "central spin" (which can be prepared in a well defined initial state, coherently manipulated and read out) is coupled to a bath of "dark" spins which can be polarized and collectively controlled but cannot be directly detected (Figure 2.2(a&c)). Specifically, we focus on a system that is described by the following model:

$$\begin{aligned} &H=H_{meas}+H_{int}\\ &H_{int}=|1\rangle\langle 1|\sum\lambda_i I_z^i,\ H_{meas}=b\left(t\right)\left(\kappa S_z+\xi\sum I_z^i\right)\end{aligned} \tag{2.1}$$

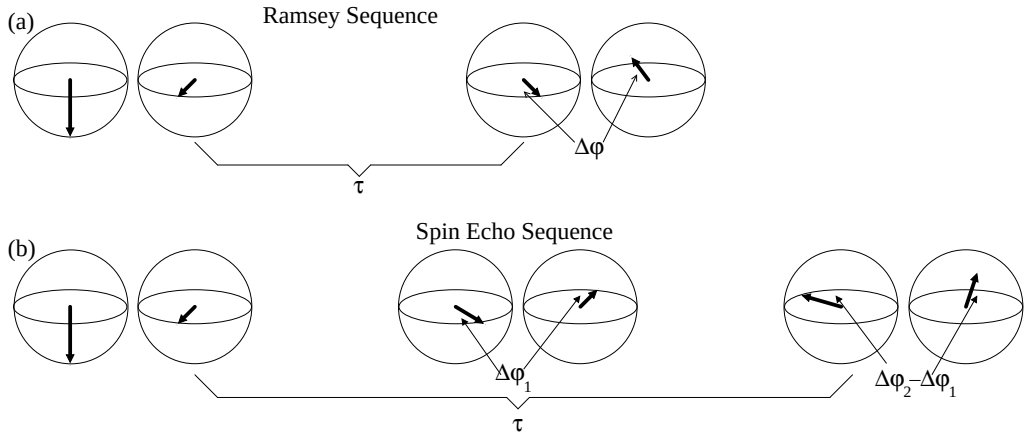

Figure 2.1: Ramsey and Spin Echo Sequences
(a) A Ramsey pulse sequence. The central spin is polarized in the state $|1\rangle$. A $-\frac{\pi}{2}_y$ pulse flips the spin onto the x-axis (with the state of the spin being $\frac{1}{\sqrt{2}}(|0\rangle + |1\rangle)$). Due to the action of the external field the spin rotates by an angle $\Delta\varphi$. A $-\frac{\pi}{2}_x$ converts this angle into a population difference between the states $|0\rangle$ and $|1\rangle$ (with the state of the spin $\sim \sin\left(\frac{\pi}{4} + \Delta\varphi\right)|1\rangle + \sin\left(\frac{\pi}{4} - \Delta\varphi\right)|0\rangle$). The state of the central spin $|0\rangle$ or $|1\rangle$ is now read out. (b) A spin echo sequence. The central spin is again prepared in the state $\frac{1}{\sqrt{2}}(|0\rangle + |1\rangle)$. Due to the action of the external field the spin rotates by $\Delta\varphi_1$. A π_y pulse echoes out any static noise. The spin then processes along the x-y plane by an angle $\Delta\varphi_2$. A $\frac{\pi}{2}_x$ converts the total angle into a population difference between the states $|0\rangle$ and $|1\rangle$. The state of the sensor spin is now $\sim \sin\left(\frac{\pi}{4} + \Delta\varphi_2 - \Delta\varphi_{21}\right)|1\rangle + \sin\left(\frac{\pi}{4} - \Delta\varphi_2 + \Delta\varphi_1\right)|0\rangle$. The state of the central spin $|0\rangle$ or $|1\rangle$ is now read out.

where λ_i are the couplings between the sensor and environment spins, while κ and ξ are couplings to the external field of the central spin and the dark spins respectively. Here $|0\rangle$, $|1\rangle$, S_z refer to the central spin while $|\uparrow\rangle$, $|\downarrow\rangle$, I_z^i refer to dark spins. We have set $\hbar = 1$. We assume that all perturbations to this model, such as couplings between the dark spins, are small compared to the couplings between the sensor and environment spins λ_i. This condition can be accommodated by say running a homonuclear decoupling sequence such as WAHUHA [46] on the dark spins in parallel with our pulse sequence, see also Section 2.5. We shall consider two cases: one where H_{int} can be turned on and off at will and is much larger in magnitude then any other time scales in the system (for example in laser mediated ion interactions), and the second when H_{int} is intrinsic to the material and of the same order of magnitude as the relevant sensing time (for example dipole dipole interactions between solid state spins). In all cases we will assume coherent control over the spins say by NMR pulses. In particular this means that we have the ability to interconvert $I_z \leftrightarrow I_x \leftrightarrow I_y$ in the Hamiltonian Equation (2.1) above at will.

2.3 Method

2.3.1 Ideal case (controlled interactions and full polarization)

To illustrate this method we consider the idealized case when the coupling between the central spin and the dark spins are in our control, that is can be turned on and off at will, and the dark spins are initialized in a pure state: $|\uparrow\uparrow ... \uparrow\rangle$. Consider the circuit shown in Figure 2.2(b). The pulse sequence shown there is a modification of a spin-echo sequence. First, the central spin is prepared in an equal superposition of the two internal states $|0\rangle + |1\rangle$ (dropping normalization). There is a $\frac{\pi}{2}_y$ pulse on the dark spins; then H_{int} is turned on and off briefly and there is a final $-\frac{\pi}{2}_y$ pulse on the dark spins. Since $e^{i\frac{\pi}{4}I_y}e^{-i\lambda|1\rangle\langle 1|I_z}e^{-i\frac{\pi}{4}I_y} = e^{-i\lambda|1\rangle\langle 1|I_x}$ these three pulses have the same effect as a controlled rotation by angle λ in the x direction. The system evolves under the action of the external

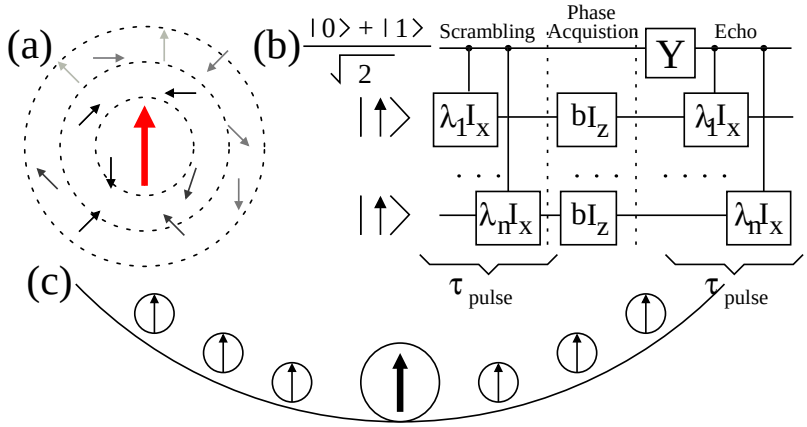

Figure 2.2: Central Spin
(a) A central spin is coupled to a spin bath. (b) A simplified circuit describing the pulse sequence. The gates λI_x represent controlled rotations $e^{-i\lambda I_x}$ of the dark spins. These are compound pulses, as explained in the main text, obtained via the interaction between the central and dark spins $e^{-iH_{int}}$ and pulses on the dark spins. The gates bI_z are rotations e^{-ibI_z} due to the external field $e^{-iH_{meas}}$. The $\bullet$ symbols represent controlled $|1\rangle$ operations. The central spin undergoes a spin-echo before measurement. The symbol Y stands for a π_y pulse on the central spin. (c) Ion implementations: there is a central ion (big arrow) and multiple sensor ions (small arrows) all confined in a harmonic potential.

field for a time τ. The central spin is then flipped with a π_y pulse (denoted by Y in the figure). There is a $\frac{\pi}{2}_y$ pulse on the dark spins. Then H_{int} is turned on and off for the same amount of time as before. There is a $-\frac{\pi}{2}_y$ pulse on the dark spins. The last three pulses are again equivalent to controlled $e^{i\lambda I_x}$ rotation. After that a $\frac{\pi}{2}_x$ pulse is applied on the central spin and the state of the central spin is read out. To understand the effect of this pulse sequence it is best to consider the state of the system at each step of the pulse sequence. The first three pulses, the ones which induce controlled x rotations of the dark spins, produce the state

$$|0\rangle |\uparrow ... \uparrow\rangle + |1\rangle |\varphi_1 ... \varphi_N\rangle , \tag{2.2}$$

where $|\varphi_i\rangle \equiv \cos(\varphi_i) |\uparrow\rangle - i \cdot \sin(\varphi_i) |\downarrow\rangle$ with $\varphi_i = \lambda_i \tau_{pulse}$. This state is then used to sense the magnetic field. The action of the magnetic field over a period τ on the central

spin is just a phase factor $\exp(i\theta_c)$ on the $|1\rangle$ component, where $\theta_c = \kappa \int_0^\tau dt b(t)$. On the states $|\varphi_i\rangle$ the action of the magnetic field is both phase acquisition and rotation. To lowest order in the magnetic field, before the second controlled rotation by $e^{-i\lambda I_x}$ the states $|\varphi_i\rangle$ thus evolve into

$$(1 - i\theta_d \sin^2 \varphi_i)\,|\varphi_i\rangle + \theta_d \sin 2\varphi_i |\varphi_i^\perp\rangle, \tag{2.3}$$

where the component $|\varphi_i^\perp\rangle$ is perpendicular to $|\varphi_i\rangle$, and $\theta_d = \xi \int_0^T dt b(t)$. After the interaction with magnetic field the central spin is flipped and a second controlled rotation is applied. Because of this second controlled rotation, if we ignore the component $\left|\varphi_i^\perp\right\rangle$, the states of the dark spins are then $|\varphi_i\rangle$ regardless of the initial state of the central spin, and the effect of the interaction is to introduce a phase $\Phi \approx \theta_c + \theta_d \sum_i sin^2 \varphi_i$. Technically the component $\left|\varphi_i^\perp\right\rangle$ will produce decoherence of the central spin. However because all matrix elements between $\left|\varphi_i^\perp\right\rangle$ and $|\varphi_i\rangle$ vanish, this will not give any contribution (to the signal $\sim \langle S_y \rangle$) to linear order in the magnetic field. After the spin is rotated around the x-axis ($S_y \leftrightarrow S_z$) the probability for the control spin to be, e.g., in $|1\rangle$ is thus given by $P_1 \approx (1 + \Phi)/2 + O(b^2)$. The signal is proportional to Φ while the quantum projection noise still remains the same as we read out one spin only. The minimum field which can be read out for a total measuring time T is:

$$b_{min} \doteq \sqrt{\frac{\tau}{T}} \frac{1}{\Phi} \sim \frac{1}{N\xi\sqrt{T\tau}} \tag{2.4}$$

Here N is the total number of dark spins. The scaling (linear in the number of dark spins) may be verified by noting that for any distribution of $\lambda_i' s$ we may choose a τ_{pulse} such that $\left\langle sin^2\left(\lambda_i \tau_{pulse}\right)\right\rangle \geq \frac{1}{2}$ [45] leading to order one contribution from every spin. Thus for sufficiently low field, for metrology purposes, only the first order terms need be taken into account. We see that we are able to perform Heisenberg limited (with sensitivity scaling $\sim N^{-1}$) spectroscopy despite the fact that at the end of the spectroscopy sequence the

state of the dark spins is weakly entangled with the state of the central spin. Equivalently this method is a possibility to attain nearly Heisenberg limited sensitivity for metrology with a new array of correlated states (not just squeezed or GHZ (Greenberg-Horne-Zeilinger) states).

2.3.2 Intrinsic couplings & partial polarization

In the previous paragraph we were able to obtain nearly Heisenberg improvement in measurement precision by utilizing short bursts of controlled rotations (of potentially unknown magnitude). Here we would like to extend this method to the case when the interactions between the central spin and and the dark spins are "intrinsic" to the system and the time scale of this interaction is comparable to the time scale of the sensing experiment. To that end we introduce a control sequence that yields an effect similar to the circuit in Figure 2.2(b), e.g. it maps some of the phase acquired by the environment spins to the sensor spin state (see Figure 2.3). The action of the pulse sequence can be best understood using the well known equivalence between Ramsey spectroscopy and Mach-Zehnder interferometry [43, 44], where the interferometer arms describe the central spin state (see Figure 2.3(a)). It is sufficient to consider the evolution of each arm separately, replacing S_z by its eigenvalues $\{0, 1\}$ and describing the evolution in the interaction frame defined by the control pulses [46]. The Hamiltonian (Equation (2.1)) becomes time-dependent, with dark spins alternating between I_z^i and I_x^i as shown in Figure 2.3. Then, for different halves of the spin echo sequence the coupling Hamiltonian in each arm is zero ($\langle S_z \rangle = 0$) while for other halves it has the same form. In the absence of a magnetic field the evolution is thus the same along each arm, except the Hamiltonian is non-zero at different times. Adding an external field creates a phase shift between the two arms. For small field intensities we consider it as a small perturbation of the main Hamiltonian $H_{main}^{(1,2)}(t) = m_s(t) \sum \lambda_i I_\alpha^i$, where $m_s(t) = 0/1$ is the eigenvalue of $S_z(t)$, $\alpha = z/x$ depending on which interval of the spin echo we are considering, and (1,2)

refer to the upper or lower arm of the Mach-Zehnder interferometer respectively (Figure 2.3 (a)). In the interaction picture given by H_{main}, $I^i_\alpha(t)$ becomes time dependent and the system is described by the Hamiltonian $H^{1,2}_{int}(t) = \mu_B b\,(t)\left[g_C m_s(t) + g_D \sum I^i_\alpha(t)\right]$. We can now evaluate the phase difference acquired between the two arms (for finite polarization P):

$$\begin{aligned} \Phi &= g_C \mu_B \overline{B_1} P_C \left[1 + \sum P_{D_i} \cdot \tfrac{g_D \overline{B_2}}{g_C \overline{B_1}} \cdot \theta_i\right], \\ \theta_i &= 1 - \cos\left(\tfrac{\lambda_i \tau}{2}\right), \end{aligned} \tag{2.5}$$

where $\overline{B_1} = \frac{1}{\tau}\left(\int_0^{\frac{\tau}{2}} b(t) - \int_{\frac{\tau}{2}}^{\tau} b(t)\right)$ and $\overline{B_2} = \frac{1}{\tau}\int_{\frac{\tau}{2}}^{\frac{3\tau}{4}} b\,(t)$ (we are assuming that the external field is small). The factor in the square bracket is the amplification attained as compared to regular spin echo, while the measurement noise is the same, as we still read out one spin only. Note that we keep the contribution from the sensor spins and all environment spins contribute positively. For values of the couplings such that $|\lambda_i \tau| \geq \pi$, or "strongly coupled environment spins" the terms $\cos\left(\frac{\lambda_i \cdot \tau}{2}\right)$ average to zero. Each of the n_{sc} "strongly coupled" spins thus gives a contribution of order one, irrespective of the sign or exact value of the coupling. "Weakly coupled" environment spins ($\lambda_i \leq 1$) contribute instead with a factor $\propto \lambda_i^2$ and we obtain a total phase $\Phi \cong g_C \mu_B \overline{B_1} P_C \left[1 + \frac{g_D \overline{B_2}}{g_C \overline{B_1}} P_D \left(n_{sc} + \frac{1}{2}\sum{}' (\lambda_i \tau)^2\right)\right]$ (here for simplicity we have assumed one polarization for the dark spins (P_D)). In general the sensitivity enhancement scales as $\sim n_{sc} P_D$ [39, 48, 49]. We can thus achieve Heisenberg limited sensing of the external field [50].

2.4 Implementation

2.4.1 Solid state qubits (Nitrogen Vacancy centers)

As a specific application we will consider magnetic sensing using a single Nitrogen Vacancy (NV) center [51] in diamond surrounded by "dark" spins associated with Nitrogen electronic impurities. We focus on NV centers in diamond since their electronic spins

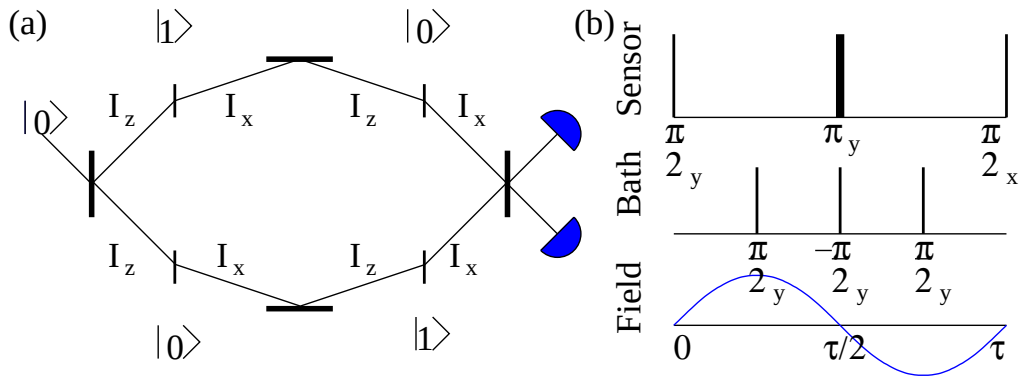

Figure 2.3: Multipulse Method.
a) Mach-Zehnder interferometer, showing the effective Hamiltonian for the bath along each arm and the state of the central spin. Note that the effective Hamiltonian for the bath spins is the same in each arm of the interferometer. b) Pulse sequence for Environment assisted magnetometry. From top to bottom: spin echo on the central spin, pulses on the environment spins, external magnetic field. This sequence can detect both AC and DC fields (with AC field shown). The pulses on the central spin produce the states shown in (a). In the frame of the pulses acting on the bath The Hamiltonian $\sim I_z$ for the dark spins alternates between $\sim I_z$ and $\sim I_x$ as shown in (a) .

(S=1) can be efficiently initialized into the $S_z = 0$ state by optical pumping and read out via state selective fluorescence, the NV center can be rendered an effective two level system by application of a magnetic field that splits the degeneracy between $S_z = \pm 1$ states. Overall the NV, N system in the presence of a magnetic field may be described by the Hamiltonian in Equation (2.1).

A high degree of coherent control has been demonstrated in these systems. In particular they have been used to manipulate individual electronic [51] and nuclear spins [52], as well as to polarize the nearby paramagnetic Nitrogen impurities using dipole-dipole coupling and resonant cross-relaxation [53, 54]. It has recently been shown that Nitrogen Vacancy (NV) impurities in diamond nanocrystals can be used to create a novel nanoscale magnetic sensor with a unique combination of sensitivity and spatial resolution [32, 33, 39]. The pulse sequence shown in Figure 2 can be used to enhance the sensitivity of such a sensor, as it maps the Zeeman phase picked up by the Nitrogen impurities onto the NV center.

2.4.2 Quantum clocks (two species ion chain)

Currently, spectroscopic measurements with trapped ions using quantum logic have achieved resolution to better then one part in 10^{15} [31, 57, 55, 59]. For this high level of performance the ions must posses the following characteristics: a stable clock transition, a cycling cooling transition, good initial state preparation and reliable final state detection. It is often convenient to use two species of ions: Logic and Spectroscopy. The Spectroscopy ions provide the clock transition while the Logic ion provides the rest. In particular at NIST some of the ion clocks employ Beryllium ($^9Be^+$) for the Logic and Aluminum ($^{27}Al^+$) for spectroscopy [60, 59] in the same Penning trap. So far only Cirac-Zoller gates have been used for the state mapping (as there is no convenient center of mass mode to achieve state transfer for all ions simultaneously). Furthermore the number of Aluminum (Spectroscopy) ions in the same Penning trap (when used for metrology purposes) has been limited to one a time [60, 59, 55, 58].

Here we propose a new metrology method that would allow for the use of Sørensen-Mølmer gates instead of Cirac-Zoller ones. This is highly advantageous as Sørensen-Mølmer gates are less prone to noise then Cirac-Zoller ones [61]. We propose to implement the circuit shown in Figure 1(a). In this scheme state dependent laser forces induce Sørensen- Mølmer like interactions between the ions with effective H_{int} given in Equation (2.1) above. The effect of the detuning of the lasers from the clock transition is well described by H_{meas}: so the circuit maps the phase due to the detuning onto the logic ion (see discussion above Equation (2.4)), which can then be fluorescent read out. As such we have attained Heisenberg limited sensing of the clock transition without individual addressability of the spectroscopy ions.

2.5 Decoherence

In this section we will focus on the NV center implementation presented in Section 2.4.1 above. We want to compare the sensitivity that can be obtained by the pulse sequence given above to that obtained with a regular spin echo pulse sequence. For a realistic comparison, we consider the same system in both cases (a sensor spin surrounded by the same spin bath) and include the effects of decoherence (external perturbations and couplings between the dark spins). Once the central spin looses phase coherence due to interactions with the bath it is no longer possible to use it for magnetometry. This limits the sensing time and consequently the magnetometer sensitivity (see discussion in paragraph two). Spin echo (as well as more sophisticated decoupling techniques [62, 46, 59]) can be used to prolong the phase coherence of the central spin. Here we argue that under realistic assumptions the coherence time for the pulse sequence presented in this chapter is not significantly shorter then the spin-echo T_2. Thus the signal amplification per unit time found above Equation (2.5) leads directly to a sensitivity enhancement.

For the pulse sequence proposed here, the signal loss due to decoherence has two causes. First, flip-flops due to dipole-dipole couplings in the bath cause the overlap of the bath wave-functions in the two arms to decay on the spin echo time scale, limiting the experiment time to the bath T_2. Indeed we have shown that the pulse sequence in Figure 2.3 echoes out the static central spin bath interaction, thus decoherence is solely due to the dynamics of the bath. Since the pulse sequence does not change the magnitude of the couplings between different spins in the bath or between the central and bath spins we do not expect a qualitative change of T_2 (in particular arguments about enhanced decoherence of entangled states such as [63] do not apply). We have verified this by Monte Carlo simulations of the signal decay for both regular spin echo and the proposed pulse sequence (see Figure 2.4). We compared them to the signal decay when no control sequence is applied (for the same environment the decay is now described by the dephasing time T_2^*). To make the distinction between the FID and spin echo very clear

we simulated a spin bath composed of spin 1/2 paramagnetic impurities, undergoing a so called WAHUHA sequence (which is designed to prolong T_2 times by averaging out the dipole-dipole coupling of the environment spins (but does not average out the coupling to the external field, see [46])). For simplicity we have assumed perfect delta function pulses.

The second source of signal loss is due to dipole-dipole interactions that scramble the direction of the environment spin polarization in a time on the order of the internal bath coherence time τ_c. Once this happens it is no longer possible to use the central spin as a control bit (see Figure 2.2(b)) and signal amplification due to the environment is lost. Since the signal for the pulse sequence is a sum of contributions from individual dark spins and since each dark spin interacts separately with the rest of the environment the relevant time scale for this source of decoherence is the coherence time of an individual spin in the bath (there is no entanglement enhanced decoherence).

We have thus demonstrated that these two effects lead to an optimum sensing time $T \sim \min\{T_2, \tau_c\}$. Since for many applications $\tau_c \geq T_2$ [46], the optimum sensing time of this pulse sequence is not significantly shorter then those of a regular spin echo, thus sensitivity enhancement is roughly the same as signal strength enhancement.

2.6 Conclusions

In this chapter we proposed a scheme to enhance magnetic field sensing with a single spin by exploiting the possibility to polarize and coherently control the bath. For solid state implementations we are able to exploit the dark spins and preserve roughly the same coherence times as a regular spin echo so we obtain sensitivity enhancement. For ion implementations we can use imperfect Sørensen-Mølmer gates for Heisenberg limited sensitivity. Our method has the potential to be applied more generally. It opens the possibility to use a large class of states to get Heisenberg limited sensitivity enhancement for metrology tasks. We expect that this method can be extended to spin 1/2 systems

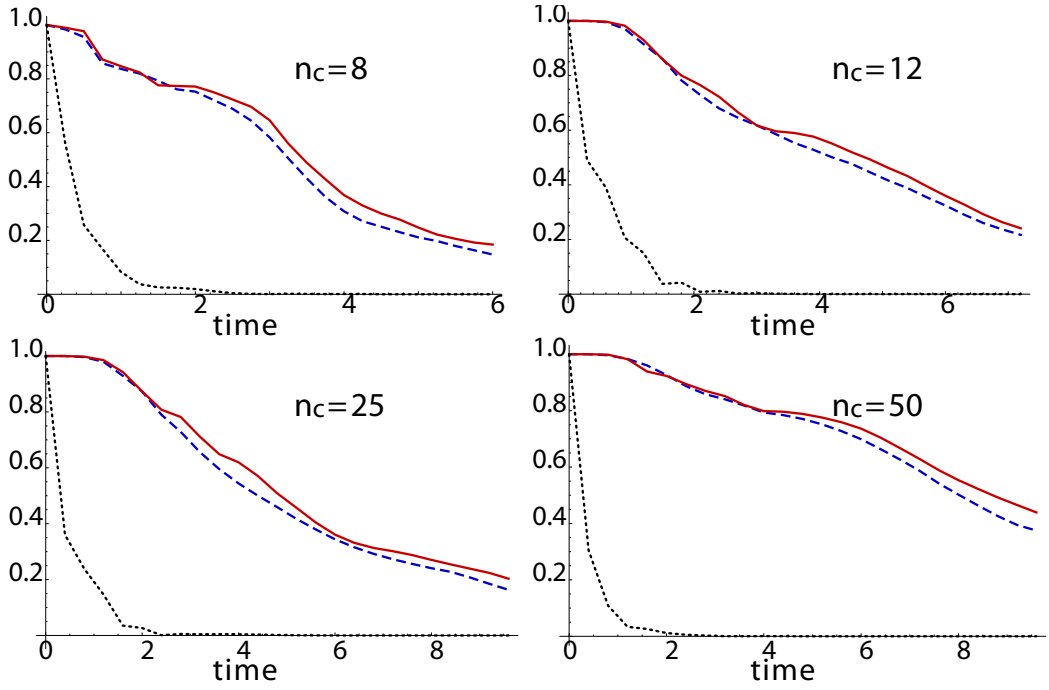

Figure 2.4: WAHUHA results.
Monte-Carlo simulations of normalized signal decay for regular spin echo sequence (Blue), modified spin echo sequence (Red) and no echo (Yellow). A leading order cluster expansion was used [56]. 20 dark spins were randomly placed in a cube of side-length $\sqrt[3]{20}$. The bright spin was placed in the center; the couplings among spins were dipole-dipole. We have set $g\mu_B \equiv 1\,[m]^{3/2}\,[s]^{-1/2}$ to get rid of dimensionful quantities. WAHUHA sequences with 8, 12, 25 and 50 cycles per echo interval respectively were simulated. We have taken an ensemble average over 10 Monte Carlo simulations to obtain each curve. Note that there is no qualitative change between regular and new spin echo sequences.

with same sign couplings, to higher spins and more sophisticated pulse sequences.

3 Decay Rates For Majorana Fermions

3.1 Introduction

Recently there have been numerous proposals to create Majorana zero modes in solid state heterojunctions, superconducting wires and optical lattices. Putatively the information stored in qubits constructed from these modes is protected from various forms of decoherence. Here we present a generic method to study the effect of external perturbations on these modes. We focus on the case where there are no interactions between different Majorana modes either directly or through intermediary fermions. To quantify the rate of loss of the information stored in the Majorana modes we study the two-time correlators for qubits built from them. We analyze a generic gapped fermionic environment (bath) interacting via tunneling with different components of the qubit (different Majorana modes). We present examples with both static and dynamic perturbations (noise), and using our formalism we derive a rate of information loss, for Majorana memories, that depends on the spectral density of both the noise and the fermionic bath.

3.2 Overview

Topological quantum computation requires the existence of topologically ordered states whose low energy excitations follow non-Abelian statistics. The subspace of states corresponding to a fixed number of quasiparticles is degenerate, to an exponential precision, in the separation between quasiparticles, and an exchange of the positions of these any-

onic excitations, also known as braiding, leads to a unitary transformation within this low energy subspace. These unitary operations are insensitive to the exact path used to perform the braiding operation and in many cases, for an appropriate encoding, braiding operations correspond to "standard" one- and two-qubit gates within the low energy subspace. These operations can be used as building blocks for fault tolerant quantum computation.

There are many candidate systems for experimental realizations of topological phases of matter with these properties. There is preliminary evidence that the $\nu = 5/2$ fractional quantum Hall state may have non-Abelian excitations [64, 65, 66]. Spin-triplet $p_x + ip_y$ pairing superfluidity occurs in the A-phase of ^{3}He [67, 68] and in strontium ruthenates [69, 70, 71, 72, 73, 74], in which half quantum vortices would be non-Abelian [75, 76]. There are also proposals to realize chiral p-wave superconductors in ultra-cold atom systems [77, 78, 79]. Furthermore there have been many advances towards producing topological states of matter in layered heterojunction systems [80, 81, 82, 83, 84, 86, 87, 88, 89, 90, 91, 92, 93].

Virtually all current experimentally viable proposals for platforms for topological quantum computation only support Ising type anyons which are carried by Majorana fermion modes. Colloquially speaking these fermions are half of a regular fermion. More precisely they are self-adjoint operators γ_i which can be written as a sum of an annihilation and creation operator for one fermion mode and which satisfy the algebra:

$$\{\gamma_i, \gamma_j\} = 2\delta_{ij}, \ \gamma_i^\dagger = \gamma_i \tag{3.1}$$

Any two Majorana fermion operators can be combined into a regular fermion mode c and its adjoint $c^\dagger$ via $c = \frac{1}{2}(\gamma_1 + i\gamma_2)$ and $c^\dagger = \frac{1}{2}(\gamma_1 - i\gamma_2)$.

The topological qubit is made up of four spin polarized MBSs (Majorana Bound States) γ_1, γ_2, γ_3 and γ_4 [94]. These can be combined into two sets of creation and annihilation

operators:

$$\begin{aligned} c_1 &= \tfrac{1}{2}(\gamma_1 + i\gamma_2) \qquad & c_1^\dagger &= \tfrac{1}{2}(\gamma_1 - i\gamma_2) \\ c_2 &= \tfrac{1}{2}(\gamma_3 + i\gamma_4) \qquad & c_2^\dagger &= \tfrac{1}{2}(\gamma_3 - i\gamma_4) \end{aligned} \tag{3.2}$$

For the logical basis it is convenient to work in the even fermion parity subspace. The qubit basis can be chosen to be $|+_L\rangle \equiv |00\rangle$ and $|-_L\rangle \equiv |11\rangle$ where the 0's and 1's refer to the occupation numbers relative to the complex fermion operators in Equation (3.2). Because of fermion parity conservation, any operation that does not entangle the states with the environment cannot mix even and odd fermion parity states for the qubits. As such, all gates acting on the topological qubit should not take the system out of the logical subspace. Furthermore all the operators of the single spin Clifford group may be produced by braiding the four vortices of our qubit leading to potentially topologically protected gates [95]. Also the various single qubit operations in our logic basis may be conveniently written in terms of the Majorana operators. For future use we note that in this encoding

$$\sigma^z = -i\gamma_1\gamma_2,\ \sigma^x = -i\gamma_2\gamma_3,\ \sigma^y = i\gamma_1\gamma_3. \tag{3.3}$$

Here all the sigma matrices are with respect to the logic basis $|+_L\rangle$ and $|-_L\rangle$. We will primarily be interested in correlators of the form:

$$\langle \sigma^z(0)\,\sigma^z(\mathrm{T})\rangle = -\langle \gamma_1(0)\,\gamma_2(0)\,\gamma_1(\mathrm{T})\,\gamma_2(\mathrm{T})\rangle\,. \tag{3.4}$$

We will proceed to calculate these below.

The Majorana operators are zero modes of some mean field Hamiltonian $[H_{\mathrm{MF}},\,\gamma_i] = 0$ so it can be argued that these modes are protected from decoherence as the mean field Hamiltonian when restricted to the subspace generated by these modes is zero. One of the open tasks of topological quantum computation is associated with understanding the

extent of this protection. This is the subject of this chapter.

3.3 Summary of main ideas

In this section we outline the setup of the rest of the chapter. We present the relevant Hamiltonian and discuss its basic properties. We describe the type of qubit we will focus on in the text, a localized Majorana mode, and give an overview of some other encodings we shall not consider in this chapter. We describe the kinds of calculations of memory coherence we are going to do in this chapter. We also give a section by section outline.

We begin our discussion with relevant Hamiltonians. The Majorana fermions interact with the external environment via tunneling type Hamiltonians. On symmetry grounds, for a single Majorana mode, any such interaction may be written as:

$$H_{\text{int}} = \gamma \int d^d r \left[u_0(\vec{r})\, \Phi^\dagger(\vec{r})\, \Psi^\dagger(\vec{r}) - u_0^*(\vec{r})\, \Psi(\vec{r})\, \Phi(\vec{r}) \right]. \tag{3.5}$$

Here $u_0(\vec{r})$ is the localized mode function associated with the Majorana bound state, $\Phi(\vec{r})$ is any local bosonic field, which in the simplest case is a tunneling amplitude (complex number) and $\Psi(\vec{r})$ is a regular (complex) fermion field. In this chapter we will analyze multiple Majorana fermions coupled to different types of environments via Hamiltonians of the form given in Equation (3.5). Furthermore the fermions in the bath will always be assumed to be gapped, for example, electrons in an insulating or superconducting material (environments composed of gapless fermions, instead, would obviously lead to decoherence).

There are many examples of microscopic situations where Hamiltonians of the form given in Equation (3.5) arise, one is as follows. If one writes the mode expansion of the electron creation and annihilation operators in the (superconducting) system of interest,

one finds that:

$$\begin{pmatrix} \psi\left(\vec{r},\, t\right) \\ \psi^{\dagger}\left(\vec{r},\, t\right) \end{pmatrix} = \gamma \begin{pmatrix} u_0\left(\vec{r}\right) \\ u_0^{*}\left(\vec{r}\right) \end{pmatrix} + \sum_{|E|>0} a_E\, e^{-iEt} \begin{pmatrix} u_E\left(\vec{r}\right) \\ v_E\left(\vec{r}\right) \end{pmatrix} . \tag{3.6}$$

Here a_E stands for the eigenoperators of the BdG equations, with non-zero energies, while u_E and v_E are the components of the corresponding eigenmode of the BdG equations. γ is the Majorana fermion corresponding to the zero energy mode. Now consider an insulating substrate below a system which may be described by Equation (3.6) above. A concrete example is given by the bulk of a topological insulator in tunneling contact with a superconductor as shown in Reference [96]. For a static Hamiltonian the bulk and surface states are orthogonalized, but dynamical effects such as phonons or two-level defect systems can alter the original Hamiltonian and turn on a hybridization. This perturbation takes the form of a tunneling between the electrons: $H_{\text{int}} = \int d^d r\ \Phi\left(\vec{r}\right)\ \Psi^{\dagger}\left(\vec{r}\right)\ \Psi\left(\vec{r}\right) + \text{h. c.}$, where $\Phi\left(\vec{r}\right)$ controls the amplitude of fluctuations of the tunneling coupling. $\Phi\left(\vec{r}\right)$ can be due to phonons, two-level systems, or even classical sources of noise. The electrons $\Psi\left(\vec{r}\right)$ come from the insulating (gapped) system, which comprise the fermionic component of our bath. This illustrates one of the many ways to arrive at Hamiltonians of the form Equation (3.5).

The coupling Hamiltonian that is derived in the paragraph above is local. The terms in Equation (3.5) are local and couple to only one Majorana mode, with no long distance coupling between the modes of any form. In this chapter we shall focus on sets of baths that couple to each Majorana individually. We would like to stress now and henceforth that even by coupling to individual modes, one at a time (with no cross mode coupling), the bath can be very damaging, in many cases leading to zero coherence for long times.

Below, we look at decoherence by analyzing qubit correlations such as $\left\langle \sigma^{\text{z}}\left(0\right) \sigma^{\text{z}}\left(\text{T}\right)\right\rangle = -\left\langle \gamma_1\left(0\right) \gamma_2\left(0\right) \gamma_1\left(\text{T}\right) \gamma_2\left(\text{T}\right)\right\rangle$, which, as we show in this paper, factorizes when the baths

that couple to each Majorana are uncorrelated with one another:

$$\langle \sigma^z(0)\,\sigma^z(\mathrm{T})\rangle \;=\; \langle \gamma_1(0)\,\gamma_1(\mathrm{T})\rangle \times \langle \gamma_2(0)\,\gamma_2(\mathrm{T})\rangle\,. \tag{3.7}$$

Thus, even though the qubit is defined non-locally using spatially separated Majorana fermions, below we will show that the decay of the memory is controlled by the product of the two-time correlations of the separate Majorana modes. It then suffices to understand the effect of the bath on each Majorana fermion separately.

At this point its worthwhile to stress that the qubit encoding given above is not unique. A particularly interesting example of a different encoding, given by Akhmerov [1], is a fermion parity protected encoding. There, the qubit is made from fermion parity preserving operators:

$$\tilde{\gamma} = \gamma \prod_i (1 - 2\,c_i^\dagger\,c_i) \tag{3.8}$$

that commute with both the tunneling Hamiltonian and the Hamiltonian for the environment. Here the c_i are the operators in the mode expansion of the fermionic $\Psi(\vec{r})$ field in the bath (i here labels the mode, which can be momentum, for example). For a finite system, such as mid gap Carroli Matricon deGennes states in vortex cores, this compound qubit is very efficient. However we stress that, in the presence of a bath (say made by continuum states), the construction of an operator that is protected because of parity conservation requires a product of infinitely many operators: which is not practical or easily experimentally measurable. One could also truncate the product so as to account for a finite system, and the terms omitted are those assigned to the bath, as depicted in Figure 3.1. In this case, however, because the operator lacks degrees of freedom assigned to the bath, parity can leak to the environment decohering the qubit. As such we will ignore all "compound" encodings for the rest of the paper.

Finally, we would also like to mention that the above scheme, with simple, non-compound, Majorana encoding, generalizes to multiple qubits. One possible encoding

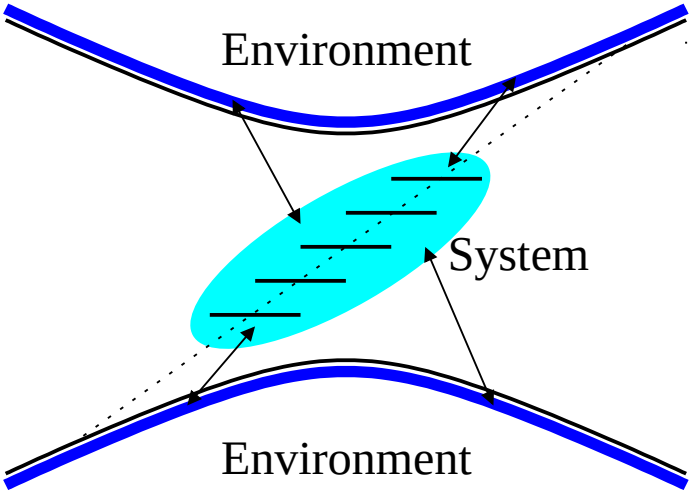

Figure 3.1: System Environment.
Depiction of the separation between system and bath degrees of freedom. For infinite baths, one cannot construct a local operator of the form Equation (3.8), one that is a product of a finite number of terms. If the product is truncated, parity leaks into the bath.

(though not the most economical) is to use four vortices and as such four Majorana modes per qubit. For this and any other encoding all possible correlators for the quantum memory may be expressed as expectation values of various products of Majorana operators [100]. All quantum coherences for our qubits may then be computed by studying Majorana mode correlators which we study below.

In carrying out this program, we will analyze two distinct types of environments: the first is when couplings $\Phi(\vec{r})$ change suddenly but remain static thereafter, and the second when the environment changes dynamically. We show that that in the static environment case the tunneling Hamiltonian merely leads to a finite depletion of the Majorana two-time correlations. In this case, much of the information stored in these modes survives for arbitrarily long times.

More generally, for dynamic environments, we obtain an expression for the rate of loss of information stored in the Majorana operators that depends on the spectral density of the noise and of the fermionic bath. We present several examples of noise that can

be studied essentially exactly, for instance classical telegraphic noise, as well as both classical and quantum Gaussian fluctuations.

The results in this chapter are presented as follows:

- In Section 3.4 we present general considerations involving the coherence properties of Majorana modes. We show that under reasonably generic initial conditions the coherence of the Majorana modes does not depend on their initial states. Furthermore we show that the two time correlation functions, coherences, factorize as a product over coherences for individual Majorana modes, that make up the quantum memory, interacting with their individual environments. As such we may reduce the problem of the coherence of the quantum memory to the problem of the coherence of one Majorana mode in tunneling contact with a (gapped) fermionic reservoir.

- In Section 3.5 we take a first step towards a calculation of the coherence of a single Majorana mode. We begin by describing the Keldysh technique relevant to Majorana modes. We present combinatorial tricks that make it possible to efficiently convert Keldysh computations using a mixture of Majorana and regular fermionic modes into a more familiar computation which uses only regular fermion modes. We then present an example where, for simplicity, we treat the fermions in the bath as free (non-relaxing approximation). We also present a general formula for the coherence of a Majorana qubit that is used several times in the remaining analysis.

- In Section 3.6 we present several related classical models for the fluctuations of the bath. We solve these models essentially exactly, by mapping the problem of the coherence of a single Majorana mode to the problem of a particle undergoing classical diffusion. We use this technique to study classical fluctuations of the tunneling amplitudes and energy levels of the reservoir (we primarily focus on

Gaussian fluctuations). In all cases we find decoherence with a rate that depends on the spectral density of the fluctuations in the reservoir. In many cases the decoherence due to an individual fermion mode has a power law time dependence but it will turn out that a bath made of many weakly interacting modes leads to exponential decay of coherence for intermediate times.

- In Section 3.7 we conclude. In light of the results discussed in the is chapter, we critically examine the degree in which quantum memories can be encoded using Majorana fermions when these are in contact with a dynamical environment. We show that the coherence of the Majorana mode is controlled by the coherence of the bath it interacts with.

- In Appendix B we present many technical calculations relevant for this chapter. For ease of reference we mention that in B.1 we compute exact dressed zero modes for static quadratic Hamiltonians, which we use to verify the validity of our results in Section 3.5. In Appendix B.2 we present a rather technical calculation of a Majorana mode interacting with a fermionic bath with fully quantum mechanical Gaussian fluctuations. To leading order we find a decay similar to classical computations. In Appendix B.3 we present various technical calculations, used throughout the rest of the text. In particular, in Appendix B.3.1 we show that our results are independent of coding subspace, in Appendix B.3.3 we present some technical arguments (which are used in Section 3.6) in favor of weak (negligible) coupling of the fluctuation for the various fermionic modes. In the rest of the appendix we derive formulas used in the main text.

3.4 Dynamics

We begin with a study of the general properties of the dynamics of a system of Majorana modes. We will focus on a computation of correlators involving Majorana operators.

This will allow us to study the coherence properties of a topological quantum memory which is based on qubits made up of localized zero energy modes. In this section we will adhere to very general Hamiltonians and we will study only properties that are essentially independent of the form of this Hamiltonian. This will set us up for studies of specific types of Hamiltonians in Section 3.5. From the outset, we would like to specify the initial conditions or equivalently the density matrix when the system is initialized at $t = 0$. We will assume that initially the density matrix factorizes into a product of the form:

$$\rho_{\text{tot}} = \rho_{\text{Maj}} \otimes \prod_i \rho_{\text{env}_\text{i}} \tag{3.9}$$

Here ρ_{tot} is the density matrix for the entire system, while ρ_{Maj} represents and arbitrary non-equilibrium density matrix for the Majorana modes. The $\rho_{\text{env}_\text{i}}$ are arbitrary, not-necessarily equilibrium, density matrices for the environments of the individual Majorana modes. No specific "ensemble" is assumed. This form is a reasonable, consistent assumption for the initial states of system plus bath, particularly so, as many experimental methods of initialization produce such states.

For our qubit memory persistence between times t_1 and t_2 is captured by the two-time correlators such as $\langle \sigma^z(t_1)\, \sigma^z(t_2) \rangle$. We note that, because the initial, $t = 0$, state breaks time-translation invariance, generically these correlators are functions of both t_1 and t_2. Here we shall focus specifically on correlations, like $\langle \sigma^z(0)\, \sigma^z(\mathrm{T}) \rangle$, between the state prepared at $t = 0$ and the state at a later time $t = \mathrm{T}$ which characterize the degree to which the information encoded in the qubit at the initial time survives interaction with the bath when it is retrieved at a later time T.

The key results of this section, which are used repeatedly later in the text, may be summarized by saying that even though the factorization form given in Equation (3.9) does not survive Hamiltonian evolution the expectation values of various correlators like $\langle \sigma^z(0)\, \sigma^z(\mathrm{T}) \rangle$ or equivalently products of Majorana fermions, to be defined precisely in

Equations (3.13) and (3.14) below, do factorize into products of expectation values for individual Majorana modes. This factorization survives for arbitrary times.

3.4.1 General ideas

We will consider a set of Majorana modes each interacting with its own fermionic environment, see Equation (3.9). We will see that there is decoherence even without direct interactions between different Majorana modes or between their respective environments. One can show that, in the limit when the spatial separation between the Majorana modes is large, the case when multiple Majorana modes interact with a common fermionic bath reduces to the case of uncorrelated non-interacting baths (see Appendix B.3.2). The Hamiltonian pertinent to each mode may be written as:

$$H_\alpha \;=\; \sum_{i=1}^{N_\alpha} \left[\gamma_\alpha \left(B_{i,\alpha}\, c_{i,\alpha} - c_{i,\alpha}^\dagger\, B_{i,\alpha}^\dagger \right) + H_\alpha^{\text{bath}} \left(\{ c_{i,\alpha}, c_{i,\alpha}^\dagger, B_{i,\alpha}, B_{i,\alpha}^\dagger \} \right) \right]. \quad (3.10)$$

Here $B_{i,\alpha}$ are some bosonic modes and $\alpha = \{1, 2, ...\}$ labels the Majorana modes. The total Hamiltonian is given by $H = \sum_\alpha H_\alpha$. We will be interested in correlators of the form $\langle \gamma_{\alpha_1}\, \gamma_{\alpha_2} \ldots \gamma_{\alpha_k}\, \gamma_{\alpha_1}(t_1)\; \gamma_{\alpha_2}(t_2) \ldots \gamma_{\alpha_{\rm k}}(t_k) \rangle$. Here all operators are in the Heisenberg picture, and $\gamma_\alpha(t)$ is given by

$$\gamma_\alpha(t) = \left(\widetilde{\mathcal{T}}\; e^{i \int_0^t H_\alpha(\tau) d\tau} \right) \;\; \gamma_\alpha \;\; \left(\mathcal{T}\; e^{-i \int_0^t H_\alpha(\tau) d\tau} \right) , \quad (3.11)$$

where $\mathcal{T}$ and $\widetilde{\mathcal{T}}$ stand for time-ordered and anti-time-ordered products, respectively. Notice that $\gamma_\alpha(t) = \gamma_\alpha^\dagger(t)$ at all times.

Now, by Taylor expanding the time-ordered and anti-time-ordered exponentials in Equation (3.11), taking various commutators, grouping terms and using the fact that $\gamma_\alpha^2 = 1$, we may write that

$$\gamma_\alpha(t) = \gamma_\alpha\, \mathcal{B}_\alpha(t) + \mathcal{F}_\alpha(t), \quad (3.12)$$

with $\mathcal{B}_\alpha(t)$ and $\mathcal{F}_\alpha(t)$ having no factors of γ_α. Because $\gamma_\alpha(t)$ must be fermionic (this can be seen from the fact that the Hamiltonian and all its powers are bosonic) we may deduce that $\mathcal{B}_\alpha(t)$ and $\mathcal{F}_\alpha(t)$ are, respectively, bosonic and fermionic operators. By the conservation of fermion parity we know that the expectation value of any operator $\langle \mathcal{F}_\alpha(t) \rangle = 0$. Finally, because $\gamma_\alpha(t)$ is Hermitian, it also follows from the properties above that $\mathcal{B}_\alpha(t)$ and $\mathcal{F}_\alpha(t)$ are Hermitian as well.

Now, it follows that

$$\begin{aligned} \langle \gamma_\alpha\, \gamma_\alpha(t) \rangle &= \langle \mathcal{B}_\alpha(t) \rangle + \langle \gamma_\alpha\, \mathcal{F}_\alpha(t) \rangle \\ &= \langle \mathcal{B}_\alpha(t) \rangle + \langle \gamma_\alpha \rangle\, \langle \mathcal{F}_\alpha(t) \rangle \\ &= \langle \mathcal{B}_\alpha(t) \rangle\ , \end{aligned} \tag{3.13}$$

where we used going from the first to the second line of Equation (3.13) that the environments and the Majorana states are initially disentangled so expectation values factorize. Note that this comes about because in the Heisenberg picture the expectation values for operators are taken with respect to the initial state, at $t = 0$. For the third line we have used that the expectation value of any fermionic operator $\langle \mathcal{F}_\alpha(t) \rangle$ should be zero. Note that because $\mathcal{B}_\alpha(t)$ is Hermitian this implies that $\langle \gamma_\alpha\, \gamma_\alpha(t) \rangle \in \mathbb{R}$.

The following factorization formula can be similarly showed:

$$\begin{aligned} \langle \gamma_{\alpha_1} \dots \gamma_{\alpha_\mathrm{k}} \gamma_{\alpha_1}(t_1) \dots \gamma_{\alpha_\mathrm{k}}(t_k) \rangle &= (-1)^{k(k-1)/2} \prod_{j=1}^{k} \langle \mathcal{B}_{\alpha_\mathrm{j}}(t_j) \rangle \\ &= (-1)^{k(k-1)/2} \prod_{j=1}^{k} \langle \gamma_{\alpha_j}\, \gamma_{\alpha_j}(t_j) \rangle\ , \end{aligned} \tag{3.14}$$

for distinct α_j, $j = 1, \dots, k$. To show this expression, one uses Equation (3.12) and again that the expectation values are computed with respect to the initial density matrix given in Equation (3.9) which has the property that the environments are uncorrelated with each other and with the initial Majorana states. We see that this factorization formula is

independent of the initial state of the density matrix of the bath. As such our formalism captures highly non-equilibrium initial conditions.

3.4.2 Qubit memory correlations

The degree of persistence of memories assembled using Majorana fermions can be quantified by the correlation between the qubit state, encoded as in Equation (3.3), at two times 0, T:

$$\begin{aligned} \langle \sigma^z(0)\,\sigma^z(\mathrm{T})\rangle &= -\langle \gamma_1(0)\,\gamma_2(0)\,\gamma_1(\mathrm{T})\,\gamma_2(\mathrm{T})\rangle \\ &= \langle \gamma_1(0)\,\gamma_1(\mathrm{T})\rangle \times \langle \gamma_2(0)\,\gamma_2(\mathrm{T})\rangle\,. \end{aligned} \tag{3.15}$$

Notice that the factorization implies that, even though the qubit is defined non-locally using two spatially separated Majorana fermions, the decay of the memory is controlled by the product of the two-time correlations of the two separate Majorana modes. In particular, the decoherence rate is independent of the initial state of the quantum memory (that is correlators of the form $\langle \gamma_1 \gamma_2 \rangle$ do not enter the result).

Thus in the case of uncoupled well separated Majorana modes each interacting with its own environment the task of determining the persistence of topological quantum memories based on Majorana fermions is reduced to the calculation of the coherences $\langle \gamma_\alpha(0)\,\gamma_\alpha(\mathrm{T})\rangle$ in the presence of different fermionic environments. We carry out this program henceforth.

3.5 Keldysh calculation of coherence

We now proceed to describe the technical details associated with studying dynamics. For generality and later use we will study both static and time dependent Hamiltonians. Based on the discussion given in Section 3.4 for the purposes of computing coherences it

will be sufficient to focus on a single Majorana mode. As such we will drop the subscript α, see Equation (3.10), henceforth.

3.5.1 General observations

We will convert the computation of the Majorana correlations into a Keldysh calculation carried out using only the bosons and regular complex fermions inside the reservoir. (For a review of standard Keldysh techniques see e.g. [101, 102, 103]) We will calculate the following correlator:

$$\langle \gamma\left(0\right)\gamma\left(T\right)\rangle = \left\langle \gamma\ \left(\widetilde{\mathcal{T}}\ e^{+i\int_0^{\mathrm{T}} H(\tau)\,d\tau}\right)\ \gamma\ \left(\mathcal{T}\ e^{-i\int_0^{\mathrm{T}} H(\tau)\,d\tau}\right)\right\rangle\ . \tag{3.16}$$

Here the expectation value is taken relative to the density matrix ρ_0 at $\tau = 0$ while $\mathcal{T}$ and $\widetilde{\mathcal{T}}$ stand for time ordering and time antiordering respectively. To make the computations tractable we will assume that $\rho_0 = \rho_{\mathrm{therm}} \otimes \rho_{\mathrm{Maj}}$. Here ρ_{Maj} is any initial density matrix acting on the subspace of the Majorana modes while ρ_{therm} is the thermal density matrix for the regular fermion modes.

To compute the correlator in Equation (3.16), we will use Equation (3.10) and work in the interaction picture with respect to the rest of the Hamiltonian $H^{\mathrm{bath}}\left(\{c_{\mathrm{i}}\,, c_{\mathrm{i}}^{\dagger}, B_{\mathrm{i}}\,, B_{\mathrm{i}}^{\dagger}\}\right)$. We will expand the ordered exponentials in powers of H and collect and contract all the γs to eliminate them. In what follows will show that

$$\langle \gamma\left(0\right)\gamma\left(T\right)\rangle = \left\langle \left(\widetilde{\mathcal{T}}\ e^{-\int_0^{\mathrm{T}} \mathrm{O}(\tau)\,d\tau}\right)\ \left(\mathcal{T}\ e^{-\int_0^{\mathrm{T}} \mathrm{O}(\tau)\,\mathrm{d}\tau}\right)\right\rangle \equiv \left\langle \mathcal{T}_c\ e^{-\sum_a \int_0^{\mathrm{T}} \mathrm{O}(\tau^a)\mathrm{d}\tau^a}\right\rangle\ , \tag{3.17}$$

where $\mathrm{O}\left(\tau\right) = \sum_{\mathrm{i}=1}^{\mathrm{N}}\left(B_i\left(\tau\right)c_i\left(\tau\right) - B_i^{\dagger}\left(\tau\right)c_i^{\dagger}\left(\tau\right)\right)$, and $\mathcal{T}_{\mathrm{c}}$ stands for the Keldysh ordering that combines the forward and backward propagation, and the index $a =$ t, b labels the two pieces (forward and backward) of the ordered product. (Notice though that the operator $\mathrm{O}\left(\tau\right)$ in the exponential comes with the same sign in the $\mathcal{T}$ and $\widetilde{\mathcal{T}}$ products.)

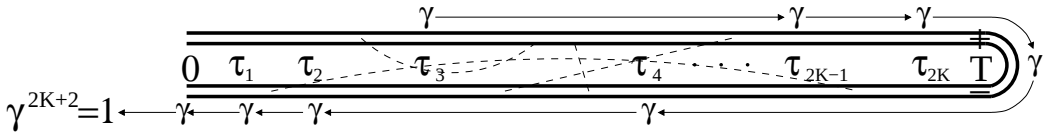

Figure 3.2: Keldysh Contour.
The Keldysh contour determining the coherence of the Majorana zero mode. We consider $2K$ insertions of our interaction Hamiltonian $\pm i\gamma \sum_{i=1}^{N} \left(B_i c_i - B_i^\dagger c_i^\dagger \right)$ into the Keldysh contour with $\pm$ referring to the forward in time and backwards in time branches. Several interaction insertions are shown by dashed lines. To convert this contour to a "regular" Keldysh calculation we commute the Majorana modes (γ terms) including the one at $\tau = \mathrm{T}$ till they are all located at $\tau = 0$ as shown. In the text we describe how to compute commutators appropriately.

Below we give the essential arguments needed to derive Equation (3.17). To carry out this program, let us introduce a short-hand notation $H = \gamma \sum_{i=1}^{N} \left(B_i c_i - B_i^\dagger c_i^\dagger \right) \equiv \gamma \left(\mathbf{Bc} - \mathbf{B}^\dagger \mathbf{c}^\dagger \right)$. Now expand Equation (3.16) in powers of H, and focus on the term with $N_\mathrm{b} + N_\mathrm{t}$ insertions, with N_b from the expansion of the $\widetilde{\mathcal{T}}$-ordered exponential and N_t from that of the $\mathcal{T}$-ordered exponential. By fermion parity conservation and using our assumption that the system-bath initial density matrix is factorized we know that $N_\mathrm{b} + N_\mathrm{t} = 2K$ is even. The insertions of our interaction Hamiltonian are of the form

$$\begin{aligned} &\overbrace{\{\gamma\}}^{\tau=0} \underbrace{\left[i\gamma \left(\mathbf{Bc} - \mathbf{B}^\dagger \mathbf{c}^\dagger \right) (t_1^b) \right] \cdots \left[i\gamma \left(\mathbf{Bc} - \mathbf{B}^\dagger \mathbf{c}^\dagger \right) (t_{N_\mathrm{b}}^\mathrm{b}) \right]}_{\text{bottom insertions}} \times \\ &\times \overbrace{\{\gamma\}}^{\tau=\mathrm{T}} \underbrace{\left[-i\gamma \left(\mathbf{Bc} - \mathbf{B}^\dagger \mathbf{c}^\dagger \right) (t_1^t) \right] \cdots \left[-i\gamma \left(\mathbf{Bc} - \mathbf{B}^\dagger \mathbf{c}^\dagger \right) (t_{N_\mathrm{t}}^\mathrm{t}) \right]}_{\text{top insertions}} . \end{aligned} \tag{3.18}$$

We show in curly brackets $\{\gamma\}$ the modes at $\tau = \mathrm{T}$ and at $\tau = 0$, to help single them out for constructing the argument below. Our strategy to convert this calculation to a "regular" Keldysh calculation will be to move the Majorana modes (γ terms), including the $\{\gamma\}$ at $\tau = \mathrm{T}$, by taking appropriate commutators, till they are all at the left hand side, adjacent to the $\{\gamma\}$ inserted at $\tau = 0$. We will move along the contour ordering

direction (see Figure 3.2). We will then use the relation $\gamma^{2K+2} = 1$ to eliminate these modes altogether. All that remains is a computation of the commutators. Because of the form of the Hamiltonian, computing commutators is equivalent to computing an overall sign for the term in the expansion. By noting that the Hamiltonian is bosonic we obtain that the overall sign is only due to the anti-commutation of the γ's with the c_i and $c_i^\dagger$ inside the $\left(\mathbf{Bc} - \mathbf{B}^\dagger\mathbf{c}^\dagger\right)$ terms. We shall move each γ mode to the very left in two steps: we first move the mode at $\tau = \mathrm{T}$ to the very left towards $\tau = 0$; then we move all the remaining modes there as well.

In the first part of the procedure is to obtain the contribution, to the overall sign, of the Majorana fermion inserted at $\tau = \mathrm{T}$. We note that the number of -1 signs it picks up depends on its position along the contour relative to the other modes it picks up one -1 sign for very mode it passes so there is an overall sign of $(-1)^{N_\mathrm{b}}$.

Now for the rest working from left to right, the first Majorana mode that needs to be moved picks up no -1 signs as it does not pass over a $\left(\mathbf{Bc} - \mathbf{B}^\dagger\mathbf{c}^\dagger\right)$ term, but the second picks up one -1 sign as it passes over one such term. Similarly, the third picks up two (-1) signs, and so forth. Finally the $2K$th Majorana mode (last to be moved, sitting all the way to the right) picks up $2K - 1$ factors of -1. The product of these factors yields $(-1)^{K(2K-1)} = (-1)^K = (-i)^{N_\mathrm{t}+N_\mathrm{b}}$.

Thus eliminating the γ's in Equation (3.18) leads to an overall sign $(-i)^{N_\mathrm{b}+N_\mathrm{t}} \times (-1)^{N_\mathrm{b}}$, which then allows us to replace terms of the form Equation (3.18) by

$$\begin{aligned}\underbrace{\left[-\left(\mathbf{Bc} - \mathbf{B}^\dagger\mathbf{c}^\dagger\right)(t_1^\mathrm{b})\right]\cdots\left[-\left(\mathbf{Bc} - \mathbf{B}^\dagger\mathbf{c}^\dagger\right)(t_{N_\mathrm{b}}^\mathrm{b})\right]}_{\text{bottom insertions}} \times \\ \times \underbrace{\left[-\left(\mathbf{Bc} - \mathbf{B}^\dagger\mathbf{c}^\dagger\right)(t_1^\mathrm{t})\right]\cdots\left[-\left(\mathbf{Bc} - \mathbf{B}^\dagger\mathbf{c}^\dagger\right)(t_{N_\mathrm{t}}^\mathrm{t})\right]}_{\text{top insertions}} .\end{aligned} \tag{3.19}$$

These are precisely the terms that appear in the series expansion of Equation (3.17), and therefore we can continue the calculation utilizing this expression. We should point

out that for complex fermions coming from Majorana insertion $\mathcal{T}_c$ corresponds to literal ordering on the Keldysh contour, without any fermionic minus signs, because the original Hamiltonian was bosonic [this can also be seen step-by-step in going from Equation (3.18) to Equation (3.19)]. This fact leads to the modified sign for the fermionic $\mathcal{T}_c$-ordering:

$$\begin{aligned}
&\mathcal{T}_c\left[c_i^\dagger\left(t_1\right)c_i\left(t_2\right)\right]\equiv\\
&\equiv\begin{cases}
\theta\left(t_1-t_2\right)\ c_i^\dagger\left(t_1\right)c_i\left(t_2\right)+\theta\left(t_2-t_1\right)\ c_i\left(t_2\right)c_i^\dagger\left(t_1\right) & ,\ t_1,t_2 \text{ on top}\\
c_i^\dagger\left(t_1\right)c_i\left(t_2\right) & ,\ t_1 \text{ on bottom}, t_2 \text{ on top}\\
c_i\left(t_2\right)c_i^\dagger\left(t_1\right) & ,\ t_1 \text{ on top}, t_2 \text{ on bottom}\\
\theta\left(t_2-t_1\right)\ c_i^\dagger\left(t_1\right)c_i\left(t_2\right)+\theta\left(t_1-t_2\right)\ c_i\left(t_2\right)c_i^\dagger\left(t_1\right) & ,\ t_1,t_2 \text{ on bottom}\ .
\end{cases}
\end{aligned}\tag{3.20}$$

Now, we turn our attention to the computation of Equation (3.17). We do so in steps, computing the expectation values by first tracing the fermions $(c_i\,,\,c_i^\dagger)$ and then subsequently tracing the bosonic degrees of freedom. Even in the case where there are interactions for the fermions, we can still treat the theory as quadratic in the fermions and include the interactions (with photons or phonons) as a coupling of the fermionic bilinears with the mediating bosons, which we label by ϕ. Alternatively, we may think of the fields ϕ fields as Hubbard-Stratonovich decoupling fields [101, 102].

We can thus write

$$\begin{aligned}
&\left\langle \mathcal{T}_{\mathrm{c}}\, e^{-\sum_a \int_0^{\mathrm{T}}\left(\mathbf{Bc}-\mathbf{B}^\dagger\mathbf{c}^\dagger\right)\left(\tau^a\right)\,\mathrm{d}\tau^a}\right\rangle=\\
&=\mathcal{Z}^{-1}\ \int\left(\prod_a \mathcal{D}\mathbf{B}_a\,\mathcal{D}\mathbf{B}_a^\dagger\right)\ e^{i\mathcal{S}_{\mathbf{B}}\left[\mathbf{B}_a\,\mathbf{B}_a^\dagger\right]}\ \int\left(\prod_a \mathcal{D}\phi_a\,\mathcal{D}\phi_a^\dagger\right)\ e^{i\mathcal{S}_\phi\left[\phi_a\,\phi_a^\dagger\right]}\times\\
&\qquad\times\ \exp\left(\tfrac{1}{2}\sum_{a,b}\ \int_0^{\mathrm{T}}\mathrm{d}\tau_1^a\int_0^{\mathrm{T}}\mathrm{d}\tau_2^b\ \ \left\langle\mathcal{T}_c\left[\left(\mathbf{Bc}-\mathbf{B}^\dagger\mathbf{c}^\dagger\right)\left(\tau_1^a\right)\ \left(\mathbf{Bc}-\mathbf{B}^\dagger\mathbf{c}^\dagger\right)\left(\tau_2^b\right)\right]\right\rangle_{\mathbf{c},\mathbf{c}^\dagger}\right)\ .
\end{aligned}\tag{3.21}$$

We remind the reader that all functional integrals are along the Keldysh contour. The action $\mathcal{S}_\phi$ is that of the interaction mediator field ϕ and contains the dressing from the integration of the fermions, which are integrated out first as explained above. The

normalization $\mathcal{Z}$ is

$$\mathcal{Z} = \int \left(\prod_a \mathcal{D}\mathbf{B}_a \, \mathcal{D}\mathbf{B}_a^\dagger \right) \, e^{i\mathcal{S}_{\mathbf{B}}[\mathbf{B}_a \, \mathbf{B}_a^\dagger]} \int \left(\prod_a \mathcal{D}\phi_a \, \mathcal{D}\phi_a^\dagger \right) \, e^{i\mathcal{S}_\phi[\phi_a \, \phi_a^\dagger]} \, . \tag{3.22}$$

This procedure works because it possible to calculate partition functions, Green's functions, integrate fields out etc. along any contour, in particular along the Keldysh contour as used here. We then express the fermionic correlators in terms of their Green's function,

$$\begin{aligned} &\left\langle \mathcal{T}_{\mathrm{c}} \left[\left(\mathbf{B}\mathbf{c} - \mathbf{B}^\dagger \mathbf{c}^\dagger \right) (\tau_1^a) \, \left(\mathbf{B}\mathbf{c} - \mathbf{B}^\dagger \mathbf{c}^\dagger \right) \left(\tau_2^b \right) \right] \right\rangle_{\mathbf{c},\mathbf{c}^\dagger} = \\ &= -B_i(\tau_1^a) \, {B_j}^\dagger \left(\tau_2^b \right) \left\langle \mathcal{T}_{\mathrm{c}} \left[c_i \left(\tau_1^a \right) {c_j}^\dagger \left(\tau_2^b \right) \right] \right\rangle - {B_i}^\dagger(\tau_1^a) \, B_j \left(\tau_2^b \right) \left\langle \mathcal{T}_{\mathrm{c}} \left[{c_i}^\dagger(\tau_1^a) \, c_j \left(\tau_2^b \right) \right] \right\rangle \equiv \\ &\equiv -\mathbf{B} \left(\tau_1^a \right) \, G_{\mathrm{F,e}}^\phi \left(\tau_1^a, \tau_2^b \right) \, \mathbf{B}^\dagger \left(\tau_2^b \right) - \, \mathbf{B}^\dagger \left(\tau_1^a \right) \, G_{\mathrm{F,h}}^\phi \left(\tau_1^a, \tau_2^b \right) \, \mathbf{B} \left(\tau_2^b \right) \end{aligned} \tag{3.23}$$

where the $G_{\mathrm{F,e}}^\phi \left(\tau_1^a, \tau_2^b \right)$ and $G_{\mathrm{F,h}}^\phi \left(\tau_1^a, \tau_2^b \right)$ are, respectively, the electron and hole fermionic Green's function, and we have used the fact that the bosonic fields $\mathbf{B}$, $\mathbf{B}^\dagger$ can be treated as c-numbers as they are inside the bosonic path integral. As stated previously $G_{\mathrm{F,e}}^\phi \left(\tau_1^a, \tau_2^b \right)$ and $G_{\mathrm{F,h}}^\phi \left(\tau_1^a, \tau_2^b \right)$ are slightly unusual Green's functions, with no fermionic minus signs (only plus signs), as shown in Equation (3.20). Let us define $D_{\mathrm{F}}^\phi \left(\tau_1^a, \tau_2^b \right) = \, G_{\mathrm{F,h}}^\phi \left(\tau_1^a, \tau_2^b \right) + \, G_{\mathrm{F,e}}^\phi \left(\tau_2^b, \tau_1^a \right)$, so we can then write

$$\begin{aligned} \langle \gamma \left(0 \right) \gamma \left(T \right) \rangle = \mathcal{Z}^{-1} \, &\int \left(\prod_a \mathcal{D}\mathbf{B}_a \, \mathcal{D}\mathbf{B}_a^\dagger \right) \, e^{i\mathcal{S}_{\mathbf{B}}[\mathbf{B}_a \, \mathbf{B}_a^\dagger]} \int \left(\prod_a \mathcal{D}\phi_a \, \mathcal{D}\phi_a^\dagger \right) \, e^{i\mathcal{S}[\phi_a \, \phi_a^\dagger]} \\ &\times \, \exp \left(-\frac{1}{2} \sum_{a,b} \int_0^{\mathrm{T}} \mathrm{d}\tau_1^a \int_0^{\mathrm{T}} \mathrm{d}\tau_2^b \, \mathbf{B}^\dagger \left(\tau_1^a \right) \, D_{\mathrm{F}}^\phi \left(\tau_1^a, \tau_2^b \right) \, \mathbf{B} \left(\tau_2^b \right) \right) \end{aligned} \tag{3.24}$$

We remark that the expression in Equation (3.24) was derived without any approximations. It holds for interacting electrons as well, as long as the interactions are included via an external bosonic field denoted by ϕ above. Furthermore we would like to note that though it is not used anywhere in this paper, but a similar path integral formulation using Grassmann variables may be done without any decoupling fields, for regular quartic

$\sim \Psi^{\dagger}(\vec{x})\,\Psi^{\dagger}(\vec{x})\,\Psi(\vec{x})\,\Psi(\vec{x})$ fermionic interactions. A systematic Keldysh diagrammatic perturbation theory may be derived from it.

For future use we note that to compute the coherence of a Majorana mode it is often enough to compute the four diagrams shown in Figure (3.3). Following Equation (3.24), their sum may be explicitly written as:

$$\begin{aligned} V(T) &\equiv \sum_{a,b} \int_0^{\mathrm{T}} \mathrm{d}\tau_1^a \int_0^{\mathrm{T}} \mathrm{d}\tau_2^b \;\mathbf{B}^{\dagger}(\tau_1^a)\; D_{\mathrm{F}}^{\phi}\left(\tau_1^a,\tau_2^b\right)\; \mathbf{B}\left(\tau_2^b\right) \\ &= 2\sum_i \Bigg\{ \int_0^{\mathrm{T}} d\tau_1 \int_0^{\mathrm{T}} d\tau_2 \Big[\mathcal{T}\left({B_i}^{\dagger}\left(\tau_1^{\mathrm{t}}\right) B_i\left(\tau_2^{\mathrm{t}}\right)\right) \times \\ &\qquad \times \left(\theta(\tau_1-\tau_2)\left\langle c_i^{\dagger}(\tau_1)\, c_i(\tau_2)\right\rangle + \theta(\tau_2-\tau_1)\left\langle c_i(\tau_2)\, c_i^{\dagger}(\tau_1)\right\rangle\right) \\ &\quad + \widetilde{\mathcal{T}}\left({B_i}^{\dagger}\left(\tau_1^{\mathrm{b}}\right) B_i\left(\tau_2^{\mathrm{b}}\right)\right) \times \\ &\qquad \times \left(\theta(\tau_2-\tau_1)\left\langle c_i^{\dagger}(\tau_1)\, c_i(\tau_2)\right\rangle + \theta(\tau_1-\tau_2)\left\langle c_i(\tau_2)\, c_i^{\dagger}(\tau_1)\right\rangle\right) \\ &\quad + \left({B_i}^{\dagger}\left(\tau_1^{\mathrm{t}}\right) B_i\left(\tau_2^{\mathrm{b}}\right)\left\langle c_i^{\dagger}(\tau_1)\, c_i(\tau_2)\right\rangle + B_i\left(\tau_1^{\mathrm{t}}\right) B_i^{\dagger}\left(\tau_2^{\mathrm{b}}\right)\left\langle c_i(\tau_1)\, c_i^{\dagger}(\tau_2)\right\rangle\right)\Big]\Bigg\} \end{aligned} \tag{3.25}$$

Here $\mathcal{T}$, $\widetilde{\mathcal{T}}$ refer to time ordering and time anti-ordering operators. This form places the time ordering or antiordering terms ($\mathcal{T}\left({B_i}^{\dagger}\left(\tau_1^{\mathrm{t}}\right) B_i\left(\tau_2^{\mathrm{t}}\right)\right)$) with the appropriate fermion correlators so it can be used directly in calculations without having to use a path integral. The factor of two going from the first to the second line comes from a symmetry $\tau_1 \leftrightarrow \tau_2$ (which also allowed us to simplify Equation (3.25) above to contain six rather then twelve terms). Because of exponentiation of disconnected diagrams, if we can safely ignore higher order correlations among the B_i's, we may write that:

$$\langle \gamma(0)\,\gamma(T)\rangle = \mathrm{e}^{-\frac{1}{2}\langle V(T)\rangle}\ . \tag{3.26}$$

A quick way to derive the extra factor of $\frac{1}{2}$ in Equation (3.26) above is by noting that it is a symmetry factor associated with the ability to permute the two Majorana insertions without changing the diagram [alternatively we can do a combinatorial check,

or use Equation (3.24)].

Let us illustrate with a few simple examples how one can use the expression for the Majorana correlations $\langle \gamma(0)\,\gamma(T)\rangle$ in Equation (3.24) to calculate the the decay rates of topological memories. We then deploy this expression in detailed studies for fluctuating Hamiltonians in Section 3.6.

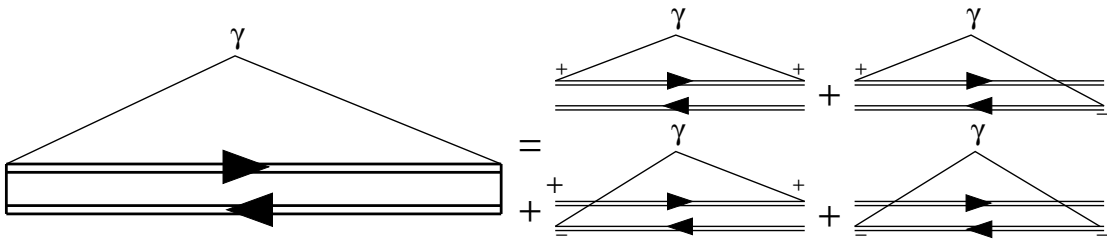

Figure 3.3: One Loop Diagrams.
The four diagrams relevant to calculating $V(T)$ in the main text. We need to sum over four possible orderings of the Majorana insertions on the Keldysh contour. The value is given by a sum of terms like ${B_i}^{\dagger}\left(\tau_1^{\mathrm{t}}\right) B_i\left(\tau_2^{\mathrm{b}}\right)\left\langle c_i^{\dagger}(\tau_1)\, c_i(\tau_2)\right\rangle$.

3.5.2 Simple examples

Let us consider simple cases where the B_i are simply constants Γ_i, switched on at $\tau = 0$. In this case the expression in Equation (3.24) simplifies to

$$\begin{aligned}\langle \gamma(0)\,\gamma(T)\rangle = \mathcal{Z}^{-1} & \int\left(\prod_a \mathcal{D}\phi_a\,\mathcal{D}\phi_a^{\dagger}\right)\, e^{i\mathcal{S}[\phi_a\,\phi_a^{\dagger}]} \\ & \times\ \exp\left(-\frac{1}{2}\sum_{a,b}\int_0^{\mathrm{T}}\mathrm{d}\tau_1^a\int_0^{\mathrm{T}}\mathrm{d}\tau_2^b\ \mathbf{\Gamma}^{\dagger}\, D_{\mathrm{F}}^{\phi}\left(\tau_1^a,\tau_2^b\right)\ \mathbf{\Gamma}\right) \\ & = \exp\left(-\frac{1}{2}\sum_{a,b}\int_0^{\mathrm{T}}\mathrm{d}\tau_1^a\int_0^{\mathrm{T}}\mathrm{d}\tau_2^b\ \mathbf{\Gamma}^{\dagger}\,\overline{D}_F^{(2)}\left(\tau_1^a,\tau_2^b\right)\ \mathbf{\Gamma}\ +\ \ldots\right)\end{aligned} \tag{3.27}$$

where $\overline{\mathrm{D}}_{\mathrm{F}}^{(2)}\left(\tau_1^a,\tau_2^b\right) = \overline{\mathrm{G}}_{\mathrm{F,h}}^{(2)}\left(\tau_1^a,\tau_2^b\right) + \overline{\mathrm{G}}_{\mathrm{F,e}}^{(2)}\left(\tau_2^b,\tau_1^a\right)$, with $\overline{\mathrm{G}}_{\mathrm{F,h}}^{(2)}$ and $\overline{\mathrm{G}}_{\mathrm{F,e}}^{(2)}$ exact 2-point electron and hole Keldysh propagators, including the effects of interactions. To be explicit at this level of approximation our formalism handles all the dynamics of the ϕ_a fields but

treats fermionic interactions to quadratic order. The ... stand for terms of order $\mathcal{O}(\mathbf{\Gamma}^4)$ that involve the 4-point Green's functions $\overline{\mathrm{G}}^{(4)}$. We shall not do so in this text, but by including these $\mathcal{O}(\mathbf{\Gamma}^4)$ and higher terms it is possible to handle all fermionic interactions as well.

Taking into account all the four cases in the sum over top and bottom insertions $\sum_{a,b}$, one can write

$$\frac{1}{2}\sum_{a,b}\int_0^{\mathrm{T}}\mathrm{d}\tau_1^a\int_0^{\mathrm{T}}\mathrm{d}\tau_2^b\ \mathbf{\Gamma}^\dagger\,\overline{\mathrm{D}}_{\mathrm{F}}^{(2)}\left(\tau_1^a,\tau_2^b\right)\ \mathbf{\Gamma}=\sum_{i,j}\int_0^{\mathrm{T}}\mathrm{d}\tau_1\int_0^{\mathrm{T}}\mathrm{d}\tau_2\ \ \Gamma_i^*\left(\langle\{c_i^\dagger(\tau_1),c_j(\tau_2)\}\rangle\right)\Gamma_j \tag{3.28}$$

We now consider a case where this formula will be particularly useful. We Consider the case when the bath is described by the Hamiltonian

$$H=\gamma\sum_{i=1}^{N}\left(\Gamma_i c_i-\Gamma_i^* c_i^\dagger\right)+\sum_{i=1}^{N}\epsilon_i c_i^\dagger c_i\ . \tag{3.29}$$

In this case we have

$$\langle\{c_i^\dagger(\tau_1),c_j(\tau_2)\}\rangle=\delta_{ij}\ e^{-i\epsilon_{\mathrm{i}}(\tau_1-\tau_2)} \tag{3.30}$$

with ϵ_i the energy of mode i. It follows by substitution in Equation (3.28) and then in Equation (3.24) that

$$\langle\gamma\,(0)\,\gamma\,(\mathrm{T})\rangle=\mathrm{e}^{-2\sum_i|\Gamma_i|^2|\int_0^{\mathrm{T}}d\tau\ e^{-i\epsilon_i\tau}|^2}\ , \tag{3.31}$$

or

$$\langle\gamma\,(0)\,\gamma\,(\mathrm{T})\rangle=\mathrm{e}^{-4\sum_i\frac{|\Gamma_i|^2}{\epsilon_i^2}[1-\cos(\epsilon_i T)]}\ . \tag{3.32}$$

If the bath has energy eigenenergies ϵ_i away from zero energy (*i.e.*, there is a gap $\tilde{\epsilon}<|\epsilon_i|$), we may drop the oscillating terms in the limit of $\mathrm{T}\gg 1/\tilde{\epsilon}$, so we can write

$$\langle\gamma\,(0)\,\gamma\,(\mathrm{T})\rangle\approx e^{-4\sum_i\frac{|\Gamma_i|^2}{\epsilon_i^2}}\ ,\quad \mathrm{T}\gg 1/\tilde{\epsilon}\ . \tag{3.33}$$

In this case, the Majorana memory decays to T independent plateaus at large times. Thus, as long as the sum $\sum_i \frac{|\Gamma_i|^2}{\epsilon_i^2}$ converges, the memory is retained to a finite extent. This result is confirmed by a time-independent re-diagonalization in the presence of the Γ_i, which is shown explicitly in Appendix B.1 where a new exact zero mode is calculated. Here we simply note that the finite depletion found in this case is a simple consequence of the fact that the modes change once the coupling is switched on. Also, we compute the sum $\sum_i \frac{|\Gamma_i|^2}{\epsilon_i^2}$, and find it to be finite, for a specific tunneling model in Appendix B.3.4.

Zero temperature limit

We would like to present rather general analysis of the decay rate for a zero temperature fully quantum environment. We will see that in this case also the decay saturates for long times. We begin by simplifying Equations 3.25 and 3.26 for this case. In this case all terms of the form $B_i^\dagger\left(\tau_1^{\mathrm{t}}\right) B_i\left(\tau_2^{\mathrm{t}}\right)$ may be replaced by the appropriate expectation values: $\left\langle B_i^\dagger\left(\tau_1\right) B_i\left(\tau_2\right)\right\rangle$. In this case we may sum directly the four diagrams in Figure 3.3 in the same manner as Equations 3.25 and 3.26 to obtain that:

$$\begin{aligned}
\left\langle \gamma\left(0\right)\gamma\left(T\right)\right\rangle &= \prod_i \exp\left(-2\int_0^T\int_0^T d\tau_1 d\tau_2 \left\{\left\langle B_i^\dagger\left(\tau_1\right) B_i\left(\tau_2\right)\right\rangle \times \left\langle c^\dagger\left(\tau_1\right) c\left(\tau_2\right)\right\rangle\right.\right. \\
&+ \left.\left.\left\langle B_i\left(\tau_1\right) B_i^\dagger\left(\tau_2\right)\right\rangle \times \left\langle c\left(\tau_1\right) c^\dagger\left(\tau_2\right)\right\rangle\right\}\right) \\
&\cong \prod_i \exp\left(-2\int_0^T\int_0^T d\tau_1 d\tau_2 \left\langle B_i\left(\tau_1\right) B_i^\dagger\left(\tau_2\right)\right\rangle e^{-i\epsilon_i\left(\tau_1-\tau_2\right)}\right) \qquad (3.34)
\end{aligned}$$

In the last step we have assumed that $\left\langle c^\dagger\left(\tau_1\right) c\left(\tau_2\right)\right\rangle \cong 0$ at zero temperature. Furthermore at zero temperature we may simplify $\left\langle B_i\left(\tau_1\right) B_i^\dagger\left(\tau_2\right)\right\rangle$ by writing that

$$\begin{aligned}
\left\langle B_i\left(\tau_1\right) B_i^\dagger\left(\tau_2\right)\right\rangle &= \sum_n \left\langle 0\right| B_i\left(\tau_1\right)\left|n\right\rangle \left\langle n\right| B_i^\dagger\left(\tau_2\right)\left|0\right\rangle \\
&= \sum_n \left|\left\langle 0\right| B_i\left(0\right)\left|n\right\rangle\right|^2 e^{-i\omega_n\left(\tau_1-\tau_2\right)} \qquad (3.35)
\end{aligned}$$

Here $|0\rangle$ is the ground state of the reservoir while $|n\rangle$ are the excited states. Substi-

tuting this into Equation 3.34 above we get that:

$$\begin{aligned}\langle\gamma(0)\gamma(T)\rangle &= \prod_i \exp\left(-4\sum_n \frac{|\langle 0|B_i(0)|n\rangle|^2}{(\epsilon_i+\omega_n)^2}\left(1-\cos\left((\epsilon_i+\omega_n)T\right)\right)\right) \\ &\cong \prod_i \exp\left(-4\sum_n \frac{|\langle 0|B_i(0)|n\rangle|^2}{(\epsilon_i+\omega_n)^2}\right) \end{aligned} \tag{3.36}$$

From this we see that the coherence of a Majorana fermion in contact with a zero temperature quantum reservoir saturates at long times similarly to the static case studied above.

3.6 Fluctuating Hamiltonians

So far we have studied static Hamiltonians. To gain further insight it is interesting to extend our results to fluctuating couplings (which may come from time dependent classical fluctuations or from quantum dynamics). We shall focus on three cases, in all three the fermionic action is quadratic. In the first case we study we consider the situation when the B_i are simply replaced by classical variables Γ_i, like we did in Section 3.5.2, but now they depend on time. The second case is that when the energies ϵ_i of the electrons in the bath fluctuate in time, because of environmental fluctuations. The third case is a generalization of the first one, where we treat the B_i quantum mechanically with their fluctuations governed by a quadratic action. We treat the first two cases here, and the third, more technical one, in Appendix B.2.

In the first two cases, one can generalize the expression in Equation (3.31) simply by taking $\Gamma_i \to \Gamma_i(\tau)$ or $\epsilon_i \to \epsilon_i(\tau)$:

$$\begin{aligned}\langle\gamma(0)\gamma(T)\rangle &= \mathrm{e}^{-2\sum_i\left|\int_0^{\mathrm{T}} d\tau\, \Gamma_i(\tau)\, e^{-i\int_0^\tau dt\,\epsilon_i(t)}\right|^2} \\ &= \prod_i \mathrm{e}^{-2\left|\int_0^{\mathrm{T}} \mathrm{d}\tau\, \Gamma_i(\tau)\, e^{-i\int_0^\tau dt\,\epsilon_i(t)}\right|^2}, \end{aligned} \tag{3.37}$$

and then average over statistical fluctuations of the $\Gamma_i(\tau)$ and $\epsilon_i(\tau)$.

The computation of the Majorana correlations can be greatly simplified as follows. Notice that, for each mode i, the argument in the exponential in Equation (3.37) can be viewed as the magnitude square of the position $\vec{Z}_i$ of a particle moving in two-dimensions, or alternatively the modulus square of a complex number Z_i moving on the plane:

$$Z_i(\mathrm{T}) = \sqrt{2}\int_0^{\mathrm{T}} d\tau\ \Gamma_i(\tau)\ \mathrm{e}^{-\mathrm{i}\int_0^\tau dt\,\epsilon_i(t)}\ , \tag{3.38}$$

with

$$\langle\gamma\,(0)\,\gamma\,(T)\rangle = \prod_{\mathrm{i}} \mathrm{e}^{-|\vec{Z}_i|^2}\ . \tag{3.39}$$

Below we will argue both in the cases of fluctuating amplitudes $\Gamma_i(\tau)$ and energies $\epsilon_i(\tau)$ that the probability distribution for the "position" $\vec{Z}_i$ is Gaussian:

$$\mathrm{P}(\vec{Z}_i) = \frac{1}{2\pi\sigma_i^2(\mathrm{T})}\ \exp\left(-\frac{1}{2}\frac{|\vec{Z}_i|^2}{\sigma_i^2(\mathrm{T})}\right)\ , \tag{3.40}$$

with $\sigma_i(\mathrm{T})$ the time-dependent width of the distribution, which we will compute below for each case. With this Gaussian distribution for the $\vec{Z}_i$, we can compute the average Majorana correlation,

$$\begin{aligned}
\overline{\langle\gamma\,(0)\,\gamma\,(\mathrm{T})\rangle} &= \prod_i \int d^2Z_i\ P(\vec{Z}_i)\ e^{-|\vec{Z}_i|^2} \\
&= \prod_i \left[1+2\,\sigma_i^2(\mathrm{T})\right]^{-1} \\
&\approx \exp\left[-2\sum_i \sigma_i^2(\mathrm{T})\right]\ .
\end{aligned} \tag{3.41}$$

In the last step we assumed that there are many modes in the fermionic bath, each making a small contribution (or order inverse volume) so we may re-exponentiate the product. The examples below are studied using this expression.

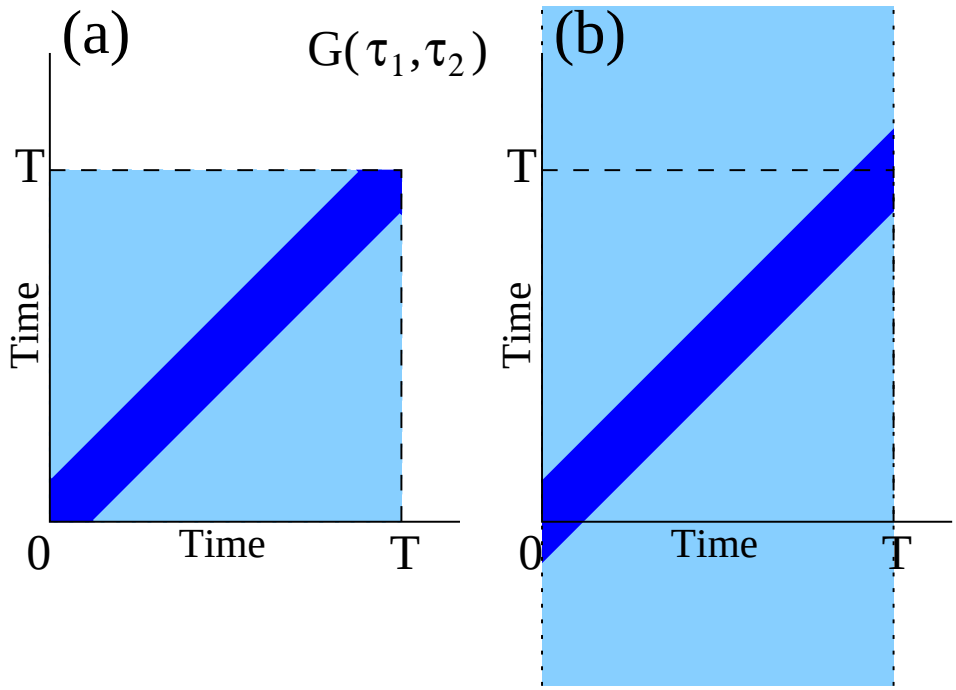

Figure 3.4: Integration Areas.
The two time correlators of the tunneling amplitude $G_\Gamma(\tau_1, \tau_2) = \langle \Gamma^*(\tau_1)\Gamma(\tau_2)\rangle$. a) The shaded region represents the actual area of integration for Equation (3.44). The darker stripe represents the area of large values for the correlator. This represents strong correlations in the tunneling amplitudes. From this we see that the majority of the integrals appearing in Equation (3.44) come from times when $\tau_1 \cong \tau_2$. b) A simplified integration area. The darkly shaded area of large correlators does not change significantly. As such geometrically we see that this should not change the values of the various correlation functions we are studying. From this it is particularly easy to derive the estimates used in Equation (3.48), in particular the linear in T scaling can now be derived by simply changing co-ordinates in the integral in Equation (3.44).

3.6.1 Fluctuating amplitudes

The fluctuations of the Γ_i are assumed to be Gaussian distributed according to

$$\mathrm{P}\left(\{\Gamma_{\mathrm{i}}(\tau),\Gamma_{\mathrm{i}}^{*}(\tau)\}\right)=\mathcal{N}^{-1}\;e^{-\frac{1}{2}\int_{-\infty}^{\infty}d\tau_1\int_{-\infty}^{\infty}d\tau_2\;\Gamma_{\mathrm{i}}^{*}(\tau_1)\;G_{\Gamma_i}^{-1}(\tau_1,\tau_2)\;\Gamma_{\mathrm{i}}(\tau_2)}\;. \tag{3.42}$$

Let us show that the distribution of the $\mathrm{P}(\vec{Z}_i)$ is Gaussian, and relate $\sigma_i(\mathrm{T})$ to the fluctuations of the Γ_i. That the distribution $\mathrm{P}(\vec{Z}_i)$ should be Gaussian is not surprising since at long times the particle is diffusing. We can write for the characteristic function distribution (Fourier transform of the probability distribution $\mathrm{P}(\vec{Z}_i)$);

$$\begin{aligned}
\tilde{P}\left(\vec{k}\right) &= \int d^2\vec{\mathrm{Z}}_i\;P(\vec{\mathrm{Z}}_i)\;e^{-i\vec{k}\cdot\vec{Z}_i}\\
&= \mathcal{N}^{-1}\int\mathcal{D}\Gamma_i\,\mathcal{D}\Gamma_i^{*}\;\;\mathrm{e}^{-\frac{1}{2}\int_{-\infty}^{\infty}d\tau_1\int_{-\infty}^{\infty}d\tau_2\;\Gamma_i^{*}(\tau_1)\;G_{\Gamma_i}^{-1}(\tau_1,\tau_2)\;\Gamma_i(\tau_2)}\\
&\qquad\qquad\times e^{-i\frac{1}{2}k^{*}\sqrt{2}\int_0^{\mathrm{T}}d\tau\;\Gamma_i(\tau)\;e^{-i\epsilon_i\tau}}\;\times e^{-i\frac{1}{2}k\sqrt{2}\int_0^{\mathrm{T}}d\tau\;\Gamma_i^{*}(\tau)\;e^{+i\epsilon_i\tau}}\\
&= \exp\left(-\frac{1}{2}\left|k\right|^2\times 2\times\int_0^{\mathrm{T}}d\tau_1\;\int_0^{\mathrm{T}}d\tau_2\;\;e^{-i\epsilon_i\tau_1}\;G_{\Gamma_i}(\tau_1,\tau_2)\;e^{+i\epsilon_i\tau_2}\right)\;.
\end{aligned} \tag{3.43}$$

Therefore, the distribution $P\left(\vec{Z}_i\right)$ is Gaussian, with a variance given by

$$\sigma_i^2(\mathrm{T})=2\int_0^{\mathrm{T}}d\tau_1\;\;\int_0^{\mathrm{T}}d\tau_2\;\;e^{-i\epsilon_i\tau_1}\;G_{\Gamma_i}(\tau_1,\tau_2)\;e^{+i\epsilon_i\tau_2}\;. \tag{3.44}$$

If the noise correlations are invariant under time-translation, then $G_{\Gamma_i}(\tau_1,\tau_2)=G_{\Gamma_i}(\tau_1-\tau_2)$. We can expand these correlations in frequency domain,

$$G_{\Gamma_i}(\tau_1-\tau_2)=\int_{-\infty}^{\infty}d\omega\;\tilde{G}_{\Gamma_i}(\omega)\;e^{-i\omega(\tau_1-\tau_2)}. \tag{3.45}$$

We proceed to compute $\sigma_i^2(\mathrm{T})$ in Equation (3.44) for two distinct cases of low and of high frequency noise.

Case I: Low-frequency noise

In this case, we shall assume that all frequencies ω for which $\tilde{G}_{\Gamma_i}(\omega)$ has significant weight fall below the fermionic energies ϵ_i. It the follows that

$$\begin{aligned} \sigma_i^2(\mathrm{T}) &= 2\int_{|\omega|\ll\tilde{\epsilon}} d\omega \sum_i \frac{1-\cos[(\epsilon_i+\omega)T]}{(\epsilon_i+\omega)^2}\,\tilde{G}_{\Gamma_i}(\omega) \\ &\approx 2\sum_i \frac{1}{\epsilon_i^2}\int_{|\omega|\ll\tilde{\epsilon}} d\omega\,\tilde{G}_{\Gamma_i}(\omega)\,. \end{aligned} \tag{3.46}$$

We thus arrive at a correlation decay, for the Majorana modes, of the form

$$\overline{\langle\gamma\,(0)\,\gamma\,(\mathrm{T})\rangle} \approx \exp\left[-4\sum_i \frac{1}{\epsilon_i^2}\int_{|\omega|\ll\tilde{\epsilon}} d\omega\,\tilde{G}_{\Gamma_i}(\omega)\right]. \tag{3.47}$$

The coefficient in the exponent depends on the spectral weight of the noise. From Parceval's theorem, $\int_{-\infty}^{\infty} d\omega\,\tilde{G}_{\Gamma_i}(\omega) = \overline{|\Gamma_i(t)|^2}$, so the prefactor depends on the intensity of fluctuations of the couplings $\Gamma_i(t)$ in time. When the fluctuations are large, for example when the $\Gamma_i(t)$ are tied to thermally induced vibrations in two dimensional systems, there is large decoherence.

We remark that even in the cases when $\sigma_i^2(\mathrm{T}\to\infty)$ is bounded, the value may be rather large, and the Majorana correlation is *exponential* in this value. Therefore keeping the error to within reasonable bounds for quantum error correction to be applicable can be a tall order. In this sense, the Majorana qubit is not necessarily any more robust than other proposed qubit platforms.

Case II: High-frequency noise

In this case we compute $\sigma_i^2(\mathrm{T})$ assuming that the correlations $G_{\Gamma_i}(\tau_1-\tau_2)$ decay in time, so one can break the $\tau_{1,2}$ integrals into center of mass: $(\tau_1+\tau_2)/2$ and relative coordinates

$\tau_1 - \tau_2$ integrals, and in the limit of large T one has

$$\sigma_i^2(\mathrm{T}) \xrightarrow[\mathrm{T\ large}]{} 2\mathrm{T}\ \tilde{G}_\Gamma(\epsilon_i)\ , \tag{3.48}$$

where $\tilde{G}_\Gamma(\epsilon_i)$ is the Fourier transform of $\mathrm{G}_\Gamma(\tau)$ at frequency ϵ_i. We further clarify this in Fig. (3.4).

We thus arrive at a correlation decay, for the Majorana modes, of the form

$$\overline{\langle \gamma\,(0)\,\gamma\,(\mathrm{T})\rangle} \ \approx\ \exp\left[-4\,\mathrm{T}\sum_i \tilde{G}_\Gamma(\epsilon_i)\right]\ . \tag{3.49}$$

Notice that this expression has meaning only if the $\tilde{G}_\Gamma(\omega)$ has spectral weight above the gap $\tilde{\epsilon}$. If not, one has to treat the problem in the low frequency limit discussed above.

Non zero expectation values

One can generalize this result for when the Γ_i fluctuations are centered around a non-zero value Γ_i^0. In this case,

$$P(\vec{Z}_i) = \frac{1}{2\pi\sigma_i^2(\mathrm{T})}\ \exp\left(-\frac{1}{2}\frac{|\vec{Z}_i - \vec{Z}_i^0(\mathrm{T})|^2}{\sigma_i^2(\mathrm{T})}\right)\ \ , \tag{3.50}$$

where

$$Z_i^0(\mathrm{T}) = \sqrt{2}\Gamma_i^0\ \int_0^{\mathrm{T}} d\tau\ e^{-i\epsilon_i\tau} = \sqrt{2}i\,\Gamma_i^0\ \frac{e^{-i\epsilon_i\mathrm{T}}-1}{\epsilon_i}\ \ , \tag{3.51}$$

which lead to

$$\overline{\langle \gamma\,(0)\,\gamma\,(\mathrm{T})\rangle} \ =\ \prod_i \frac{e^{-\frac{|Z_i^0(\mathrm{T})|^2}{1+2\sigma_i(\mathrm{T})}}}{1+2\sigma_i(\mathrm{T})}\ . \tag{3.52}$$

Notice that we recover the static result Equation (3.32) of the previous section if there is no disorder $[\sigma_i(\mathrm{T}) = 0]$. Indeed we see that $\langle \gamma\,(0)\,\gamma\,(\mathrm{T})\rangle = \prod_i e^{-|Z_i^0(\mathrm{T})|^2}$.

In the particular case of high-frequency noise (non-zero $G_{\Gamma_i}(\epsilon_i)$), one obtains in the

large T limit one obtains

$$\overline{\langle \gamma(0)\,\gamma(\mathrm{T})\rangle} \xrightarrow[\mathrm{T\ large}]{} \prod_i \left[1 + 4T\widetilde{G}_\Gamma(\epsilon_i)\right]^{-1}, \tag{3.53}$$

which agrees with the case where the fluctuations are centered around zero shown in Equation (3.49).

Cross correlations of fluctuations

We would now like to extend our model to include cross correlations of fluctuations between the modes. Once again we focus on a Hamiltonian of the form $H_{\mathrm{Mean}} = \gamma \sum_{i=1}^{N} \left(\Gamma_i c_i - \Gamma_i^* c_i^\dagger\right) + \sum_{i=1}^{N} \epsilon_i c_i^\dagger c_i$. Here γ is a single Majorana mode and c_i , $c_i^\dagger$ are regular fermion creation and annihilation operators. In our model we will allow for Gaussian classical dynamics for the coupling constants Γ_i with possible cross correlations between the couplings. More precisely, we will assume that the probability distribution of couplings may be written as:

$$\begin{aligned} \mathrm{P}\left(\{\Gamma_{\mathrm{i}}(\tau), \Gamma_{\mathrm{i}}^*(\tau)\}\right) &= \mathcal{Z}^{-1} \int\int \mathcal{D}\left\{\Gamma_i^*(\tau), \Gamma_i(\tau)\right\} \times \\ &\times \exp\left(\frac{-1}{2}\int_{-\infty}^{\infty}\int_{-\infty}^{\infty} d\tau_1 d\tau_2 \sum_{i,j} G_{i,j}^{-1}(\tau_1,\tau_2)\,\Gamma_i^*(\tau_1)\,\Gamma_j(\tau_2)\right) \end{aligned} \tag{3.54}$$

Next we introduce the $\vec{\mathcal{Z}} \equiv (\mathcal{Z}_1, ...\mathcal{Z}_N) \in \mathbb{C}^N$ with $\mathcal{Z}_i(\mathrm{T}) = \sqrt{2}\int_0^{\mathrm{T}} d\tau\ \Gamma_i(\tau)\ \mathrm{e}^{-\mathrm{i}\int_0^\tau dt\,\epsilon_i(t)}$. With this notation we may write that:

$$\langle \gamma(0)\,\gamma(T)\rangle = e^{-\vec{\mathcal{Z}}^\dagger \vec{\mathcal{Z}}} \tag{3.55}$$

Which is just a rewriting of Equation (3.39). Next following Equation (3.43) we may

write that:

$$\begin{aligned}
\tilde{P}\left(\vec{\mathcal{K}}\right) &= \int d^2\mathcal{Z}_1 \int d^2\mathcal{Z}_2 \int d^2\mathcal{Z}_3 .... \int d^2\mathcal{Z}_N \; P(\vec{\mathcal{Z}})\, e^{\frac{-i}{2}\left(\vec{\mathcal{Z}}^\dagger \vec{\mathcal{K}} + \vec{\mathcal{K}}^\dagger \vec{\mathcal{Z}}\right)} \\
&= \mathcal{N}^{-1} \int \mathcal{D}\Gamma_i \, \mathcal{D}\Gamma_i^* \;\; \mathrm{e}^{-\frac{1}{2}\int_{-\infty}^{\infty} d\tau_1 \int_{-\infty}^{\infty} d\tau_2 \; \Gamma_i^*(\tau_1)\, G_{ij}^{-1}(\tau_1,\tau_2)\, \Gamma_j(\tau_2)} \\
&\qquad \times e^{-i\frac{1}{2}\sqrt{2}\sum_i \mathcal{K}_i^* \int_0^{\mathrm{T}} d\tau \; \Gamma_i(\tau)\, e^{-i\epsilon_i \tau}} \;\; \times e^{-i\frac{1}{2}\sqrt{2}\sum_i \mathcal{K}_i \int_0^{\mathrm{T}} \int_0^{\mathrm{T}} d\tau \; \Gamma_i^*(\tau)\, e^{+i\epsilon_i \tau}} \\
&= \exp\left(-\frac{1}{2} \times 2 \times \sum_{i,j} \mathcal{K}_i^* \mathcal{K}_j \int_0^{\mathrm{T}} d\tau_1 \;\; \int_0^{\mathrm{T}} d\tau_2 \;\; e^{-i\epsilon_i \tau_1} \; G_{ij}(\tau_1,\tau_2) \; e^{+i\epsilon_j \tau_2} \right) . \quad (3.56)
\end{aligned}$$

From this equation we see that the distribution $P\left(\vec{\mathcal{Z}}\right)$ is a Gaussian with a covariance matrix $\boldsymbol{\sigma}\left(\mathrm{T}\right)$ given by:

$$\boldsymbol{\sigma_{ij}}\left(\mathrm{T}\right) \equiv 2 \int_0^{\mathrm{T}} d\tau_1 \;\; \int_0^{\mathrm{T}} d\tau_2 \;\; e^{-i\epsilon_i \tau_1} \; G_{ij}(\tau_1,\tau_2) \; e^{+i\epsilon_j \tau_2} \quad (3.57)$$

Combining and simplifying we may write that:

$$\left\langle \gamma\left(0\right) \gamma\left(\mathrm{T}\right) \right\rangle = \frac{1}{\det\left(\mathbb{I} + 2\boldsymbol{\sigma}\left(\mathrm{T}\right)\right)} \quad (3.58)$$

Here $\mathbb{I}$ is the identity matrix ($\mathbb{I}_{ij} = \delta_{ij}$). We can also generalize to the case where the couplings have a non-zero expectation value, $\Gamma_i = \Gamma_i^0 + \delta\Gamma_i$, with the $\delta\Gamma_i$ having a probability distribution given by Equation (3.54). In this case, we obtain:

$$\left\langle \gamma\left(0\right) \gamma\left(\mathrm{T}\right) \right\rangle = \frac{\exp\left(-\vec{\mathcal{Z}}_0^\dagger\left(\mathrm{T}\right) \left(\mathbb{I} + 2\boldsymbol{\sigma}\left(\mathrm{T}\right)\right)^{-1} \vec{\mathcal{Z}}_0\left(\mathrm{T}\right) \right)}{\det\left(\mathbb{I} + 2\boldsymbol{\sigma}\left(\mathrm{T}\right)\right)} \quad (3.59)$$

Here, similarly to Section 3.6.1, we have introduced the vector $\vec{\mathcal{Z}}_0$ whose i'th component is given by: $\mathcal{Z}_{0,i}\left(\mathrm{T}\right) = \sqrt{2} i \, \Gamma_i^0 \, \frac{e^{-i\epsilon_i \mathrm{T}} - 1}{\epsilon_i}$.

3.6.2 Fluctuating energies

Let us consider the case where the energies undergo Gaussian fluctuations in time, around some average value: $\epsilon_{\rm i}(\tau) = \epsilon_{\rm i} + \delta\epsilon_{\rm i}(\tau)$ with $\langle \delta\epsilon_i(\tau_1)\,\delta\epsilon_i(\tau_2)\rangle = G_i(\tau_1,\,\tau_2)$. Let $\varphi(\tau) \equiv \int_0^\tau dt\ \delta\epsilon_i(t)$. If the $\delta\epsilon_i(\tau)$ are short-time correlated the quantity:

$$\overline{[\varphi(\tau_1) - \varphi(\tau_2)]^2} \equiv G_\varphi^2(\tau_1 - \tau_2) \tag{3.60}$$

will grow linearly in $|\tau_1 - \tau_2|$. We note that the phases $\varphi_i(\tau)$ execute random walks in this case.

The magnitude square of the "position" of the Z_i has average

$$\begin{aligned}
\overline{|Z_i({\rm T})|^2} &= 2\ \ |\Gamma_i|^2 \int_0^{\rm T} d\tau_+ \int_0^{\rm T} d\tau_-\ \ e^{+i\epsilon_i\tau_+}\ \overline{e^{+i[\varphi(\tau_+)-\varphi(\tau_-)]}}\ e^{-i\epsilon_i\tau_-} \\
&= 2\ \ |\Gamma_i|^2 \int_0^{\rm T} d\tau_+ \int_0^{\rm T} d\tau_-\ \ e^{+i\epsilon_i\tau_+}\ e^{-\frac{1}{2}G_\varphi^2(\tau_+-\tau_-)}\ e^{-i\epsilon_i\tau_-}\ .
\end{aligned} \tag{3.61}$$

The calculation of higher moments is quite similar if the term ${\rm e}^{{\rm G}_\varphi(\tau_+-\tau_-)}$ confines the two times to be close to each other.

$$\begin{aligned}
\overline{|Z_i({\rm T})|^{2n}} &= 2^n|\Gamma_i|^{2n} \int_0^{\rm T} {\rm d}\tau_1^+ \ \ldots \int_0^{\rm T} {\rm d}\tau_{\rm n}^+ \int_0^{\rm T} {\rm d}\tau_1^- \ \ldots \int_0^{\rm T} {\rm d}\tau_{\rm n}^- \times \\
&\times\ \ \overline{e^{i\sum_j \varphi(\tau_j^+) - i\sum_j \varphi(\tau_j^-)]}}\ \ {\rm e}^{-i\epsilon_i \sum_j \tau_j^-} \\
&= 2^n|\Gamma_i|^{2n} \int_0^{\rm T} {\rm d}\tau_1^+ \ \ldots \int_0^{\rm T} {\rm d}\tau_{\rm n}^+ \int_0^{\rm T} {\rm d}\tau_1^- \ \ldots \int_0^{\rm T} {\rm d}\tau_{\rm n}^-\ \ e^{i\epsilon_i \sum_j \tau_j^+} \times {\rm e}^{-i\epsilon_i \sum_j \tau_j^-} \\
&\times\ \ \exp\left[-\frac{1}{2}\int_0^{\tau_1^+} du_1 .. \int_0^{\tau_n^+} du_n \int_0^{\tau_1^-} dv_1 .. \int_0^{\tau_n^-} dv_n \times\right. \\
&\times\ \ \left.\sum_{i=1}^{n} \{G(u_i,\,u_j) + G(v_i,\,v_j) - G(u_i,\,v_j) - G(v_i,\,u_j)\}\right] \\
&\cong\ \ 2^n\,|\Gamma_i|^{2n}\ n!\ \left(\int_0^{\rm T} d\tau_+ \int_0^{\rm T} d\tau_-\ \ e^{+i\epsilon_i\tau_+}\ e^{-\frac{1}{2}G_\varphi^2(\tau_+-\tau_-)}\ e^{-i\epsilon_i\tau_-}\right)^n \\
&=\ \ n!\ \left(\overline{|Z_i({\rm T})|^2}\right)^n .
\end{aligned} \tag{3.62}$$

For the second equality we have used the fact that the process is Gaussian. In this way we mapped the problem to the partition function of a two species Coulomb like gas. Then in the fourth line we have used a dipole approximation for the partition function. We note that this is consistent with the confining assumption as $\int_{\tau_1}^{\tau_2}\int_{\tau_1}^{\tau_2} dudvG\left(u,v\right) \propto |\tau_1-\tau_2|$ so that we have a confining linear potential between oppositely charged particles of our Coulomb gas.

We now claim that Z_i will execute diffusion because of the random phases. Indeed, these correlation functions are the moments of a Gaussian distribution with variance $\overline{|Z_i\left(\mathrm{T}\right)|^2}$. This variance can often be computed in the high-frequency case (similarly to Section 3.6.1) and for large T one can approximate

$$\overline{|Z_i(\mathrm{T})|^2} \xrightarrow[\mathrm{T\ large}]{} 2\mathrm{T}\ |\Gamma_i|^2 \int_{-\infty}^{\infty} d\tau\ \ e^{+i\epsilon_i\tau}\ e^{-\frac{1}{2}G_\varphi^2(\tau)} \ \equiv \mathrm{T}\Theta_i\ , \tag{3.63}$$

and the probability distribution is given by $\mathrm{P}\left(Z_i\left(\mathrm{T}\right)\right) \cong \frac{1}{2\pi\Theta_i^2(\mathrm{T})}\ \exp\left(-\frac{1}{2}\frac{|Z_i(\mathrm{T}))|^2}{\mathrm{T}\Theta_i^2(\mathrm{T})}\right)$. Repeating the analysis of Section 3.6.1, we get a power law decay (for each mode i) for the coherence of Majorana qubit, with a coefficient that is dependent on the Fourier transform of the exponential of the $G_\varphi^2(\tau)$ correlation function:

$$\begin{aligned}\overline{\langle\gamma\left(0\right)\gamma\left(\mathrm{T}\right)\rangle} &= \prod_{\mathrm{i}}\left[1+4\,\mathrm{T}\ |\Gamma_i|^2 \int_{-\infty}^{\infty} d\tau\ \ e^{+i\epsilon_i\tau}\ e^{-\frac{1}{2}G_\varphi^2(\tau)}\right]^{-1} \\ &\approx \exp\left[-4\,\mathrm{T}\sum_i |\Gamma_i|^2 \int_{-\infty}^{\infty} d\tau\ \ e^{+i\epsilon_i\tau}\ e^{-\frac{1}{2}G_\varphi^2(\tau)}\right]\ .\end{aligned} \tag{3.64}$$

For $G_\varphi^2(\tau) \propto |\tau|$, the Fourier transform of $e^{-\frac{1}{2}G_\varphi^2(\tau)}$ will decay as a power law in frequency. We would like to point out that if the $\epsilon_{\mathrm{i}}(\tau)$ have a correlation time $\tau_\Omega = \Omega^{-1}$, the short-time behavior of $G_\varphi^2(\tau)$ is smoothened, and the kink-singularity of at $\tau = 0$ disappears, while the long-time behavior $|\tau|$ remains the same. Using general results on Fourier transforms [106] we know that the Fourier transform of $e^{-\frac{1}{2}G_\varphi^2(\tau)}$ will decay faster than any power of frequency ω when $\omega \gg \Omega$. This indicates a good level of protection

for systems with large gaps compared to the bandwidth of the noise source.

3.6.3 Telegraph noise fluctuations of coupling amplitudes

Here we shall study classical telegraphic noise. Our model for telegraphic noise will be a $\Gamma_i(\tau)$ that switches between $\pm\Lambda_i$ with time intervals between events that are distributed randomly with characteristic frequency Ω_i^{-1}. The complex number $Z_i(\mathrm{T})$ will again perform a random walk at long times, which we will confirm by computing the moments of $|Z_i(\mathrm{T})|^2$. Let us start by computing the second moment:

$$\overline{|\mathrm{Z_i(T)}|^2} \;\; = 2 \;\; \int_0^{\mathrm{T}} d\tau_+ \int_0^{\mathrm{T}} d\tau_- \;\; e^{+i\epsilon_i\tau_+} \; \overline{\Gamma_i(\tau_+)\,\Gamma_i(\tau_-)} \; e^{-i\epsilon_i\tau_-} \; . \tag{3.65}$$

Now, $|\mathrm{Z_i(T)}|^2 \;=\; 2\Lambda_i^2 \;\; (-1)^{N_{\mathrm{flips}}(\tau_-,\tau_+)}$, where $N_{\mathrm{flips}}(\tau_-,\tau_+)$ is the number of switches between the two times $\tau_\pm$. The average

$$\begin{aligned} \overline{(-1)^{N_{\mathrm{flips}}(\tau_-,\tau_+)}} \;\; &= \;\; \sum_{N=0}^{\infty} (-1)^N \; \frac{1}{N!} \, (\Omega_i \, |\tau_+ - \tau_-|)^N \;\; e^{-\Omega_i \, |\tau_+ - \tau_-|} \\ &= \;\; e^{-2\,\Omega_i \, |\tau_+ - \tau_-|} \; , \end{aligned} \tag{3.66}$$

so we obtain

$$\overline{|\mathrm{Z_i(T)}|^2} \xrightarrow[\mathrm{T\ large}]{} 2\mathrm{T} \; \Lambda_i^2 \; \frac{4\,\Omega_i}{(2\,\Omega_i)^2 + \epsilon_i^2} \; . \tag{3.67}$$

In the appendix we compute the higher moments and show that the distribution of $Z_i(\mathrm{T})$ approaches a Gaussian, as intuitively expected from the fact that the telegraph noise causes the fictitious particle position to diffuse at times larger compared to the switching time. We obtain, similarly to the previous cases discussed above, that

$$\begin{aligned} \overline{\langle \gamma\,(0)\,\gamma\,(\mathrm{T}) \rangle} \;\; &= \;\; \prod_{\mathrm{i}} \left[1 + 2\mathrm{T} \; \Lambda_i^2 \; \frac{4\,\Omega_i}{(2\,\Omega_i)^2 + \epsilon_i^2} \right]^{-1} \\ &\approx \;\; \exp\left[-2\mathrm{T} \; \sum_i \; \Lambda_i^2 \; \frac{4\,\Omega_i}{(2\,\Omega_i)^2 + \epsilon_i^2} \right] \; . \end{aligned} \tag{3.68}$$

In the last line we assumed that there are many relevant fluctuating levels each making a small contribution so that we are able to re-exponentiate. From this we see that due to the effects of telegraph noise the information stored in the Majorana qubit is lost on a time scale $\sim \tau_{\rm typ}/\sum_i \frac{|\Lambda_i|^2}{\epsilon_i^2}$. Here $\tau_{\rm typ} \sim \Omega^{-1}$ is the typical switching rate for the regular fermion modes. This is an exponential decay of Majorana coherence with the rate given by a rational function of the the coupling strengths and frequencies of the switching. This leads to short lifetimes of Majorana modes. We would like to note that the power law term comes from the instantaneous switching process. For a finite switching speed and as such a smooth $\langle \Gamma(\tau)\Gamma(v)\rangle$ the Fourier transform in Equation (3.68) would decay faster then any rational function of ϵ_i for large ϵ_i (as compared to the inverse switching time) [106].

3.7 Conclusions

In this chapter we have studied the stability of qubits constructed from Majorana zero modes, for example using an encoding such as $\sigma^z = i\gamma_1\gamma_2$. The persistence of memory can be measured from two-time correlations such as $\langle \sigma^z(0)\sigma^z(\mathrm{T})\rangle$, which we have shown is independent of the particular state of the qubit. We have shown that the if the environments coupling to each Majorana mode are uncorrelated, then the qubit overlap function factorizes: $\langle \sigma^z(0)\sigma^z(\mathrm{T})\rangle = \langle \gamma_1(0)\gamma_1(\mathrm{T})\rangle \langle \gamma_2(0)\gamma_2(\mathrm{T})\rangle$. We then analyzed, in detail, the decay of the Majorana two-point function $\langle \gamma(0)\gamma(\mathrm{T})\rangle$, when the Majoranas couple via tunneling to fermions in a bath. We considered only baths where the fermions had a gapped single particle spectrum (gapless baths would trivially destroy coherence). We considered both cases where the tunneling amplitudes were static, and cases where they were dynamical, fluctuating either classically or quantum mechanically, say mediated by a boson bath. Some of the more technical details of the quantum mechanical fluctuations have been relegated to Appendix B.

Static tunnelings are, expectantly, not consequential leading to finite decay. Though

this serves as a way to check our generic formalism. More precisely if the fermions in the bath are non-interacting and if the tunnelings are just switched on but then kept constant thereafter, then the Majorana qubits only experience a finite depletion which we checked by explicitly rediagonalizing the non-interacting fermionic Hamiltonian with the new couplings. This result can be easily interpreted as a finite adjustment in the overlap of the qubit before and after the basis changes upon switching the tunnelings. Similarly for a zero temperature quantum environment there is no long term decay for the coherence of Majorana fermions, merely a finite depletion of the correlator $\langle \gamma(0)\,\gamma(T)\rangle$.

However, dynamic fluctuations of the tunneling amplitudes can have very serious consequences. Our analysis makes it clear that the dephasing of the Majorana correlations is tied hand-in-hand to fluctuations (spectral functions) of both the fermionic bath and the noise. In some instances, for example in the case of athermal telegraphic noise, fluctuations can destroy the Majorana memories, leading to complete decay of coherence at long times. We analyzed several types of noise in the bath, both classical and quantum. To understand the rate of information loss in experimentally relevant systems it is important to study various materials, relevant sources of noise and in general realistic spectral functions of the bath. The formalism here presented forms the basis for such analysis.

4 Exact zero modes

4.1 Introduction

In this chapter we show that for closed finite sized systems with an odd number of real fermionic modes, even in the presence of many-body interactions, there are always at least two fermionic operators that commute with the Hamiltonian. There is a zero mode corresponding to the total Majorana operator, as shown by Akhmerov [1], as well as additional linearly independent zero modes, one of which 1) is continuously connected to the Majorana mode solution in the non-interacting limit, and 2) is less prone to decoherence when the system is opened to contact with an infinite bath. We also show that in the idealized situation where there are two or more well separated zero modes each associated with a finite number of interacting fermions at a localized vortex, these modes have non-Abelian Ising statistics under braiding. Furthermore the algebra of the zero mode operators makes them useful for fermionic quantum computation [107].

4.2 Overview

Zero modes in non-interacting systems, *i.e.* eigenstates annihilated by a single-particle Hamiltonian, have a long history in physics and in mathematics. Zero energy states are associated to certain types of topological defects in the background fields in which electrons or quasiparticles propagate. The first example of such modes in physics appeared in the seminal work of Jackiw and Rebbi [108] in one-dimensional and three-dimensional

systems, where the topological defects were domain walls and hedgehogs, respectively. In both these examples the physical consequence of the zero modes is the fractionalization of electron charge. Fractional charges can also be bound to vortices in a Kékule dimerization pattern in two-dimensional graphene-like systems [109]. The zero mode solutions in two-dimensions were first found by Jackiw and Rossi [110] in the study of Dirac fermions in the background of scalar and vector gauge fields of the Abelian Higgs model. In the condensed matter context this corresponds to a superconductor (where charge cannot be fractionalized, since it is not conserved). The number of zero modes in such system of Dirac fermions in two-dimensions equals the magnitude of the net vorticity independent of the details of the profile of the Higgs fields, a result that was shown by Weinberg [111] to be tied to the index theorem.

A modern example of a physical realization of the model in Reference [110] was presented by Fu and Kane [112], who showed that a Dirac-type matrix equation governs surface excitations in a topological insulator in contact with an s-wave superconductor. A vortex in the superconducting order parameter leads to a zero mode solution. Because of the reality conditions imposed by the symmetries of the Bogoliubov-de Gennes (BdG) equations describing the superconductor within the mean-field approximation, the zero energy solutions correspond to Majorana zero modes, which are the focus of our study. Majorana fermions are self-adjoint operators γ_i which can be written as a sum of an annihilation and creation operator for one fermion mode and which satisfy the algebra:

$$\{\gamma_i, \gamma_j\} = 2\delta_{ij}, \gamma_i^\dagger = \gamma_i. \tag{4.1}$$

Because they are zero modes of some mean field Hamiltonian, $[H_{\mathrm{MF}}, \gamma_i] = 0$, these modes are in principle protected from decoherence as the mean field Hamiltonian, when restricted to the subspace generated by these modes, is zero as we observed in Chapter 3. Recently it has been argued that quantum and classical fluctuations in open infinite

systems (for example when the system is in contact to a bath) lead to decoherence of information stored in such modes [113] and also the discussion in Chapter 3. Below, instead, we shall focus on closed, finite systems, which have markedly different properties from those coupled to an infinite environment.

The purpose of this letter is to study zero modes of interacting many-body fermionic Hamiltonians, beyond mean-field approximations. We will assume that the relevant degrees of freedom may be described by an odd number of Majorana fermions, say $2N+1$ of them: $\{\gamma_1, \gamma_2, \ldots, \gamma_{2N+1}\}$.

This formalism also handles the case when complex fermions are present, as we may change basis from complex to Majorana fermions:

$$c_j = \frac{1}{2}\left(\gamma_{2j} + i\gamma_{2j+1}\right), \; c_j^\dagger = \frac{1}{2}\left(\gamma_{2j} - i\gamma_{2j+1}\right). \tag{4.2}$$

For an interacting many-body Hamiltonian, a zero mode means a Hermitian fermionic operator

$$\mathcal{O} = \sum_i \alpha_i \; \gamma_i + i \sum_{i,j,k} \beta_{i,j,k} \; \gamma_i \gamma_j \gamma_k + \ldots \; , \tag{4.3}$$

written as a multinomial with sums and products of γ_i's, that commutes with the Hamiltonian, $[H, \mathcal{O}] = 0$. For any such operator, $\mathcal{O}$, $\exp\left(itH\right)\mathcal{O}\exp\left(-itH\right) = \mathcal{O}$ for all times t. As such there is no decoherence of the information stored in the correlators of such operators.

We will find below, for systems of interacting fermions, 2^N linearly independent solutions of the form given in Equation (4.3). We will also extend our results to the case when interactions include bosonic modes (with finite dimensional Hilbert space) coupled to the Majorana modes.

4.3 Derivation

4.3.1 Quadratic Hamiltonians

Let us start, as a warm up, with the simplest case where $H^{\text{Gauss}} = i \sum_{i,j} h_{i,j}\ \gamma_i \gamma_j$ with $h_{i,j} = -h_{j,i}$ and $h_{i,j}$ real. We note that any quadratic Hamiltonian may be written in this manner. Generic eigenoperator solutions satisfying $\left[H^{\text{Gauss}}, \mathcal{O}_\lambda\right] = \lambda\, \mathcal{O}_\lambda$ are obtained by computing the commutators for operators of the form $\mathcal{O} = \sum_i \alpha_i \gamma_i$ using the relations Equation (4.1), and matching the coefficients multiplying each operator γ_i on both sides of the equation. One arrives in this manner at an eigenvalue equation for the matrix

$$\mathcal{H}^{\text{Gauss}} = 4i \begin{pmatrix} 0 & h_{1,2} & h_{1,3} & \cdots & h_{1,2N+1} \\ h_{2,1} & 0 & \ddots & & \vdots \\ h_{3,1} & \ddots & 0 & & \vdots \\ \vdots & & & \ddots & h_{2N,2N+1} \\ h_{2N+1,1} & \cdots & \cdots & h_{2N+1,2N} & 0 \end{pmatrix}. \tag{4.4}$$

The elements of the matrices $\mathcal{H}^{\text{Gauss}}$ and h are closely related because the theory is Gaussian – there will be modifications in the case of interacting systems. Note that $\mathcal{H}^{\text{Gauss}}$ is an odd-dimensional Hermitian antisymmetric matrix so it has an eigenvector with zero eigenvalue and real components $(\alpha_1, \alpha_2, \ldots, \alpha_{2N+1})$ which corresponds to the zero mode $\mathcal{O} = \sum_i \alpha_i \gamma_i$. Notice that it follows from the relations in Equation (4.1) that $\mathcal{O}^\dagger = \mathcal{O}$ and $\mathcal{O}^2 = \sum_i \alpha_i^2 \times 1$.

Let us now introduce notation so as to arrive at the same $\mathcal{H}^{\text{Gauss}}$ in a way that will be similar to the calculations for interacting systems below. Matching the coefficients multiplying each operator γ_i on both sides of the equation $\left[H^{\text{Gauss}}, \mathcal{O}_\lambda\right] = \lambda\, \mathcal{O}_\lambda$ can be achieved easily if we think of the γ_i as basis vectors and define an inner product for

operators A and B as $(A, B) \equiv \text{Coeff}_1(A^\dagger B)$, where

$$\text{Coeff}_1 \left(z \times 1 + \sum_i \alpha_i \, \gamma_i + \sum_{i,j} \beta_{i,j} \, \gamma_i \gamma_j + \dots \right) \equiv z, \tag{4.5}$$

i.e., the function $\text{Coeff}_1(\mathcal{Q})$ returns the coefficient proportional to the identity in the multinomial expansion of the operator $\mathcal{Q}$. One can check that the inner product is Hermitian, $(A, B) = (B, A)^*$ and it follows from the algebra of the γ_i's that the inner product gives $(\gamma_i, \gamma_j) = \delta_{i,j}$.

Armed with this inner product we then compute the matrix

$$\begin{aligned} \mathcal{H}_{ij}^{\text{Gauss}} &= \left(\gamma_i, \left[H^{\text{Gauss}}, \gamma_j\right]\right) \\ &= -\left(\gamma_j, \left[H^{\text{Gauss}}, \gamma_i\right]\right) = -\mathcal{H}_{ji}^{\text{Gauss}} \, , \end{aligned} \tag{4.6}$$

where the last line follows by direct computation and the fact that $h_{i,j} = -h_{j,i} \in \mathbb{R}$. Once again $\mathcal{H}_{ji}^{\text{Gauss}}$ is given by Equation (4.4) above. We thus arrive once more at the result that zero modes can be determined from null vectors of a linear eigenvector equation for a Hermitian anti-symmetric matrix $\mathcal{H}_{ij}^{\text{Gauss}}$ (of odd dimension).

4.3.2 Quartic Hamiltonian

We will consider a Hamiltonian given by:

$$H^{\text{Quart}} = i \sum_{i,j} h_{i,j} \, \gamma_i \gamma_j + \sum_{i,j,k,l} V_{i,j,k,l} \, \gamma_i \gamma_j \gamma_k \gamma_l, \tag{4.7}$$

with $h_{i,j}$ a real and anti-symmetric matrix and $V_{i,j,k,l}$ real and antisymmetric under odd permutations of i, j, k, l (we have dropped an irrelevant constant that gives a state independent energy shift). We will look for operators that commute with H^{Quart}. We will work with a vector space that is spanned by all linearly independent Hermitian modes

obtained from products of individual Majorana fermions γ_i:

$$\begin{aligned} 0\,\gamma: &\quad 1, \\ 1\,\gamma: &\quad \gamma_1, \gamma_2, \gamma_3, \ldots, \gamma_{2N+1}, \\ 2\,\gamma'\mathrm{s}: &\quad i\gamma_1\gamma_2, i\gamma_1\gamma_3, \ldots, i\gamma_{2N}\gamma_{2N+1}, \\ 3\,\gamma'\mathrm{s}: &\quad -i\gamma_1\gamma_2\gamma_3, \ldots, -i\gamma_{2N-1}\gamma_{2N}\gamma_{2N+1}, \\ \cdots: &\quad \ldots \\ 2N+1\,\gamma'\mathrm{s}: &\quad i^{(2N+1)N}\gamma_1\gamma_2\ldots\gamma_{2N+1}\,. \end{aligned} \tag{4.8}$$

There are in total $\sum_{k=0}^{2N+1}\binom{2N+1}{k} = 2^{2N+1}$ such operators, which we will denote by Υ_a, for $a = 1, \ldots, 2^{2N+1}$. For each a we define n_a to be the number of γ's in the product Υ_a, and we let $L(a) \equiv \{i_1(a), \ldots, i_{n_a}(a)\}$ be the list of indices appearing in the product Υ_a. With this notation, one can write

$$\Upsilon_a \equiv i^{\,n_a(n_a-1)/2}\,\gamma_{i_1(a)}\gamma_{i_2(a)}\cdots\gamma_{i_{n_a}(a)}. \tag{4.9}$$

The choice of phase factor guarantees that $\Upsilon_a = \Upsilon_a^\dagger$ and $\Upsilon_a^2 = 1$. Using Equation (4.9) one verifies that, up to a phase, the product of two Υ_a's gives a third: $\Upsilon_a\,\Upsilon_b = (i)^{s(a,b)}\,\Upsilon_c$, where c satisfies $L(c) = L(a) \cup L(b) \setminus L(a) \cap L(b)$ and $s\,(a,b) \in \mathbb{N}$. Without loss of generality, we shall reserve the labels $a = 1$ and $a = 2^{2N+1}$ for the identity and the total Majorana operators: $\Upsilon_1 = 1$ and $\Upsilon_{2^{2N+1}} = i^{(2N+1)N}\gamma_1\gamma_2\ldots\gamma_{2N+1} \equiv \Upsilon_{\mathrm{Maj}}$.

We can now rewrite the Hamiltonian Equation (4.7) as

$$H^{\mathrm{Quart}} = \sum_{a|n(a)=2} h_a\,\Upsilon_a + \sum_{a|n(a)=4} V_a\,\Upsilon_a\,, \tag{4.10}$$

for some coefficients h_a , V_a defined when $n(a) = 2$ or 4, respectively, and h_a, $V_a \in \mathbb{R}$. Below we will convert H^{Quart} into an operator acting on the vector space spanned by

the Υ_a's with the action being given by the linear transformation where H^{Quart} acts by commutation: $\mathcal{O} \to \left[H^{\text{Quart}}, \mathcal{O}\right]$. As a first step we extend the inner product given in Equation (4.5) above to the space spanned by Υ_a i.e. $(A, B) \equiv \text{Coeff}_1(A^\dagger B)$. One can check that the inner product is Hermitian, $(A, B) = (B, A)^*$ and the set Υ_a forms an orthonormal basis. Furthermore, up to a multiplicative constant, we see that it is also given by the usual trace inner product:

$$(A, B) = \frac{1}{2^{2N+1}} tr\left(A^\dagger B\right). \tag{4.11}$$

Here, tr is taken over the space spanned by Υ_a. Indeed this can be checked by noting that Equation (4.11) is linear, so it is sufficient to consider only terms of the form $A = \Upsilon_a$, $B = \Upsilon_b$. There are two possibilities: 1) $\Upsilon_a = \Upsilon_b$ in which case $tr\left({\Upsilon_a}^\dagger \Upsilon_b\right) = 2^{2N+1}$ (the dimension of the vector space) 2) $\Upsilon_a \neq \Upsilon_b$, for which case $tr\left({\Upsilon_a}^\dagger \Upsilon_b\right) = 0$, and Equation (4.11) holds. We now compute the matrix elements $\mathcal{H}^{\text{Quart}}_{ab}$. Since $\left[H^{\text{Quart}}, \Upsilon_b\right]$ is an anti-Hermitian operator (or i times a Hermitian operator) all the matrix elements of $\mathcal{H}^{\text{Quart}}_{ab}$ are imaginary. Now because $\{\Upsilon_b\}$ is an orthonormal set we may compute matrix elements by taking inner products:

$$\begin{aligned} \mathcal{H}^{\text{Quart}}_{ab} &= \left(\Upsilon_a, \left[H^{\text{Quart}}, \Upsilon_b\right]\right) \\ &= \frac{1}{2^{2N+1}} tr\left(\Upsilon_a H^{\text{Quart}} \Upsilon_b - \Upsilon_a \Upsilon_b H^{\text{Quart}}\right) \\ &= -\left(\Upsilon_b, \left[H^{\text{Quart}}, \Upsilon_a\right]\right) = -\mathcal{H}^{\text{Quart}}_{ba}\ , \end{aligned} \tag{4.12}$$

so $\mathcal{H}^{\text{Quart}}_{ab}$ is antisymmetric. The equality in the last line of Equation (4.12) comes from the cyclic property of trace. Therefore we arrive at a Hermitian anti-symmetric matrix $\mathcal{H}^{\text{Quart}}$. So far, this matrix has dimension $2^{2N+1} \times 2^{2N+1}$, which is even. However, one can break this matrix into four block-diagonal pieces. First, because H^{Quart} contains only even Υ_c, that is with n_c even, sectors with opposite parity are not mixed by $\mathcal{H}^{\text{Quart}}_{ab}$, so necessarily $n_a \equiv n_b \bmod 2$. Therefore we break $\mathcal{H}^{\text{Quart}}$ into blocks acting on the

fermionic and bosonic $\{\Upsilon_a\}$, each block a $2^{2N} \times 2^{2N}$ matrix. Second, notice that both the identity and the total Majorana operator commute trivially with H^{Quart}, so they each reside in a 1×1 block. The identity is in the even sector ($n_1 = 0$) and the total Majorana operator is in the odd sector ($n_{\text{Maj}} = 2N + 1$). Therefore we have broken down $\mathcal{H}^{\text{Quart}}$ into four odd-dimensional Hermitian and anti-symmetric block matrices: there are four operators that commute with the Hamiltonian H^{Quart}, or zero mode solutions. They are, in the even block, the trivial identity $\Upsilon_1 = 1$ and the Hamiltonian H^{Quart} proper, and in the odd sector the total Majorana operator Υ_{Maj} [1] and *another non-trivial solution* $\mathcal{O} = \sum_a \alpha_a \Upsilon_a$, with α_a solutions of $\sum_b \mathcal{H}^{\text{Quart}}_{ab} \alpha_b = 0$.

4.3.3 Generic Fermionic Hamiltonians

Let us allow for arbitrarily high order interactions. That is we will consider Hamiltonians of the form

$$H^{\text{Gen}} = i \sum h_{i,j} \gamma_i \gamma_j + \sum_{i,j,k,l} V_{i,j,k,l} \gamma_i \gamma_j \gamma_k \gamma_l + i \sum_{i,j,k,l,m,n} Q_{i,j,k,l,m,n} \gamma_i \gamma_j \gamma_k \gamma_l \gamma_m \gamma_n + \dots, \tag{4.13}$$

which may also be expressed as

$$H^{\text{Gen}} = \sum_{a|n(a)=2} h_a \Upsilon_a + \sum_{a|n(a)=4} V_a \Upsilon_a + \sum_{a|n(a)=6} Q_a \Upsilon_a + \dots, \tag{4.14}$$

where h_a, V_a, $Q_a, \dots \in \mathbb{R}$. We can construct the matrix $\mathcal{H}^{\text{Gen}}$ similarly to what we did above, it is still a Hermitian antisymmetric matrix. Nothing changes in the argument, and the essence is that the Hamiltonian contains only Υ_c with even n_c, and therefore one can break $\mathcal{H}^{\text{Gen}}$ into four block diagonal pieces exactly the same way we did for quartic Hamiltonians and obtain zero modes.

4.3.4 Bosonic modes

We now partially extend our ideas to the case of an odd number of Majorana fermions coupled to some bosonic modes. Our main limitation is that in order to insure convergence, to have finite dimensional matrices only – we will "truncate" the Hilbert space of the bosonic modes to a finite number of states. More precisely we will assume that the relevant Hilbert space for the bosons is M dimensional and labeled by the states $\{|1\rangle, |2\rangle ... |M\rangle\}$ [114]. As such we may represent all boson operators by $M \times M$ Hermitian matrices. One can then write a Hamiltonian that generalizes Equation (4.14):

$$\begin{aligned} H^{\text{Gen}-\text{Bose}} &= \Theta^{M\times M} + \sum_{a|n(a)=2} h_a^{M\times M} \otimes \Upsilon_a + \\ &+ \sum_{a|n(a)=4} V_a^{M\times M} \otimes \Upsilon_a + \sum_{a|n(a)=6} Q_a^{M\times M} \otimes \Upsilon_a + \dots \\ &= \sum_{a|n(a)\text{ even}} \sum_{p=1}^{M^2} W_{a,p}\, \Upsilon_a \otimes h_p \,, \end{aligned} \tag{4.15}$$

with $\Theta^{M\times M}$, $h_a^{M\times M}$, $V_a^{M\times M}$, $Q_a^{M\times M}$ Hermitian matrices and we expanded the bosonic $M\times M$ Hermitian matrices into an orthonormal basis $\{h_1,\, h_2, ...h_{M^2}\}$, with $(h_p, h_q)_{\text{Bose}} = \delta_{pq}$. The inner product is $(A, B)_{\text{Bose}} \equiv \frac{1}{M}\, tr\left(A^\dagger B\right)$. It is not too hard to see that this is a positive definite symmetric form on the space of bosonic operators [115]. Without loss of generality, we take $h_1 = 1_{M\times M}$.

We can combine the operators in the fermionic and bosonic spaces and define $\Omega_{a,p} \equiv \Upsilon_a \otimes h_p$, with the usual tensor space inner product [115]. These states are orthonormal because $(\Omega_{a,q}, \Omega_{b,q})_{\text{total}} \equiv (\Upsilon_a, \Upsilon_b) \times (h_p, h_q)_{\text{Bose}} = \delta_{a,b}\, \delta_{p,q}$. We can also check that this is expressible as a trace: $(A, B)_{\text{total}} = \frac{1}{2^{2N+1}} \frac{1}{M} tr\, \left(A^\dagger B\right)$. Here the trace is over the total space spanned by $\Omega_{a,p}$.

Armed with these combined operators, we can show that there is an exact zero mode

in exactly the same way we have done in the previous case. We need the matrix:

$$\begin{aligned} \mathcal{H}^{\text{Gen}-\text{Bose}}_{a,p;b,q} &= \left(\Omega_{a,p}, \left[H^{\text{Gen}-\text{Bose}}, \Omega_{b,q}\right]\right) \\ &= -\left(\Omega_{b,q}, \left[H^{\text{Gen}-\text{Bose}}, \Omega_{a,p}\right]\right) = -\mathcal{H}^{\text{Gen}-\text{Bose}}_{b,q;a,p} \ , \end{aligned} \tag{4.16}$$

which is Hermitian and anti-symmetric. The last equality in Equation (4.16) can be checked similarly to Equation (4.12). We then break $\mathcal{H}^{\text{Gen}-\text{Bose}}_{a,p;b,q}$ into even and odd block diagonal spaces, as before. In this way, we find two zero modes in the even sector, $\Upsilon_1 \otimes h_1 = 1 \otimes 1_{M\times M}$, and $H^{\text{Gen}-\text{Bose}}$ proper, and two zero modes in the odd sector, $\Upsilon_{\text{Maj}} \otimes 1_{M\times M}$ and *another non-trivial solution* $\mathcal{O} = \sum_{a,p} \alpha_{a,p}\, \Upsilon_a \otimes h_p$, with $\alpha_{a,p}$ solutions of $\sum_{b,q} \mathcal{H}^{\text{Quart}}_{a,p;b,q}\, \alpha_{b,q} = 0$.

4.4 Counting and structure of zero modes

Let us count all zero modes in the system. We first start with the Gaussian part of the theory, including bosons, and then later we add the interactions. Consider a Hamiltonian given by:

$$H^{\text{Gauss}} = \sum_{m=1}^{M} E_m \left|m\right\rangle \left\langle m\right| + \frac{1}{2}\sum_{j=1}^{N} \epsilon_j \ i\gamma_{2j}\gamma_{2j+1} \ . \tag{4.17}$$

(Notice that $i\gamma_{2j}\gamma_{2j+1} = 2\, c_i^\dagger c_i - 1$.) By inspection, there are $M \times 2^N$ bosonic zero modes all given by operators of the form $\mathcal{O}^{\text{Bose}}_{m,\{\theta_j\}} \equiv \left|m\right\rangle \left\langle m\right| \otimes \prod_{j=1}^{N} \left(i\gamma_{2j}\gamma_{2j+1}\right)^{\theta_j}$ with $m = 1, \ldots, M$ and $\theta_j = 0, 1$ for $j = 1, \ldots, N$. There are similarly $M\times 2^N$ fermionic zero modes, simply given by $\mathcal{O}^{\text{Fermi}}_{n,\{\theta_j\}} \equiv \mathcal{O}^{\text{Bose}}_{n,\{\theta_j\}}\ \gamma_1$. These zero modes have a nice algebraic structure: 1) they are all Hermitian, 2) an appropriate linear combination all of them square to one: $\left(\mathcal{O}^{\text{Fermi/Bose}}_{Id,\{\theta_j\}}\right)^2 = 1$, and 3) all zero modes commute: $\left[\mathcal{O}^{\text{Fermi/Bose}}_{m,\{\theta_j\}}, \mathcal{O}^{\text{Fermi/Bose}}_{m',\{\theta'_j\}}\right] = 0$. As such any one of the fermionic modes, and only one mode at a time, can be used for fermionic quantum computation [107].

Let us now show that the number of zero modes and their commutation relations do

not change in the presence of weak interactions. To do so, as a first step, consider the following family of Hamiltonians $H^{\{\delta\}} \equiv H^{\text{Gauss}} + \sum_{m,\{\theta_j\}} \delta_{m,\{\theta_j\}} \mathcal{O}^{\text{Bose}}_{m,\{\theta_j\}}$ with $\delta_{m,\{\theta_j\}} \in \mathbb{R}$, and we note that $\left\{\delta_{m,\{\theta_j\}}\right\} \in \mathbb{R}^{M\times 2^N}$. It is not to hard to see that other then for points of accidental degeneracy all zero modes of all Hamiltonians of the form $H^{\{\delta\}}$ are given by $\mathcal{O}^{\text{Fermi/Bose}}_{m,\{\theta_j\}}$. As the next step, consider zero modes of Hamiltonians given by $H^{\{\delta\},U} \equiv U^\dagger H^{\{\delta\}} U$. All the zero modes are now given by $U^\dagger \mathcal{O}^{\text{Fermi/Bose}}_{m,\{\theta_j\}} U$, and as such also satisfy conditions 1), 2), and 3) of the previous paragraph. As before, exactly one mode from the fermionic set can be used for quantum computation [107]. To complete the discussion of the counting and structure of the zero modes for interacting systems, it remains for us to show that any Hamiltonian with weak interactions can be written as a $H^{\{\delta\},U}$.

To show this, we consider the map $\mathcal{F} : U\left(M^2\times 2^{2N}\right) \oplus \mathbb{R}^{M\times 2^N} \to \mathbb{R}^{M^2\times 2^{2N}}$ given by $\mathcal{F}\left(U, \left\{\delta_{m,\{\theta_j\}}\right\}\right) = U^\dagger H^{\{\delta\}} U$. It is enough to show that the image of $U\left(M^2\times 2^{2N}\right) \oplus \mathbb{R}^{M\times 2^N}$ contains a small open neighborhood of H^{Gauss}. Indeed, as any sufficiently weakly interacting Hamiltonian can be found in a small neighborhood of a non-interacting one this would show that $U^\dagger H^{\{\delta\}} U$ is a representation of all sufficiently weakly interacting Hamiltonians. By the implicit function theorem it is enough to show that $d\mathcal{F}$ is a surjective mapping onto $\mathbb{R}^{M^2\times 2^{2N}}$. Now writing $U = e^{-i\widetilde{H}}$ we get $d\mathcal{F}\left(\widetilde{H}, \left\{\delta_{m,\{\theta_j\}}\right\}\right) = i\left[\widetilde{H},\, H^{\text{Gauss}}\right] + \sum_{m,\{\theta_j\}} \delta_{m,\{\theta_j\}} \mathcal{O}^{\text{Bose}}_{m,\{\theta_j\}}$. From this we see that all the zero modes are explicitly in the image of $d\mathcal{F}$. Since the transformation $* \to i\left[*,\, H^{Gauss}_{\{n\},\{\gamma_j\}}\right]$ is an invertible linear operator when restricted to the space of all non-zero modes, all non-zero modes are also in the image of $d\mathcal{F}$ as well. As such all of $\mathbb{R}^{M^2\times 2^{2N}}$ is in the image of $d\mathcal{F}$. This shows that up to conjugation by a unitary transformation the structure of the zero modes is the same as in the non-interacting case completing the proof.

4.5 Comparison with previous work

In Reference [1], the fermion parity operator Υ_{Maj} was discussed. This Majorana operator commutes with *any* Hamiltonian, since it is formed by the product of *all* the operators γ_i. This operator sits on its own 1×1 block of the matrix $\mathcal{H}$, for all cases studied, including in our generalization that includes bosons interacting with the fermionic modes.

In contrast, the other zero mode solutions found in the larger odd-dimensional block of $\mathcal{H}$ *do* depend on the form of the Hamiltonian. There are $M \times 2^N - 1$ of them. Furthermore one of the modes has a particularly simple structure $\mathcal{O} = e^{i\widetilde{H}} \sum_i \alpha_i \gamma_i \, e^{-i\widetilde{H}}$ which is continuously connected to the non interacting mode (consider $\mathcal{O}_t = e^{it\widetilde{H}} \sum_i \alpha_i \gamma_i \, e^{-it\widetilde{H}}$). This mode is different from the fermion parity mode [1] and, as we shall see below, for weak interactions (small $\widetilde{H}$) it is better protected from various forms of decoherence when the system is coupled to a generic bath.

4.6 Decoherence

Consider the setup shown in Figure (4.1). We consider a simple perturbing tunneling Hamiltonian of the form: $\Delta H = i \sum_i t_i \gamma_i \eta_i$, with $t_i \in \mathbb{R}$. Here η_i refer to Hermitian fermionic modes relevant to the environment. In previous works it was demonstrated that $\langle \mathcal{O}(0) \mathcal{O}(T) \rangle$ is a good measure of the coherence of a qubit composed of localized Majorana modes [113]. Here $\mathcal{O}$ is an operator used to encode the qubit, and we will assume that the qubit and environment start uncorrelated. By Taylor expanding $e^{iT\Delta H}$ and keeping only leading order terms we obtain $\langle \mathcal{O}(0) \mathcal{O}(T) \rangle =$

$$\begin{aligned} 1 - \tfrac{1}{2} T^2 \sum_{i,j} t_i t_j \{ \langle \eta_i \eta_j \rangle \times \{ \langle \mathcal{O} \gamma_i \gamma_j \mathcal{O} \rangle + \langle \mathcal{O} \gamma_i \mathcal{O} \gamma_j \rangle \} \\ + \langle \eta_j \eta_i \rangle \times \left\{ \langle \mathcal{O} \gamma_j \mathcal{O} \gamma_i \rangle + \left\langle \mathcal{O}^2 \gamma_j \gamma_i \right\rangle \right\} \} . \end{aligned} \tag{4.18}$$

We can understand how this expression scales for various operators, in particular for $\mathcal{O} = \Upsilon_a$, n_a odd, we get that $\langle \Upsilon_a(0) \Upsilon_a(T) \rangle = 1 - 2T^2 \sum_{i \in L(a)} t_i^2 \left\langle \eta_i^2 \right\rangle_{\text{Env}}$. Since $t_i^2 \left\langle \eta_i^2 \right\rangle_{\text{Env}} \geq$

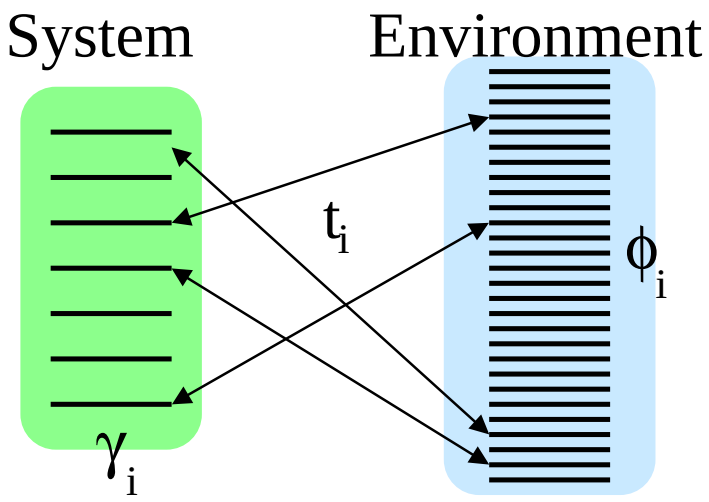

Figure 4.1: System Environment Schematic.
The system in tunneling contact with the environment. The system is composed of CdGM states [116], while the environment is everything else.

0, operators with larger n_a decohere more quickly, at least for short times. This indicates enhanced stability for operators that are similar to single Majorana fermions, like the new zero modes presented here.

4.7 Braiding

We would like to consider the idealized case of several Fermi zero modes $\{\mathcal{O}_\ell\}$, of the form $e^{i\tilde{H}_\ell}\sum_i \alpha_i^\ell \gamma_i^\ell\, e^{-i\tilde{H}_\ell}$, each corresponding to its own individual finite environment and labeled by ℓ. We further assume that the individual environments do not interact with the rest of the system. In this case because the modes are composed of sums of products of odd numbers of Majorana modes we see, following Ivanov [95], that the transformation properties of two zero modes under exchange are given by:

$$\begin{aligned} \mathcal{O}_1 &\rightarrow \mathcal{O}_2 \\ \mathcal{O}_2 &\rightarrow -\mathcal{O}_1. \end{aligned} \tag{4.19}$$

The minus sign comes when vortex 1 crosses the "cut" corresponding to vortex 2. These rules are identical to Ising braiding rules. To extend the derivation of Equation (4.19) given in [95], we must show that the many body holomony when restricted to the zero modes is zero. Indeed referring to [117, 118, 119], we know that in order to add in the many body holomony, in the Schrodinger picture, it is sufficient to consider Hamiltonian evolution within the zero energy subspace; with a Hamiltonian whose matrix elements are given by $\overline{H}_{\Omega,\Omega'} = i \langle \Omega | \frac{d}{dt} | \Omega' \rangle$. Here $|\Omega\rangle$ and $|\Omega'\rangle$ are instantaneous zero energy eigenkets. In the Heisenberg picture, this evolution corresponds to an evolution of the operators Υ_a when acted on by the Hamiltonian $\overline{\mathcal{H}}_{a,p;b,q}$, see the discussion following Equation (4.10). As such it is enough to show that any Hamiltonian $\overline{\mathcal{H}}_{a,p;b,q}$ can only have zero matrix elements within the subspace of zero modes. Indeed we know that up to a unitary transformation the structure of the zero modes is the same as in the non-interacting case, so by transforming $\overline{H} \to U^\dagger \overline{H} U \equiv \widetilde{\overline{H}}$ we reduce the problem to the non-interacting case. As such it is enough to show that any $\widetilde{\overline{H}}_{a,p;b,q} = 0$ when restricted to the space of zero modes. By linearity it is enough to consider only Hamiltonians of the form $|m\rangle \langle n| \otimes \Upsilon_b$. By explicitly taking commutators with $\mathcal{O}_{m,\{\theta_j\}}$ we see that all matrix elements within the zero energy subspace are zero ($\widetilde{\overline{H}}_{a,p;b,q} = 0$). This means that under braiding the fermionic zero modes transforms as $\mathcal{O}_{1,m,\{\theta_j\}} \to \mathcal{O}_{2,m,\{\theta_j\}}$, $\mathcal{O}_{1,m,\{\theta_j\}} \to -\mathcal{O}_{2,m,\{\theta_j\}}$ [120]. In particular the non-interacting holomony, Equation (4.19), is recovered.

4.8 Conclusions

We presented a systematic treatment of closed interacting systems with an odd number of real fermions. This formulation allowed us to find the zero mode solutions of interacting Hamiltonians, *i.e.*, operators that commute with the many-body Hamiltonian. In addition to the fermion parity operator that can be viewed as a constant of the motion for *any* Hamiltonian, we have found the solution that connects continuously to the Majorana mode for non-interacting systems as the interactions are switched off. These modes

couple more weakly than the fermion parity mode to an environment once the system is opened up to an outside infinite bath [113]. Therefore, the solutions that are continuously connected to the non-interacting Majorana modes should lead to slower decay rates in the presence of a bath. We have also verified that, under idealized conditions when multiple such modes exist, they obey Ising like statistics under braiding.

A Linked cluster expansion

A.1 Introduction

For our discussion of coherence of the pulse sequences presented in Chapter 2, see Section 2.5, we have presented numerical simulations of the coherence of a central spin under the action of various pulse sequences. In the main text we presented only a qualitative discussion and some final numerical results. Here we present in detail the numerical method used. We strive to make this appendix as self contained as possible. As such we review the linked cluster method, present derivations of the various correlators needed to compute the coherence and signal, and discuss some technical details pertinent to our specific simulation.

A.2 Unitary evolution for spin echo and related pulse sequences.

Here we derive various formulas for the signal from the spin echo sequences used in Chapter 2. These will be used in the numerical simulations. To simplify the derivation, as a first step we consider the case of a pure initial state $|\Psi_d\rangle$ for the dark spins. Consider the evolution as presented in Figure A.1(a). In this case after the total evolution under the pulse sequence the final state is $U_1\left(\frac{\tau}{2},\tau\right)U_0\left(0,\frac{\tau}{2}\right)|\Psi_d\rangle$ and $U_0\left(\frac{\tau}{2},\tau\right)U_1\left(0,\frac{\tau}{2}\right)|\Psi_d\rangle$ depending on the arm of the interferometer. Here $U_\alpha\left(\tau_i,\tau_j\right)$ are the unitary evolutions of the whole system for $S_z{=}\alpha$ for the time interval $\{\tau_i,\tau_j\}$. The signal is proportional

to the probability of the sensor spin being in the state $|0\rangle$ after the final $\frac{\pi}{2}$-pulse, which is $\propto Im\left\{\langle\Psi_d| U_1\left(\frac{\tau}{2},\tau\right) U_0\left(0,\frac{\tau}{2}\right) U_1^\dagger\left(0,\frac{\tau}{2}\right) U_0^\dagger\left(\frac{\tau}{2},\tau\right)|\Psi_d\rangle\right\}$. To proceed further we note that:

$$\begin{aligned}\langle\Psi_d| U_1\left(\tfrac{\tau}{2},\tau\right) U_0\left(0,\tfrac{\tau}{2}\right) U_1^\dagger\left(0,\tfrac{\tau}{2}\right) U_0^\dagger\left(\tfrac{\tau}{2},\tau\right)|\Psi_d\rangle = \\ Tr\,|\Psi_d\rangle\langle\Psi_d| U_1^\dagger\left(\tfrac{\tau}{2},\tau\right) U_0^\dagger\left(0,\tfrac{\tau}{2}\right) U_1\left(0,\tfrac{\tau}{2}\right) U_0\left(\tfrac{\tau}{2},\tau\right).\end{aligned} \tag{A.1}$$

We can generalize this result by using the linear dependence of the signal on the initial state and simply replacing $|\Psi_d\rangle\langle\Psi_d| \rightarrow \sum P_{|\Psi_d\rangle}|\Psi_d\rangle\langle\Psi_d| \equiv \rho$. We now rearrange the expression and get that the sensitivity is $\propto$:

$$Im\left\{Tr\left[U_1\left(\frac{\tau}{2},\tau\right) U_0\left(0,\frac{\tau}{2}\right)\rho U_1^\dagger\left(0,\frac{\tau}{2}\right) U_0^\dagger\left(\frac{\tau}{2},\tau\right)\right]\right\}. \tag{A.2}$$

Where Im vs. Re in Equation (A.2) comes from choice of phase for the last pulse. In general, for completeness, we mention that if we have any decoupling sequence such as CPMG, see Figure A.1(b) (where the Hamiltonian for the system depends on only one spin component of the central spin at a time) using reasoning similar to that given above we may write down the signal for the sequence just by inspection. It is proportional to

$$\begin{aligned}Tr\left[U_\alpha^\dagger\left(\tau_{n-2},\tau_{n-1}\right) U_\beta^\dagger\left(\tau_{n-1},\tau_{n-2}\right)...U_\gamma^\dagger\left(\tau_1,\tau_2\right) U_\delta^\dagger\left(0,\tau_1\right)\times\right. \\ \left.\times\rho U_{\widetilde{\alpha}}\left(0,\tau_1\right) U_{\widetilde{\beta}}\left(\tau_1,\tau_2\right).....U_{\widetilde{\gamma}}\left(\tau_1,\tau_2\right) U_{\widetilde{\delta}}\left(\tau_{n-1},\tau_n\right)\right].\end{aligned} \tag{A.3}$$

Here there are n time intervals for the pulse sequence $\{(0,\tau_1),(\tau_1,\tau_2),.....(\tau_{n-1},\tau_n)\}$ and the state of the central spin for the interval is $\{\alpha,\beta,.....\gamma,\delta\}$ for one arm and $\left\{\widetilde{\alpha},\widetilde{\beta},.....\widetilde{\gamma},\widetilde{\delta}\right\}$ for the other arm

A.3 Formulation of the problem

Here we would like to state the exact formulas for the signal and coherence of the pulse sequences considered in Chapter 2. We will always consider the following model Hamil-

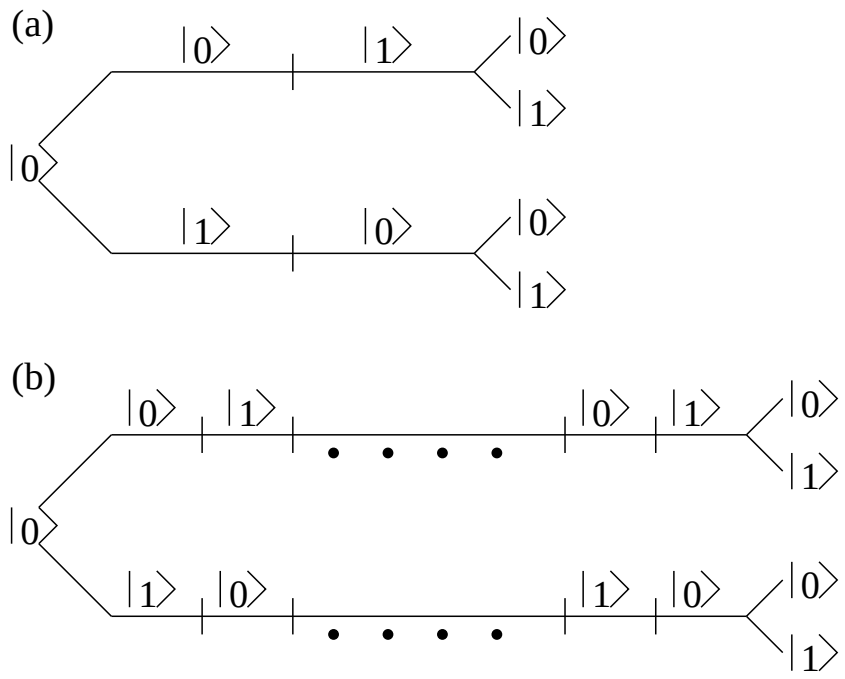

Figure A.1: Pulse Sequence Mach Zehnder.
Pulse sequences consider in the main text. (a) A spin echo sequence (b) complex CPMG type sequence. The state of the central spin is shown at each stage.

tonian:

$$H = g\mu_B b\left(t\right)\left(S_z + \sum I_z^i\right) + \sum \lambda_i S_z I_z^i + \sum \kappa_{ij}\left(3I_z^i I_z^j - \overrightarrow{I_i}\cdot\overrightarrow{I_j}\right). \tag{A.4}$$

Here κ_{ij} are the intrabath couplings (dipole-dipole interactions). The initial density matrix is given by $\rho = \bigotimes \frac{1}{2}\left(1 + P_i I_z^i\right)$. Now using Equation (A.1) and expanding to leading order in $b(t)$, the signal (for a spin echo sequence) is proportional to:

$$\begin{aligned} Sig \;\propto\; & \left[-\int_0^{\frac{\tau}{4}} Tr\left\{\sum_i U_1\left(\frac{\tau}{2}+t,\tau\right) b(t) I_z^i U_1\left(\frac{\tau}{2},\frac{\tau}{2}+t\right) U_0\left(0,\frac{\tau}{2}\right)\right.\right. \\ \times\; & \left.\left[\bigotimes \frac{1}{2}\left(1+P_j I_z^j\right)\right] U_1^\dagger\left(0,\frac{\tau}{2}\right) U_0^\dagger\left(\frac{\tau}{2},\tau\right)\right\} \\ +\; & \int_0^{\frac{\tau}{4}} \sum_i Tr\left\{U_1\left(\frac{\tau}{2},\tau\right) U_0\left(0,\frac{\tau}{2}\right) \bigotimes \frac{1}{2}\left(1+P_j I_z^j\right)\right. \\ \times\; & \left.\left. U_1^\dagger\left(0,\frac{\tau}{2}\right) U_0^\dagger\left(\frac{\tau}{2},\frac{\tau}{2}+t\right) b(t) I_z^i U_0^\dagger\left(\frac{\tau}{2}+t,\tau\right)\right\}\right] \end{aligned} \tag{A.5}$$

By considering any individual term in Equation (A.5) above we see that we have reduced the problem to finding traces of the form

$$\begin{aligned} & Tr\left\{U_1\left(\tfrac{\tau}{2}+t,\tau\right) I_z^i U_1\left(\tfrac{\tau}{2},\tfrac{\tau}{2}+t\right) U_0\left(0,\tfrac{\tau}{2}\right)\right. \\ & \qquad \left.\left[\bigotimes \tfrac{1}{2}\left(1+P_j I_z^j\right)\right] U_1^\dagger\left(0,\tfrac{\tau}{2}\right) U_0^\dagger\left(\tfrac{\tau}{2},\tau\right)\right\}. \end{aligned} \tag{A.6}$$

For completeness we will study both the coherence properties (T_2) for the pulse sequences proposed in this paper. For these calculations we will need similar traces:

$$Tr\left\{U_1\left(\frac{\tau}{2},\tau\right) U_0\left(0,\frac{\tau}{2}\right)\left[\bigotimes \frac{1}{2}\left(1+P_j I_z^j\right)\right] U_1^\dagger\left(0,\frac{\tau}{2}\right) U_0^\dagger\left(\frac{\tau}{2},\tau\right)\right\}. \tag{A.7}$$

Below we will describe an algorithm using the Linked Cluster Expansion [121, 56] to compute these traces numerically.

A.4 Linked cluster expansion (a review)

The purpose of the Linked Cluster Expansion is to generate an "easy" numerical algorithm for evaluating "short term" expectation values for spin operators for a weakly interacting spin bath. More concretely, we are interested in taking the trace of a string of spin operators

$$\Theta\left(1,2,...N\right) \equiv Tr\left\{U\left(\tau_1,\tau_2\right) I_\alpha^i .....I_\gamma^k U^\dagger\left(\tau_n,\tau_{n+1}\right)\right\}. \tag{A.8}$$

Here we are assuming a bath of N environment spins. In the trace we allow for arbitrary insertions (in arbitrary order) of the form I_η^k, $U\left(\tau_i,\tau_{i+1}\right)$, $U^\dagger\left(\tau_j,\tau_{j+1}\right)$. To make the trace systematic let us define expectations for subsets of the spin bath of the form $\Theta\left(i_1,i_2,...i_k\right) \equiv \Theta\left(1,2,...N\right)\mid_{drop}$ where $\mid_{drop}$ means that we neglect all spin operators not in the set $\{i_1,i_2,....i_k\}$ from Equation (A.8). For spin baths where, for the relevant timescale, two body and higher order interactions are small (that is single spin terms dominate $U\left(\tau_j,\,\tau_{j+1}\right)$) it is advantageous to consider only small clusters of spins for the purpose of calculating traces given by Equation (A.8). To make this small cluster expansion rigorous consider the following recursive definitions for one spin correlator: $\widetilde{\Theta}\left(i\right) \equiv \Theta\left(i\right)$, two spin correlator $\widetilde{\Theta}\left(i_1,i_2\right) \equiv \Theta\left(i_1,i_2\right) - \widetilde{\Theta}\left(i_1\right)\cdot\widetilde{\Theta}\left(i_2\right)$, three spin correlator:

$$\begin{aligned}\widetilde{\Theta}\left(i_1,i_2,i_3\right) &\equiv \Theta\left(i_1,i_2,i_3\right) - \widetilde{\Theta}\left(i_1,i_2\right)\cdot\widetilde{\Theta}\left(i_3\right) - \widetilde{\Theta}\left(i_1,i_3\right)\cdot\widetilde{\Theta}\left(i_2\right)\\ &- \widetilde{\Theta}\left(i_2,i_3\right)\cdot\widetilde{\Theta}\left(i_1\right) - \widetilde{\Theta}\left(i_1\right)\cdot\widetilde{\Theta}\left(i_2\right)\cdot\widetilde{\Theta}\left(i_3\right)\end{aligned} \tag{A.9}$$

More generally we define a k spin correlator as:

$$\widetilde{\Theta}\left(i_1,i_2,...i_k\right) = \Theta\left(i_1,i_2,...i_k\right) - \sum\left(\prod\widetilde{\Theta}\left(i_{j_1}..i_{j_l}\right)\cdot\widetilde{\Theta}\left(i_{j_{l+1}}..i_{j_{l+q}}\right)...\cdot\widetilde{\Theta}\left(i_{j_m}..i_{j_k}\right)\right), \tag{A.10}$$

where the sum is over all disjoint non-empty partitions of the set $\{i_1, i_2, ...i_k\}$. From this recursive definition it is clear that:

$$\begin{array}{l} \Theta\left(1,2,...N\right) = \widetilde{\Theta}(1,2,...N) \\ + \sum \left(\prod \widetilde{\Theta}\left(i_{j_1}..i_{j_l}\right) \cdot \widetilde{\Theta}\left(i_{j_{l+1}}..i_{j_{l+q}}\right) .... \cdot \widetilde{\Theta}\left(i_{j_m}..i_{j_k}\right) \right) \end{array} . \tag{A.11}$$

So if the procedure is taken to a sufficiently high order this algorithm yields exact expectation values. In practice it is impossible to calculate these sums to arbitrary order so it is necessary to truncate the expansion and consider correlators of order n or less. In many cases, as we shall see below, the sum over partitions in Equation (A.11) may be replaced (with only a small error) with a product over subsets of two or three spins.

A.5 Simulations

In this section we will give the technical details associated with the specific implementation of the Linked Cluster Expansion used for our simulations. To demonstrate the effectiveness of pulse sequence we have simulated coherence times and signal for regular spin echo and the proposed spin echo sequence. To simplify our computations we have simulated a bath of spin 1/2 impurities (as opposed to Nitrogen P1 centers). Explicitly the Hamiltonians for the simulations were given by $H = \sum \lambda_i S_z I_z^i + \sum \kappa_{ij} \left(3 I_z^i I_z^j - \overrightarrow{I_i} \cdot \overrightarrow{I_j} \right)$. Here $\lambda_i = \frac{g^2 \mu_B^2}{r_i^3} \left(1 - 3\cos^2\left(\theta_i\right)\right)$ while $\kappa_{ij} = \frac{g^2 \mu_B^2}{r_{ij}^3} \left(1 - 3\cos^2\left(\theta_{ij}\right)\right)$. All angles are taken with respect to the direction of the external magnetic field which is assumed parallel to the NV axis.

We have simulated a WAHUHA experiment on the dark spins. For simplicity we have neglected all pulse imperfections. To further simplify the numerics for the simulation we have calculated the leading order Magnus expansion for a WAHUHA sequence [46] by hand. For this purpose we may retain only the zeroth order central coupling term $\frac{1}{3} S_z \sum \left(I_x^i + I_y^i + I_z^i \right)$ and $H_{dip-dip}^{(2)}$ (the second order dipole dipole Hamiltonian). In the

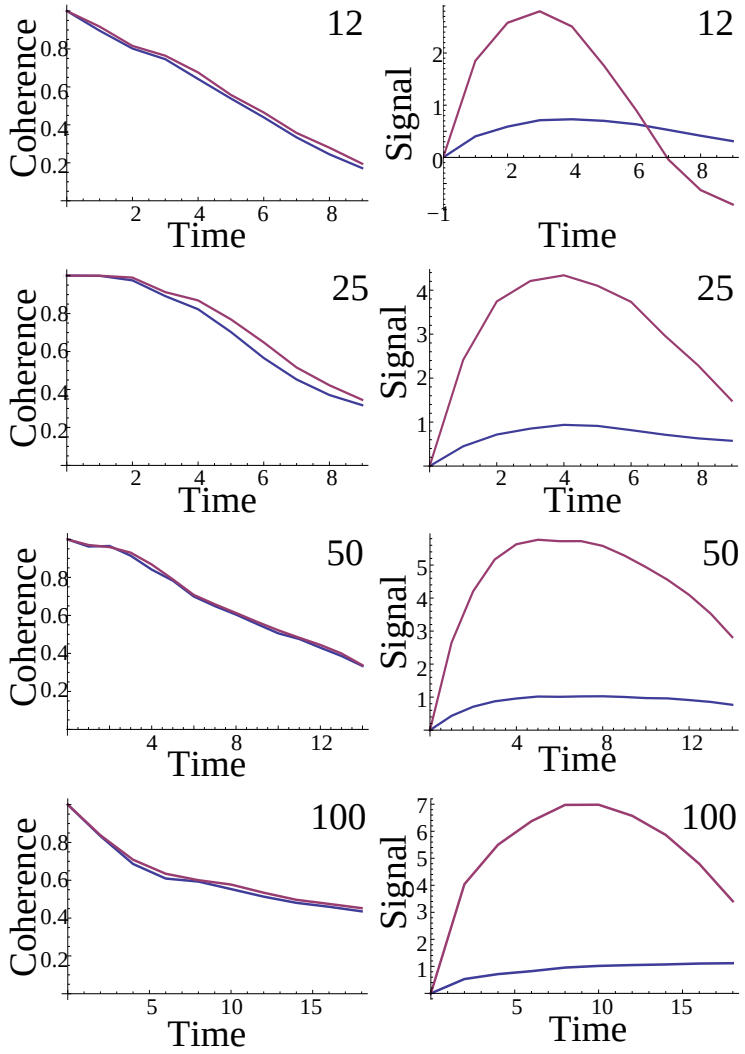

Figure A.2: Signal and Coherence WAHUHA.
Monte-Carlo simulations of normalized signal for regular spin echo sequence (Blue) and modified spin echo sequence (Red). We have also simulated the decay of coherence for both pulse sequences (shown on the left for regular spin echo (Blue) and modified spin echo (Red)). A leading order cluster expansion was used, see [121, 56]. In each case 20 dark spins were randomly placed in a cube of side-length $\sqrt[3]{20}$. The bright spin was placed in the center; the coupling between all spins was dipole-dipole. We have set $g_c = g_d \,\&\, g_c\mu_B \equiv [m]^{3/2}\,[s]^{-1/2}$ to get rid of dimensionful quantities. WAHUHA pulse sequences were simulated on all dark spins with 12, 25, 50 and 100 WAHUHA pulse cycles respectively. We have taken an ensemble average over 15 Monte-Carlo simulations to obtain each curve.

Magnus Hamiltonian all other terms are higher in order and for all time intervals of the spin echo sequence they are accompanied by at least one of the two terms given above. A straightforward but tedious calculation shows that:

$$H^{(2)}_{dip-dip} = \frac{\tau_c^2}{648}\left[\left(H^x_D - H^z_D\right), \left[H^x_D, H^y_D\right]\right]. \tag{A.12}$$

Here $H^z_D = g^2\mu_B^2 \sum_{i<k} \kappa_{ik}\left(3I^i_z I^k_z - \overrightarrow{I_i}\cdot\overrightarrow{I_k}\right)$ with analogous definitions for H^x_D and H^y_D; $\kappa_{ik} = \frac{\left(1-3\cos^2\theta_{ik}\right)}{r^3_{ik}}$ and τ_c is the length of a single elementary WAHUHA pulse sequence (e.g. $\tau_c = \frac{\tau}{\mathcal{N}\kappa}$). Now we can calculate these commutators. Because:

$$\left[3I^i_x I^k_x - \overrightarrow{I_i}\cdot\overrightarrow{I_k},\, 3I^i_y I^k_y - \overrightarrow{I_i}\cdot\overrightarrow{I_k}\right] = 0, \tag{A.13}$$

the leading order terms come from clusters of three spins. Terms coming from clusters of four spins are sub-dominant for $\propto \frac{1}{r^3}$ interactions. Indeed four spin terms will contain products proportional to $\frac{1}{r_{ij}}\frac{1}{r_{jk}}\frac{1}{r_{kl}}$ while three spin interactions will contain terms proportional to $\frac{1}{r^2_{ij}}\frac{1}{r_{jk}}$ which will dominate for two closely spaced spins (ij). For reference we explicitly display these terms here:

$$\begin{aligned}
H^{(2)}_{dip-dip} &= \frac{\tau_c^2}{54}\sum_{i<j<k}\Big\{\kappa^2_{jk}\left(\kappa_{ij}\left(2I^i_xI^k_x - I^j_yI^k_y - I^j_yI^k_y\right) + \kappa_{ki}\left(2I^i_yI^i_y - I^i_zI^k_z - I^i_zI^i_z\right)\right) \\
&+ \kappa^2_{ij}\kappa_{jk}\left(2I^i_yI^k_y - I^j_zI^k_z - I^i_zI^k_z\right) + \kappa^2_{ij}\kappa_{ki}\left(2I^k_xI^j_x - I^k_yI^i_y - I^i_yI^j_y\right) \\
&+ \kappa^2_{ik}\left(\kappa_{jk}\left(2I^i_xI^k_x - I^k_yI^j_y - I^j_yI^i_y\right) + \kappa_{ij}\left(2I^i_yI^k_y - I^j_zI^i_z - I^i_zI^k_z\right)\right) \\
&+ \kappa_{ij}\kappa_{jk}\kappa_{ki}\Big(2\left(I^i_yI^j_y + I^i_yI^j_y + I^i_yI^j_y\right) - \left(I^i_xI^j_x + I^j_xI^k_x + I^k_xI^i_x\right) \\
&- \left(I^i_zI^j_z + I^j_zI^k_z + I^k_zI^i_z\right)\Big)\Big\}
\end{aligned} \tag{A.14}$$

This formula is only correct for $I = \frac{1}{2}$. We have done Monte-Carlo simulations of the T_2 times and signals for the pulse sequences given above. For each simulation we have used 20 dark spins randomly positioned in a cube of edge length $\sqrt[3]{20}$ with the bright spin in

the middle. Each curve shown is an ensemble average over 15 Monte-Carlo simulations. The results for the coherence times and signal for regular spin echo sequences and our sequence are given in Figure A.2.

B Technical calculations for decay rates

B.1 Non interacting systems (quantum depletion)

To have yet another independent check of the results presented in Chapter 3 we would like to derive results similar to Equation (3.33) in a different way. That is we would like to show that the coherence of a Majorana mode when interacting with a static quadratic environment that undergoes a single sudden switch does not decay to zero at long times. We shall do so by explicitly diagonalizing the new static Hamiltonian and showing that it has an exact zero mode with finite overlap with the original Majorana zero mode. More precisely we will consider a model consisting of a Majorana mode interacting via tunneling with non-interacting complex fermionic modes. The Hamiltonian of our system will be:

$$H_{\text{Mean}} = \gamma \sum_{i=1}^{N} \left(\Gamma_i c_i - \Gamma_i^* c_i^\dagger \right) + \sum_{i=1}^{N} \epsilon_i c_i^\dagger c_i \tag{B.1}$$

This is the most general form of a Quadratic Hamiltonian for a system of complex fermions interacting with a single Majorana mode. We will first proceed by exactly re-diagonalizing the Hamiltonian. By taking commutators of the form $[H_{\text{Mean}}, \gamma]$, $[H_{\text{Mean}}, c_i]$ and $\left[H_{\text{Mean}}, c_i^\dagger\right]$ we may rewrite this Hamiltonian as a matrix acting on the space spanned by $\left\{\frac{\gamma}{\sqrt{2}}, c_i, c_i^\dagger\right\}$ (the factor of $\sqrt{2}$ is a normalization constant that insures that the matrix representing the Hamiltonian is Hermitian in this basis). With respect

to this basis we may write that:

$$H_{\text{Mean}} = \begin{pmatrix} 0 & \sqrt{2}\Gamma_1 & \cdots & \cdots & \sqrt{2}\Gamma_N & -\sqrt{2}\Gamma_1^* & \cdots & \cdots & -\sqrt{2}\Gamma_N^* \\ \sqrt{2}\Gamma_1^* & \epsilon_1 & 0 & \cdots & 0 & 0 & \cdots & \cdots & 0 \\ \vdots & 0 & \epsilon_2 & \ddots & \vdots & \vdots & & & \vdots \\ \vdots & \vdots & \ddots & \ddots & 0 & \vdots & & & \vdots \\ \sqrt{2}\Gamma_N^* & 0 & \cdots & 0 & \epsilon_N & 0 & \cdots & \cdots & 0 \\ -\sqrt{2}\Gamma_1 & 0 & \cdots & \cdots & 0 & -\epsilon_1 & 0 & \cdots & 0 \\ \vdots & \vdots & & & \vdots & 0 & -\epsilon_2 & \ddots & \vdots \\ \vdots & \vdots & & & \vdots & \vdots & \ddots & \ddots & 0 \\ -\sqrt{2}\Gamma_N & 0 & \cdots & \cdots & 0 & 0 & \cdots & 0 & -\epsilon_N \end{pmatrix} \tag{B.2}$$

We may now diagonalize this matrix by solving for the eigenvalues of the system $\{\lambda_\kappa\}$ with corresponding eigenvectors $\left\{V_\kappa \equiv U_\kappa \gamma + \sum_{i=1}^N U_{\kappa,i} c_i + \sum_{i=1}^N U_{\kappa,N+i} c_i^\dagger\right\}$. By direct substitution into the equation $HV_\kappa = \lambda_\kappa V_\kappa$ we see that:

$$\begin{aligned} U_{\kappa,i} &= \frac{\sqrt{2}\Gamma_i^*}{\lambda_\kappa - \epsilon_i} U_\kappa, \\ U_{\kappa,N+i} &= -\frac{\sqrt{2}\Gamma_i}{\lambda_\kappa + \epsilon_i} U_\kappa \end{aligned} \tag{B.3}$$

Here we have ignored the "top line" of H_{Mean} in Equation (B.2). Substituting Equation (B.3) into the "top line" of H_{Mean} we get that:

$$\lambda_\kappa U_\kappa = \sum_i \sqrt{2}\Gamma_i U_{\kappa,i} - \sum_i \sqrt{2}\Gamma_i^* U_{\kappa,N+i} \tag{B.4}$$

$$= \sum_i \frac{4\lambda_\kappa |\Gamma_i|^2}{(\lambda_\kappa)^2 - (\epsilon_i)^2} U_\kappa, \tag{B.5}$$

We can now obtain eigenvalue equations:

$$\lambda_\kappa = 0, \text{ or } 1 = 4\sum_i \frac{|\Gamma_i|^2}{(\lambda_\kappa)^2 - (\epsilon_i)^2} \tag{B.6}$$

Now substituting $\lambda_0 = 0$ into Equation (B.4) we get that:

$$\begin{aligned} 1 &= |U_0|^2 + \sum_{i=1}^{N} |U_{0,i}|^2 + \sum_{i=1}^{N} |U_{0,N+i}|^2 \\ &= |U_0|^2 \left(1 + 4\sum_{i=1}^{N} \frac{|\Gamma_i|^2}{\epsilon_i^2}\right) \end{aligned} \tag{B.7}$$

From this we see that the overlap of the new zero mode with the original mode stays finite (which would lead to non-zero coherence for arbitrarily long times) whenever:

$$\sum_{i=1}^{N} \frac{|\Gamma_i|^2}{\epsilon_i^2} < \infty \tag{B.8}$$

This result is similar to Equation 3.33 in the main text, which demonstrates finite coherence for the Majorana mode subject to the same condition as B.8. This condition is true for any finite system. Furthermore the overlap of this mode with the original zero energy mode is depleted by a factor of:

$$\begin{aligned} &\left(1 + \sum_{i=1}^{N} |U_{0,i}|^2 + \sum_{i=1}^{N} |U_{0,N+i}|^2\right)^{-1/2} \\ &\qquad = \left(1 + 4\sum_i \frac{|\Gamma_i|^2}{\epsilon_i^2}\right)^{-1/2}. \end{aligned} \tag{B.9}$$

Since non-zero modes should show no coherence at long times the coherence of a Majorana mode should be depleted by a similar factor, which is highly similar to Equation 3.33 in the main text. Below in Appendix B.3.4 we will show that the condition given in Equation B.8 is satisfied for mean field like infinite systems.

B.2 Quantum fluctuations

We would like to extend the previous results, see Section 3.6, to the case where the couplings Γ_i are allowed to have quantum fluctuations. That is we will allow for different fluctuations for the backwards and forwards time paths. Once again we will focus on a single Majorana mode which may be well described by a Hamiltonian of the form $H_{\text{Mean}}\left(\Gamma_i,\, \Gamma_i^*\right) = \gamma \sum_{i=1}^{N} \left(\Gamma_i c_i - \Gamma_i^* c_i^\dagger\right) + \sum_{i=1}^{N} \epsilon_i c_i^\dagger c_i$. Here γ is a single Majorana mode and $c_i,\, c_i^\dagger$ are regular fermion creation and annihilation operators. In our model we will allow for Gaussian quantum dynamics for the coupling constants Γ_i. We will not be able to emulate the diffusion equation derivation given in Section B.3.4 but we will provide a brute force resummation of the leading order terms contributing to coherence. The key difficulty in modifying the approach of Section B.3.4 to the case of quantum noise is that because of the various theta functions, see e.g. Equations (3.25) & (B.12), the fermionic part of the correlation function cannot be written in a factorisable form $G_F\left(\tau_1,\, \tau_2\right) \neq \widetilde{G_{1F}}\left(\tau_1\right) \times \widetilde{G_{2F}}\left(\tau_2\right)$ (or a sum of such terms). As such we cannot simply study the diffusion of one or several modes, see e.g. Equation (3.38), but we have to study the diffusion of an infinite number of degrees of freedom (which is more difficult). We now proceed with the computation, by using Equation (3.25) we may write that:

$$
\begin{aligned}
\left\langle \gamma\left(0\right)\gamma\left(T\right)\right\rangle \;&=\; \mathcal{N}\int\int\mathcal{D}\left\{\mathbf{\Gamma}^\dagger,\mathbf{\Gamma}\right\}\exp\left(-\frac{1}{2}\sum_{a,b}\int_0^{\mathrm{T}}d\tau_1^a\int_0^{\mathrm{T}}d\tau_2^b\mathbf{\Gamma}^\dagger\left(G_F^{(2)}\left(\tau_1^a,\tau_2^b\right)\right)^{-1}\mathbf{\Gamma}\right)\\
&\times\;\gamma\exp\left(i\widetilde{\mathcal{T}}\int_0^{\mathrm{T}}\left\{H_{\text{Mean}}\left(\mathbf{\Gamma}^\dagger\left(\tau\right),\mathbf{\Gamma}\left(\tau\right)\right)\right\}d\tau\right)\\
&\times\;\gamma\exp\left(-i\mathcal{T}\int_0^{\mathrm{T}}\left\{H_{\text{Mean}}\left(\mathbf{\Gamma}^\dagger\left(\tau\right),\mathbf{\Gamma}\left(\tau\right)\right)\right\}d\tau_2\right)\\
&=\;\mathcal{N}\int\int\mathcal{D}\left\{\mathbf{\Gamma}^\dagger,\mathbf{\Gamma}\right\}\exp\left(-\frac{1}{2}\sum_{a,b}\int_0^{\mathrm{T}}d\tau_1^a\int_0^{\mathrm{T}}d\tau_2^b\mathbf{\Gamma}^\dagger\left(\overline{G}_F^{(2)}\left(\tau_1^a,\tau_2^b\right)\right)^{-1}\mathbf{\Gamma}\right)\\
&\times\;\exp\left(-\frac{1}{2}\sum_{a,b}\int_0^{\mathrm{T}}d\tau_1^a\int_0^{\mathrm{T}}d\tau_2^b\;\mathbf{\Gamma}^\dagger\,\overline{D}_{\mathrm{F}}^{(2)}\left(\tau_1^a,\tau_2^b\right)\;\mathbf{\Gamma}\right)
\end{aligned}
\tag{B.10}
$$

Here $\mathrm{G}_F^{(2)} = \otimes_i \begin{pmatrix} G_{11}^i(\tau_1,\tau_2) & G_{12}^i(\tau_1,\tau_2) \\ G_{21}^i(\tau_1,\tau_2) & G_{22}^i(\tau_1,\tau_2) \end{pmatrix}$, $\mathcal{N} = \det G_F^{(2)}$ and $\overline{D}_{\mathrm{F}}^{(2)}\left(\tau_1^a,\tau_2^b\right)$ was defined in Equation (3.27). We note that Equation (3.26) does not apply as there are correlations between the Γ's. As such we must compute a functional determinant as shown in Equation (B.10) above. We now use the equation:

$$\int\int dz_1...dz_n dz_1^*...dz_n^* \exp\left(-\frac{1}{2}\vec{z}^\dagger G^{-1}\vec{z}\right) = (2\pi)^n \det(\mathrm{G}) \tag{B.11}$$

Which is true even for an arbitrary (not necessarily Hermitian) matrix G. We will provide an independent proof of this result in Appendix B.3. Now noting that the determinant of a block diagonal matrix factorizes and writing out the form of $\overline{D}_{\mathrm{F}}^{(2)}\left(\tau_1^a,\tau_2^b\right)$ say by using Equation (3.25) we can show that:

$$\begin{aligned} \langle\gamma(0)\,\gamma(\mathrm{T})\rangle^{-1} &= \prod_{\mathrm{i}} \det\left\{ \mathbb{I} + 2\begin{pmatrix} G_{11}^i(\tau_1,\tau_2) & G_{12}^i(\tau_1,\tau_2) \\ G_{21}^i(\tau_1,\tau_2) & G_{22}^i(\tau_1,\tau_2) \end{pmatrix} \right. \\ &\times \left. \begin{pmatrix} \theta(t_1-t_2)\left\langle c_i^\dagger(t_1)c_i(t_2)\right\rangle & \left\langle c_i^\dagger(t_1)\,c_i(t_2)\right\rangle \\ +\theta(t_2-t_1)\left\langle c_i(t_2)c_i^\dagger(t_1)\right\rangle & \\ \left\langle c_i(t_2)\,c_i^\dagger(t_1)\right\rangle & \theta(t_2-t_1)\left\langle c_i^\dagger(t_1)c_i(t_2)\right\rangle \\ & +\theta(t_1-t_2)\left\langle c_i(t_2)c_i^\dagger(t_1)\right\rangle \end{pmatrix} \right\} \end{aligned} \tag{B.12}$$

We have inserted the forms of the various matrices explicitly. What remains is to evaluate the functional determinant in Equation (B.12) above. First by conjugating all matrices above with the matrix $\frac{1}{\sqrt{2}}\begin{pmatrix} \mathbb{I} & \mathbb{I} \\ \mathbb{I} & -\mathbb{I} \end{pmatrix}$ (here $\mathbb{I}$ stands for the identity matrix on

$[0,\mathrm{T}]\times[0,\mathrm{T}]$) we may write that:

$$\begin{aligned}
&\langle\gamma(0)\,\gamma(\mathrm{T})\rangle^{-1}= \\
&\prod_i \det\left\{\mathbb{I}+2\begin{pmatrix} 0 & G_i^R \\ G_i^A & G_i^K\end{pmatrix}\times\right. \\
&\left.\times\begin{pmatrix} 0 & \theta(t_1-t_2)\left\{\left\langle c_i^\dagger(t_1)c_i(t_2)\right\rangle - \left\langle c_i(t_2)c_i^\dagger(t_1)\right\rangle\right\} \\ \theta(t_2-t_1)\left\{\left\langle c_i(t_2)c_i^\dagger(t_1)\right\rangle - \left\langle c_i^\dagger(t_1)c_i(t_2)\right\rangle\right\} & \left\langle c_i(t_2)\,c_i^\dagger(t_1)\right\rangle+\left\langle c_i^\dagger(t_1)\,c_i(t_2)\right\rangle\end{pmatrix}\right\} \\
&=\prod_i \det\left\{\mathbb{I}+2\begin{pmatrix} 0 & G_i^R \\ G_i^A & G_i^K\end{pmatrix}\begin{pmatrix} 0 & \widetilde{G_i^R} \\ \widetilde{G_i^A} & \widetilde{G_i^K}\end{pmatrix}\right\}
\end{aligned} \tag{B.13}$$

We would like to note the unusual bosonic minus signs in $\widetilde{G_i^R}$ & $\widetilde{G_i^A}$ in Equation (B.13) above. The rest of this section is an evaluation of the determinant in Equation (B.13) above. Using the identity $\det(\mathbb{I}+M)=\exp\left(\sum\frac{-1^n}{n}\mathrm{Tr}\left(M^n\right)\right)$ we may write that

$$\langle\gamma(0)\,\gamma(\mathrm{T})\rangle \;=\; \exp\left(\sum\tfrac{-2^n}{n}\mathrm{Tr}\left(\sum_{i_1,i_2,..i_{2n}}\prod G_i^{i_{2k-1},i_{2k}}\widetilde{G_i^{i_{2k},i_{2k+1}}}\right)\right) \tag{B.14}$$

Here $i_j=1$ or 2 and $(i_k,\,i_{k+1})\neq(1,\,1)$. To proceed further we will now evaluate each of the traces (to leading order for large T). As such we need to evaluate integrals of the form:

$$\begin{aligned}
&\textstyle\int_0^{\mathrm{T}}d\tau_1\int_0^{\mathrm{T}}d\tau_2..\int_0^{\mathrm{T}}d\tau_{2n}\times \\
&\Big\{\Big(\Big[G_i^{A/R/K}(\tau_1-\tau_2)\times\left(\theta(\tau_2-\tau_1)/\theta(\tau_1-\tau_2)/1\right)\Big]\times \\
&\times\Big[G_i^{A/R/K}(\tau_3-\tau_4)\times\left(\theta(\tau_2-\tau_1)/\theta(\tau_1-\tau_2)/1\right)\Big]\times \\
&....\times\Big[G_i^{A/R/K}(\tau_{2n-1}-\tau_{2n})\times\left(\theta(\tau_{2n-1}-\tau_{2n})/\theta(\tau_{2n}-\tau_{2n-1})/1\right)\Big]\Big)\times \\
&\times\left(\left[e^{-i\epsilon_i(\tau_2-\tau_3)-\kappa_i|\tau_2-\tau_3|}\times\left((1-2n_i)\,\theta(\tau_{2n-1}-\tau_{2n})/(2n_i-1)\,\theta(\tau_{2n}-\tau_{2n-1})/1\right)\right]\times\right. \\
&\left.....\times\left[e^{-i\epsilon_i(\tau_{2n}-\tau_1)-\kappa_i|\tau_{2n}-\tau_1|}\times\left((1-2n_i)\,\theta(\tau_1-\tau_{2n})/(2n_i-1)\,\theta(\tau_{2n}-\tau_1)/1\right)\right]\right)\Big\}
\end{aligned} \tag{B.15}$$

Here for future convenience we have written out the various theta functions involved

and for simplicity assumed relaxation time approximation for the fermion Greens functions. The terms $A/R/K$ refer to advanced/retarded/Keldysh Green's functions while the various options for the theta functions shown in the brackets correspond to the respective green's functions $(A/R/K)$. We now need to evaluate these integrals. As a first step we take advantage of the short range of our correlation functions (see Figure (3.4)) to change range of integration limits for the variables $\tau_1, \tau_3, ...\tau_{2n-1}$ from $(0, \mathrm{T})$ to $(-\infty, \infty)$. We also shift the variables of integration calling $u_i \equiv \tau_{2i-1} - \tau_{2i}$, $v_i \equiv \tau_{2i}$. Combing all these changes we get that the any term in expansion in Equation (B.14) e.g. Equation (B.15) may be written as:

$$\begin{aligned}
&\int_{-\infty}^{\infty} du_1 \int_{-\infty}^{\infty} du_2 .... \int_{-\infty}^{\infty} du_n \times \\
&\left(G_i^{A/R/K}(u_1) \times e^{-i\epsilon_i u_1 - \kappa_i |u_1|} \times \left(\theta(-u_1)/\theta(u_1)/1\right)\right) \times \\
&..... \times \left(G_i^{A/R/K}(u_n) \times e^{-i\epsilon_i u_n - \kappa_i |u_n|} \times \left(\theta(-u_n)/\theta(u_n)/1\right)\right) \times \\
&\times \int_0^T dv_1 \int_0^T dv_2 .... \int_0^T dv_n \times \\
&\left(\theta(v_2 - v_1 + u_2)/\theta(v_1 - v_2 - u_2)/1\right) ..... \left(\theta(v_1 - v_n + u_1)/\theta(v_n - v_1 - u_1)/1\right)
\end{aligned} \tag{B.16}$$

We may further simplify this expression by noting that all the correlation functions $G_i^{A/R/K}$ are dominated by small values of u so that we may approximate $\theta(v_2 - v_1 + u_2) \cong \theta(v_2 - v_1)$ and similarly for other θ functions. Substituting we get that the integrals simplify:

$$\begin{aligned}
&\left\{ \prod_{j=1}^{n} \int_{-\infty}^{\infty} G_i^{A/R/K}(u_j)\, e^{-i\epsilon_i u_j - \kappa_i |u_j|} \cdot \left(\theta(-u_i)/\theta(u_i)/1\right)\right\} \times \\
&\left\{ \int_0^T dv_1 .. \int_0^T dv_n \prod_{j=1}^{n} \left(\theta(v_{j+1} - v_j)/\theta(v_j - v_{j+1})/1\right)\right\}
\end{aligned} \tag{B.17}$$

In Appendix B.3 we will further simplify the expression in Equation (B.17) above. Here we will merely compute the leading order term for the semi classical case where $G_i^K \gg G_i^R, G_i^A$. In this case a single term (containing only G_i^K contributions) dominates

at each order of integration and we may write that:

$$\mathrm{Tr}\left(\sum_{i_1,i_2,..i_{2n}}\prod G_i^{i_{2k-1},i_{2k}}\widetilde{G_i^{i_{2k},i_{2k+1}}}\right)\cong\left(\widehat{G_i^K}\left(\epsilon_i-i\kappa_i\right)\cdot\mathrm{T}\right)^n \tag{B.18}$$

Here $\widehat{G_i^K}\left(\epsilon_i-i\kappa_i\right)$ is the "Fourier transform" of the Keldysh Green's function evaluated at energy ϵ_i and decay term κ_i. Combining these results we recover the semiclassical result that:

$$\begin{aligned}\left\langle\gamma\left(0\right)\gamma\left(\mathrm{T}\right)\right\rangle &= \prod_i\frac{1}{1+2\mathrm{T}\widehat{G_i^K}\left(\epsilon_i-i\kappa_i\right)} \\ &= \prod_i\frac{1}{1+2\mathrm{T}\left(\widehat{G_i}\left(\epsilon_i-i\kappa_i\right)+\widehat{G_i}\left(-\epsilon_i+i\kappa_i\right)\right)} \\ &\cong \exp\left(-2\mathrm{T}\sum_i\left(\widehat{G_i}\left(\epsilon_i-i\kappa_i\right)+\widehat{G_i}\left(-\epsilon_i+i\kappa_i\right)\right)\right)\end{aligned} \tag{B.19}$$

In the second step we have used a relation between Keldysh and time ordered correlation functions and in the last step we have assumed that there are many relevant fermionic modes in the bath so that we can safely exponentiate each term. Further corrections to this result are given in Appendix B.3.

B.3 Various tedious calculations and proofs

B.3.1 Parity eigenvalues (coding subspace)

In the main text (see Section 3.2) we presented a specific encoding of the Majorana qubit that used the even Majorana fermion parity subspace for its coding space. Throughout the main text we computed expectation values of the form:

$$\left\langle\gamma_1\left(0\right)\gamma_2\left(0\right)\gamma_1\left(T\right)\gamma_2\left(T\right)\right\rangle=-\left\langle\sigma^z\left(0\right)\sigma^z\left(T\right)\right\rangle. \tag{B.20}$$

We claimed that this is a good representation of the fidelity of our quantum memory. There could be further concern that we are over or under estimating the fidelity by including in the expectation value $\langle\gamma(0)\gamma...\gamma(\mathrm{T})\rangle$ processes that included final states that do not have an even fermion parity [123]. Here we show that for two time correlation functions such processes never contribute to this expectation value so no further measurements or corrections are needed to adjust for such processes. Even though we do not focus on this case in the main text we will show that the above statement is not correct for multitime correlators. We will also show what modifications must be made in the multitime case.

Two time correlators

We start by showing that no modifications are necessary in the two time correlators case (again focusing on the four Majorana fermion qubit). Indeed consider $\prod_+$ and $\prod_-$ projectors into even and odd Majorana fermion parity subspaces ($\prod_+ + \prod_- = 1$, $\prod_\pm^2 = \prod_\pm$ and $\prod_+ \prod_- = 0$). Since the initial state of the Majorana qubit has even fermion parity, we may write that:

$$\begin{aligned}
&\langle\sigma^{\mathrm{z}}(0)\,\sigma^{\mathrm{z}}(\mathrm{T})\rangle = \left\langle\prod_+ \sigma^{\mathrm{z}}(0)\,\sigma^{\mathrm{z}}(\mathrm{T})\prod_+\right\rangle \\
&= \left\langle\prod_+ \sigma^{\mathrm{z}}(0)\left(\prod_+ + \prod_-\right)\sigma^{\mathrm{z}}(\mathrm{T})\prod_+\right\rangle \\
&= \left\langle\prod_+ \sigma^{\mathrm{z}}(0)\prod_+ \sigma^{\mathrm{z}}(\mathrm{T})\prod_+\right\rangle \\
&= \left\langle\sigma^{\mathrm{z}}(0)\prod_+ \sigma^{\mathrm{z}}(\mathrm{T})\prod_+\right\rangle
\end{aligned} \tag{B.21}$$

In the third step we have used the fact that $\left[\sigma^{\mathrm{z}}(0)\,,\,\prod_\pm\right] = 0$ to get rid of the term $\prod_+ \sigma^z(0)\prod_- = 0$. From this we see that we may as well project out the odd fermion parity subspace, e.g. $\sigma^{\mathrm{z}}(\mathrm{T}) \to \prod_+ \sigma^{\mathrm{z}}(\mathrm{T})\prod_+$ and not worry about errors involving non-coding subspaces (these errors do not contribute to expectation values). The same sort of argument may be made for any two time correlator of the fermion modes and any encoding subspace. Indeed based on the form of the previous proof to ensure that the

non-coding subspace does not contribute to the expectation values all we need is a coding system such that the logic operators do not take us out of the encoding space (which is always the case). So no further corrections are needed in this case.

Multi-time correlators

In the multi time case in order to only consider terms within the even fermion parity subspace it is necessary to project out the odd fermion parity states explicitly; that is convert $\mathcal{O}_i(\mathrm{T}) \rightarrow \prod_+ \mathcal{O}_i(\mathrm{T}) \prod_+$. There are still many simplifications in the case of three time correlations. In this case similarly to what we did above one can check that it is only necessary to project out once just before the last operator. For example:

$$\begin{aligned} &\langle \sigma^{\mathrm{z}}(0)\, \sigma^{\mathrm{z}}(\tau_1)\, \sigma^{\mathrm{z}}(\tau_2) \rangle \rightarrow \left\langle \sigma^{\mathrm{z}}(0)\, \sigma^{\mathrm{z}}(\tau_1) \prod\nolimits_+ \sigma^{\mathrm{z}}(\tau_2) \right\rangle = \\ &\tfrac{-\mathrm{i}}{2} \langle \gamma_1\gamma_2\gamma_1(\tau_1)\, \gamma_2(\tau_1)\, (1+\gamma_1\gamma_2\gamma_3\gamma_4)\, \gamma_1(\tau_2)\, \gamma_2(\tau_2) \rangle , \end{aligned} \tag{B.22}$$

which we can calculate using the methods derived in this paper.

B.3.2 Cross correlations between Majorana baths

In the bulk of the text we have discussed the case when the different baths surrounding the Majorana fermions are uncorrelated, or equivalently that interactions between modes that couple to different Majorana fermions are negligible. In this section we shall discuss the effects of such interactions, and indeed argue that they may well be neglected in the case of well separated Majorana modes: modes whose separation is much greater then the scattering length in the bath medium.

First we begin by arguing that the initial conditions which we have selected in this paper, of uncorrelated distant baths, are likely to be highly favorable for the coherence of a qubit composed of Majorana fermions. Indeed, focusing on two Majorana modes, we note that the coherence of the qubit may be expressed as $\left\langle \gamma_1\gamma_2\, e^{iH\mathrm{T}}\, \gamma_1\gamma_2\, e^{-iH\mathrm{T}} \right\rangle$. We now consider two Majorana modes each interacting with the same fermionic environment:

in particular we will focus on a shared modes f_ϵ with energy ϵ, coupling to both γ_1 and γ_2 through a Hamiltonian of the form $H = \gamma_1 \sum_\epsilon \left(\Gamma_1^\epsilon f_\epsilon - \Gamma_1^{\epsilon *} f_\epsilon^\dagger\right) + \gamma_2 \sum_\epsilon \left(\Gamma_2^\epsilon f_\epsilon - \Gamma_2^{\epsilon *} f_\epsilon^\dagger\right)$. Here $\Gamma_{1,2}^\epsilon$ are just complex tunneling amplitudes, for simplicity. Taylor expanding the exponentials in the equation above, we obtain non-zero contributions to the coherence (the expectation value given above) that contain cross terms involving both of Γ_1^ϵ and Γ_2^ϵ:

$$\begin{aligned} &-2\langle\gamma_1\gamma_2\rangle \int_0^{\mathrm{T}} dt_1 \int_0^{\mathrm{T}} dt_2 \sum_\epsilon \langle\left[\left(\Gamma_1^\epsilon f_\epsilon(t_1) - \Gamma_1^{\epsilon *} f_\epsilon^\dagger(t_1)\right), \left(\Gamma_2^\epsilon f_\epsilon(t_2) - \Gamma_2^{\epsilon *} f_\epsilon^\dagger(t_2)\right)\right]\rangle \\ &= 2\langle\gamma_1\gamma_2\rangle \int_0^{\mathrm{T}} dt_1 \int_0^{\mathrm{T}} dt_2 \sum_\epsilon \Gamma_1^{\epsilon *}\Gamma_2^\epsilon \left(\langle f_\epsilon(t_2) f_\epsilon^\dagger(t_1)\rangle - \langle f_\epsilon^\dagger(t_1) f_\epsilon(t_2)\rangle\right) + \text{h.c.} \quad \text{(B.23)} \end{aligned}$$

These are the interference terms that do not appear for Majorana fermions interacting with separate baths, but appear due to a common bath. For short times any non-zero terms like those lead to decoherence. Indeed, since it is impossible to have higher then unity coherence, these terms must contribute negatively to the performance of a qubit composed of Majorana fermions.

However we would like to now argue that this effect can easily be avoided in realistic experimental situations by simply keeping the Majorana fermions far apart. First note that individual f modes that are localized cannot have large tunneling overlaps with two distant Majoranas, so $\Gamma_1\Gamma_2^* \cong 0$. Therefore only extended modes can contribute to the interference terms. Now, each such mode contains a normalization factor proportional to inverse square root of volume, so individually they contribute zero in the thermodynamic limit. As such, in order to get a non-zero value for the term shown in Equation (B.23) we need to integrate over the contributions of all the extended states. To do so first recall Equation (3.5) or Equation (B.26) below which state that $\Gamma_{1,2}^\epsilon \sim \int dr\ u_{1,2}(r) \times v_\epsilon(r)$. Here $u_{1,2}$ is the wavefunction of the Majorana mode while v_ϵ is the wavefunction of the mode f_ϵ. Assuming a pointlike $u_{1,2}$ or dividing the integral into portions of negligible extent we may write that $\Gamma_{1,2}^\epsilon \propto v_\epsilon(r_{1,2})$, where $r_{1,2}$ are the locations of the two Majorana

modes. In this case, we can relate terms entering Equation (B.23) to single-particle Green's functions for the bath electrons:

$$\begin{aligned}
&\sum_{\epsilon} \Gamma_1^{\epsilon *} \Gamma_2^{\epsilon} \, \langle f_\epsilon(t_2) f_\epsilon^\dagger(t_1) \rangle \\
&\propto \sum_{\epsilon} v_\epsilon^* \left(r_1\right) v_\epsilon \left(r_2\right) \, \langle f_\epsilon(t_2) f_\epsilon^\dagger(t_1) \rangle \\
&= G\left(r_1 \, , \, t_1 \, ; \, r_2 \, , \, t_2\right) \, . \qquad \text{(B.24)}
\end{aligned}$$

In a realistic material there are always sources of decorrelation, in particular lattice disorder and phonons. It is not too difficult to show that[97, 99, 98] these sources lead to an exponential decay of $G\left(r_1 \, , \, t_1 \, ; \, r_2 \, , \, t_2\right)$ in space with a characteristic length given by the mean free path of the material. The mean free path is directly related to phonon and impurity scattering strengths[98, 97, 99]. Since this reasoning indicates an exponential suppression of these interference effects with distance, and since it is not possible to use these interference effects to enhance coherence anyway, we have ignored the possibility of the Majorana modes sharing a common bath in the text.

B.3.3 Partial justification of independently fluctuating modes.

In Section 3.6 we presented some results for the coherence of a single Majorana mode in the presence of a fluctuating environment. While we covered both diagonal fluctuations and cross correlations between different modes of our environment, we mostly focused on the case of diagonal fluctuations. Furthermore our results on cross-correlations are technical and in practice difficult to apply. Here we shall present a partial justification indicating that diagonal fluctuations are dominant over cross correlations. Weak correlations do exist so no "theorem" indicating a lack of cross-correlations can be presented. We will however present arguments supporting independent correlations in three key cases: when there is a high degree of symmetry for the problem, when there is "disorder averaging" of the continuum states and tunnel couplings have short correlation length,

or to leading order in perturbation when the fluctuations are weak.

High degree of symmetry

Many Hamiltonians have a high degree of symmetry. For example for a p-wave superconductor with a single vortex supporting a single Majorana mode the vortex core states have rotational symmetry. Most external Hamiltonians causing fluctuations in the vortex core are invariant under this rotational symmetry and as such they may be written in block diagonal form with each block corresponding to a different eigenstate of the rotation operator. As such fluctuations corresponding to different angular momentum eigenstates are decoupled from each other (uncorrelated), justifying this assumption in this case. More generally fermionic modes corresponding to different irreducible representations (diagonal blocks) of some fluctuation Hamiltonian have uncorrelated fluctuations. This in part justifies the assumptions used in Section 3.6.

Short correlation length & disorder averaging

We shall now focus on a particularly simple, but realistic, model of tunnel couplings between the Majorana mode and the regular fermion modes in the superconductor. We shall assume point like tunneling with an effective coupling that may be written as:

$$\begin{aligned} H_{\text{tun}} &= \gamma \sum_i \left\{ c_i \left(\int d^2 r \left\{ \Xi\left(r,\,\tau\right) u_0\left(r\right) u_i\left(r\right) - \Xi^*\left(r,\,\tau\right) v_0\left(r\right) v_i\left(r\right) \right\} \right) \right. \\ &+ \left. c_i^\dagger \left(\int d^2 r \left\{ \Xi\left(r,\,\tau\right) u_0\left(r\right) v_i^*\left(r\right) - \Xi^*\left(r,\,\tau\right) v_0\left(r\right) u_i^*\left(r\right) \right\} \right) \right\}. \end{aligned} \tag{B.25}$$

Here $u_i\left(r\right)$ and $v_i\left(r\right)$ are the creation and annihilation components of the modes c_i while $u_0\left(r\right)$ and $v_0\left(r\right)$ are the creation and annihilation components of the Majorana mode and Ξ is a tunneling amplitude. For a similar coupling form see e.g. Equations (B.45), & (3.5). From this we see that within our model the coupling functions in

Equation (2.1) is given by:

$$\Gamma_i(\tau) = \int d^2r \left\{ \Xi(r,\tau)\, u_0(r)\, u_i(r) - \Xi^*(r,\tau)\, v_0(r)\, v_i(r) \right\}. \tag{B.26}$$

The correlation function is given by $\langle \Gamma_i^*(\tau_1)\, \Gamma_j(\tau_2) \rangle =:$

$$\begin{aligned}
&= -\int d^2r_1 \int d^2r_2 \left\langle \Xi(r_1,\tau_1)\, \Xi^*(r_2,\tau_2)\, u_0(r_1)\, v_0(r_2)\, u_i(r_1)\, u_j^*(r_2) + \right. \\
&\qquad \left. + \Xi(r_1,\tau_1)\, \Xi^*(r_2,\tau_2)\, u_0(r_1)\, v_0(r_2)\, v_i(r_1)\, v_j^*(r_2) \right\rangle \\
&\cong -\int d^2r \left\{ F(\tau_1,\tau_2) \left\langle |u_0(r)|^2\, u_i(r)\, u_j^*(r) \right\rangle + F^*(\tau_1,\tau_2) \left\langle |u_0(r)|^2\, v_i(r)\, v_j^*(r) \right\rangle \right\} \\
&\cong -\int d^2r \left\{ F(\tau_1,\tau_2) \left\langle |u_0(r)|^2\, \mathcal{U}_i(r)\, \delta_{ij} \right\rangle + F^*(\tau_1,\tau_2) \left\langle |u_0(r)|^2\, \mathcal{V}_i(r)\, \delta_{ij} \right\rangle \right\}
\end{aligned} \tag{B.27}$$

Here we able to simplify our expressions by assuming that $\langle \Xi(\vec{r}_1,\tau_1)\, \Xi^*(\vec{r}_2,\tau_2) \rangle \cong F(\tau_1,\tau_2)\, \delta(\vec{r}_1 - \vec{r}_2)$ for some $F(\tau_1,\tau_2)$ and that $\langle \Xi(\vec{r}_1,\tau_1)\, \Xi^*(\vec{r}_2,\tau_2) \rangle \cong 0$. We have also performed a disorder average over the bath states $u_i(r)\, u_j(r) \sim \delta_{ij}$. This averaging works well for continuum states.

Weak fluctuations

In many situations there are many fermionic modes responsible for the decoherence of the Majorana mode and the coupling to any one mode is quite weak. In this case even if the fluctuations between the different fermion modes are strongly cross correlated the diagonal correlations dominate decoherence. Indeed, to show this we first recall the formula for the coherence of a Majorana correlator given in Section 3.6.1: $\langle \gamma(0)\, \gamma(\mathrm{T}) \rangle = \det{}^{-1}(\mathbb{I} + 2\boldsymbol{\sigma}(\mathrm{T}))$. We now simplify this formula. First, letting the eigenvalues of $\boldsymbol{\sigma}$ be $\{\lambda_i\}$, we obtain that:

$$\begin{aligned}
\langle \gamma(0)\, \gamma(\mathrm{T}) \rangle &= \prod_i \frac{1}{1+2\lambda_i} \\
&\cong \exp\left(-2 \sum \lambda_i \right) = \exp\left(-2\mathrm{Tr}(\boldsymbol{\sigma}) \right)
\end{aligned} \tag{B.28}$$

In the second step we have assumed that many eigenvalues contribute to the product so we can exponentiate. From this we see explicitly that in many cases with weak fluctuations only diagonal terms of the matrix σ matter. These are one particle terms $\boldsymbol{\sigma_{ii}}(\mathrm{T}) \equiv 2\int_0^{\mathrm{T}} d\tau_1 \int_0^{\mathrm{T}} d\tau_2 \; e^{-i\epsilon_i\tau_1} G_i(\tau_1,\tau_2)\, e^{+i\epsilon_i\tau_2}$ and as such are much easier to handle.

B.3.4 Proofs and clarifications of Equations. (B.11), (B.17), & (3.68)

Equation (B.11).

Here we wish to prove Equation (B.11) for arbitrary (not necessarily Hermitian) matrices. As a first step we wish to prove an analogous expression for real Gaussian integrals. More precisely we wish to show that for an arbitrary possibly complex $n \times n$ matrix M and an integral over $\mathbb{R}^n$ we may write that:

$$\int dx_1 ... dx_n \exp\left(-\frac{1}{2}\vec{x}^T M \vec{x}\right) = \frac{(2\pi)^{n/2}}{\left(\det\left(\frac{M+M^T}{2}\right)\right)^{1/2}} \tag{B.29}$$

To prove this we first note that $\sum_{i,j} x_i M_{ij} x_j = \frac{1}{2}\sum x_i \left(M_{ij} + M_{ji}\right) x_j$. As such we may safely transform $M \to \frac{1}{2}\left(M + M^T\right)$. Next we may use Takagi's decomposition for symmetric matrices [122] to write that $\frac{1}{2}\left(M + M^T\right) = UDU^T$. Where U is a unitary matrix and D is a diagonal one. From this we see that

$$\int dx_1 ... dx_n \exp\left(-\frac{1}{2}\vec{x}^T M \vec{x}\right) = \frac{(2\pi)^{n/2}}{\left(\det\left(D\right)\right)^{1/2} \det\left(U\right)} = \frac{(2\pi)^{n/2}}{\left(\det\left(\frac{1}{2}\left(M + M^T\right)\right)\right)^{1/2}} \tag{B.30}$$

The extra factor of $\det(U)$ comes from the Jacobian of the change of variables. To proceed to the complex case we begin by writing $\vec{z} = \vec{x} + i\vec{y}$, $\vec{z}^* = \vec{x} - i\vec{y}$. Then we may write that:

$$\vec{z}^\dagger G^{-1} \vec{z} = \begin{pmatrix} \vec{x}^T & \vec{y}^T \end{pmatrix} \begin{pmatrix} G^{-1} & iG^{-1} \\ -iG^{-1} & G^{-1} \end{pmatrix} \begin{pmatrix} \vec{x} \\ \vec{y} \end{pmatrix} \tag{B.31}$$

As such we may write that:

$$\begin{aligned}
&\int\int dz_1..dz_n dz_1^*..dz_n^* \exp\left(-\tfrac{1}{2}\vec{z}^\dagger G^{-1}\vec{z}\right) \\
&= \int\int dx_1..dx_n dy_1..dy_n \exp\left(-\tfrac{1}{2}\begin{pmatrix} \vec{x}^T & \vec{y}^T \end{pmatrix}\begin{pmatrix} G^{-1} & iG^{-1} \\ -iG^{-1} & G^{-1} \end{pmatrix}\begin{pmatrix} \vec{x} \\ \vec{y} \end{pmatrix}\right) \\
&= (2\pi)^n \left(\det\left[\tfrac{1}{2}\left(\begin{pmatrix} G^{-1} & iG^{-1} \\ -iG^{-1} & G^{-1} \end{pmatrix} + \begin{pmatrix} G^{-1} & iG^{-1} \\ -iG^{-1} & G^{-1} \end{pmatrix}^T\right)\right]\right)^{-\frac{1}{2}}
\end{aligned} \tag{B.32}$$

Next we note that:

$$\begin{aligned}
&\tfrac{1}{2}\begin{pmatrix} G^{-1}+G^{-1T} & i\left(G^{-1}-G^{-1T}\right) \\ -i\left(G^{-1}-G^{-1T}\right) & G^{-1}+G^{-1T} \end{pmatrix} = \\
&= \begin{pmatrix} 1 & i \\ 0 & 1 \end{pmatrix}\begin{pmatrix} G^{-1} & 0 \\ \frac{-i}{2}\left(G^{-1}-G^{-1T}\right) & G^{-1T} \end{pmatrix}\begin{pmatrix} 1 & -i \\ 0 & 1 \end{pmatrix}
\end{aligned} \tag{B.33}$$

Since

$$\begin{aligned}
&\det\begin{pmatrix} 1 & -i \\ 0 & 1 \end{pmatrix} = \det\begin{pmatrix} 1 & i \\ 0 & 1 \end{pmatrix} = 1, \\
&\det\begin{pmatrix} G^{-1} & 0 \\ \frac{-i}{2}\left(G^{-1}-G^{-1T}\right) & G^{-1T} \end{pmatrix} = \det\left(G^{-1}\right)\det\left(G^{-1T}\right)
\end{aligned} \tag{B.34}$$

We get that

$$\begin{aligned}
&\int\int dz_1...dz_n dz_1^*...dz_n^* \exp\left(-\tfrac{1}{2}\vec{z}^\dagger G^{-1}\vec{z}\right) = \\
&= (2\pi)^n \left(\det\left(G^{-1}\right)\det\left(G^{-1T}\right)\right)^{-1/2} = (2\pi)^n \det\left(G\right)
\end{aligned} \tag{B.35}$$

This reproduces Equation (B.11).

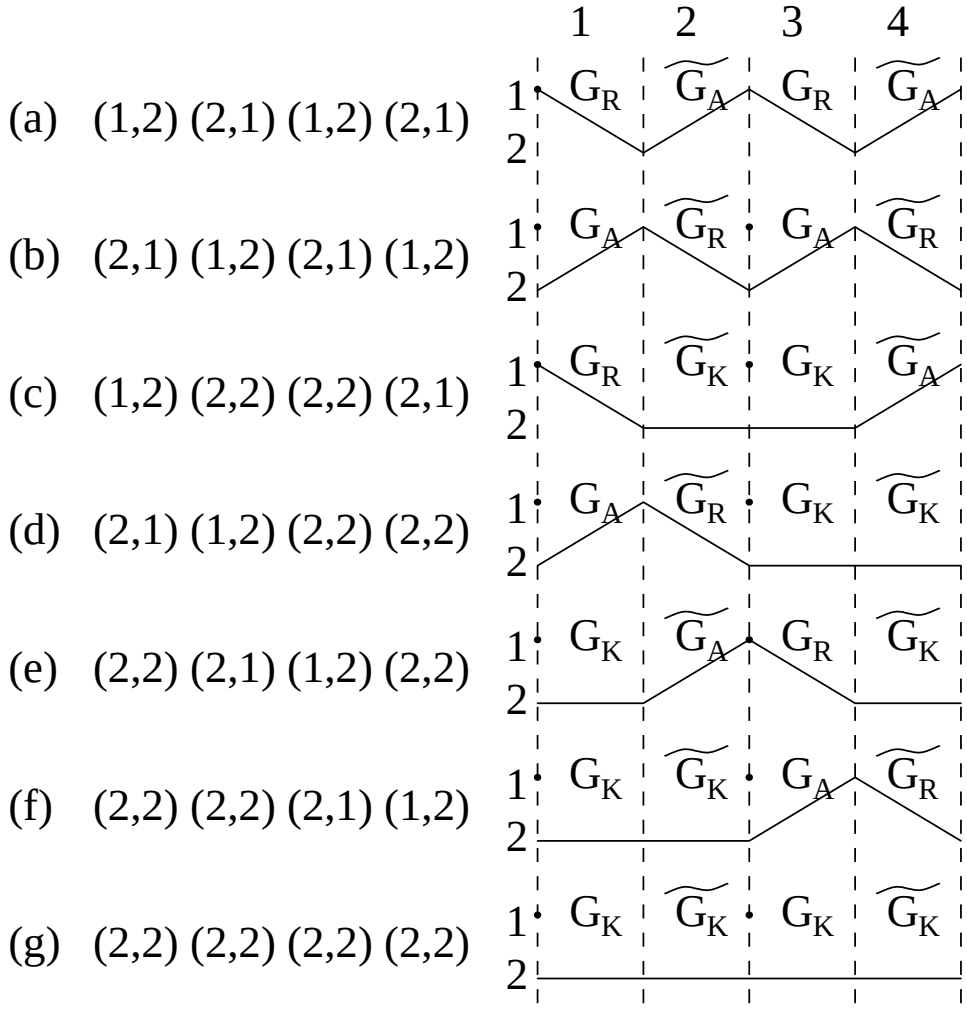

Figure B.1: Leading Order Greens Functions.

In this figure we consider the second order term in Equation (B.17) above. We picture the seven terms contributing to $\mathrm{Tr}\left\{\left(\begin{pmatrix} 0 & G_i^R \\ G_i^A & G_i^K \end{pmatrix}\begin{pmatrix} 0 & \widetilde{G_i^R} \\ \widetilde{G_i^A} & \widetilde{G_i^K} \end{pmatrix}\right)^2\right\}$ with lines connecting indices in the Keldysh matrix, e.g. (1, 2) stands for $G^{(1,2)} = G^R$. Each entry corresponds to a Green's function. The biggest term contains four Keldysh Green's functions (pictured last (g)). The six subleading terms are also shown.

Equation (B.17)

Here we would like to further simplify the sums in Equations (B.17) and (B.14) as well as obtain more accurate estimates. We begin with Equation (B.17) above. By considering the form of the indices in the trace we see that we may represent any term in the expansion for $\mathrm{Tr}\left\{\left(\begin{pmatrix} 0 & G_i^R \\ G_i^A & G_i^K \end{pmatrix}\begin{pmatrix} 0 & \widetilde{G_i^R} \\ \widetilde{G_i^A} & \widetilde{G_i^K} \end{pmatrix}\right)^n\right\}$ as a set of broken lines with periodic boundary conditions with each line representing an appropriate Green's function (see Figure (B.1)). In the quasi classical limit the biggest contribution comes from the term $Tr\left\{\left(G_i^K\widetilde{G_i^K}\right)^n\right\} \simeq \mathrm{T}^n\left(G_i^K\left(\epsilon_i - i\kappa_i\right)\right)^n$. The last equality may be obtained by noting that the various terms in Equation (B.17) factorize. By noting that most of Equation (B.17) factorizes we may compute the subleading term including combinatorial factors in the semiclassical expansion, it is $\frac{n}{4}\mathrm{T}^n\left(\widehat{G_i^K}\left(\epsilon - i\kappa_i\right)\right)^{n-1}\left(\widehat{G_i^R}\left(\epsilon - i\kappa_i\right) + \widehat{G_i^A}\left(\epsilon + i\kappa_i\right)\right)$ (for n ≥ 1). This term would correspond to diagrams (c)-(f) in Figure (B.1). As such we obtain that:

$$\begin{aligned}
\langle\gamma\left(0\right)\gamma\left(\mathrm{T}\right)\rangle &\cong \prod_i \exp\left\{\sum_{n=0}^{\infty}\frac{(-2)^n}{n}\mathrm{T}^n\left(\widehat{G_i^K}\left(\epsilon_i - i\kappa_i\right)\right)^n + \right. \\
&+ \left.\sum_{n=1}^{\infty}\frac{(-2)^n}{4}\mathrm{T}^n\left(\widehat{G_i^K}\left(\epsilon_i - i\kappa_i\right)\right)^{n-1}\left(\widehat{G_i^R}\left(\epsilon_i - i\kappa_i\right) + \widehat{G_i^A}\left(\epsilon_i + i\kappa_i\right)\right)\right\} \\
&\cong \prod_i \frac{1}{1 + 2\mathrm{T}\widehat{G_i^K}\left(\epsilon_i - i\kappa_i\right)}\exp\left(-\frac{1}{2}\mathrm{T}\left(\widehat{G_i^R}\left(\epsilon_i - i\kappa_1\right) + \widehat{G_i^A}\left(\epsilon_i + i\kappa_i\right)\right)\right. \\
&\times \left.\frac{1}{1 + 2\mathrm{T}\widehat{G_i^K}\left(\epsilon_i - i\kappa_i\right)}\right) \qquad \text{(B.36)} \\
&\cong \left[\prod_i \exp\left(-2\mathrm{T}\widehat{G_i^K}\left(\epsilon_i - i\kappa_i\right)\right)\right] \\
&\times \left[\prod_i \exp\left(-\frac{\widehat{G_i^R}\left(\epsilon_i - i\kappa_i\right) + \widehat{G_i^A}\left(\epsilon_i + i\kappa_i\right)}{4\widehat{G_i^K}\left(\epsilon_i - i\kappa_i\right)}\right)\right]
\end{aligned}$$

In the final step we have taken the large T limit. As such we recover the semiclassical approximation and the leading order quantum correction.

Equation (3.68)

We would like to derive Equation (3.68). As a first step we will calculate the n-point correlation function for telegraphic noise. We will find that it is short ranged and this will allow us to calculate the distribution of the "displacement" field $Z_i(\mathrm{T})$ (see Equation (3.38)) within the dipole approximation. We will find that the distribution is Gaussian at which point Equation (3.68) will follow. First we motivate the dipole approximation used in Section 3.6.3. To do so we compute the n-point correlation function for tunneling amplitudes acted on by telegraph noise and observe that it is exponentially short ranged. That is we extend Equations (3.65) & (3.66) from the main text by showing that for the i'th mode, $t_1 < t_2 < ... < t_N$, and for N even [124]:

$$\left\langle \prod_{j=1}^{N} \Gamma(t_j) \right\rangle = \Lambda_i^N \exp\left(-\frac{2}{\tau_i} \sum_{j=1}^{N} (t_{2j} - t_{2j-1}) \right). \tag{B.37}$$

To do so we first we recall the result that for telegraph noise the probability of having exactly K flips in some set of interval whose total length in L is given by $\frac{1}{K!}\left(\frac{L}{\tau_i}\right)^K \exp\left(-\frac{L}{\tau_i}\right)$ [125]. Now we know that $\Pi_{i=1}^{N}\Gamma(\tau_i) = \pm\Lambda_i^N$ depending on whether an odd or an even number of the $\Gamma(\tau_i) = -\Lambda$. At this point it is a straightforward combinatorial argument to show that:

$$\{\#\Gamma(\tau_i) = -\Lambda\} = \left\{ \sum_{j=1}^{N} \#\text{ Flips in } [t_{2j-1}, t_{2j}] \right\} \pmod 2 \tag{B.38}$$

Combing these results we get that:

$$\begin{aligned} \left\langle \prod_{j=1}^{N} \Gamma(t_j) \right\rangle &= \sum_{n=0}^{\infty} (-1)^n \frac{1}{n!} \left(\frac{L}{\tau_i}\right)^n \exp\left(-\frac{L}{\tau_i}\right) \\ &= \exp\left(-2\frac{L}{\tau_i}\right) \end{aligned} \tag{B.39}$$

Here $L = \sum_{j=1}^{N} (t_{2j} - t_{2j-1})$. As such we obtain the result in Equation (B.37). Now we wish to calculate $2n$ point function of the displacement field, see Equation (3.38). It

is given by:

$$\begin{aligned}
&\left\langle \left|Z_i\left(\mathrm{T}\right)\right|^{2n}\right\rangle = \\
&2^{2n}\int\mathcal{D}\left\{\Gamma_i\left(\tau_1\right)\right\}P\left\{\Gamma_i\left(\tau\right)\right\}\int_0^T d\tau_1...\int_0^T d\tau_{2n}\prod_i\exp\left(\vartheta_k i\epsilon_i\tau_k\right)\left\langle\prod_k\Gamma\left(\tau_k\right)\right\rangle \\
&=\left(2\Lambda\right)^{2n}\times\lim_{\delta\to0}\sum_{P_{2n}}\left\{\sum_{l=0}^{2n}\times\right. \\
&\times\left\{\left(-1\right)^{2n-l}\exp\left(\sum_{j=1}^{l}\left\{\left(\vartheta_{P_{2n}(j)}i\epsilon_i+\delta\right)+2\left(-1\right)^j\Omega_i\right\}\mathrm{T}\right)\right\}\times \\
&\left.\times\left(\prod_{j=1}^{l}\frac{1}{\sum_{k=j}^{l}\left(\vartheta_{P_{2n}(k)}i\epsilon_i+\delta+2(-1)^k\Omega_i\right)}\right)\times\left(\prod_{j=l+1}^{2n}\frac{1}{\sum_{k=l+1}^{j}\left(\vartheta_{P_{2n}(k)}i\epsilon_i+\delta+2(-1)^k\Omega_i\right)}\right)\right\}
\end{aligned} \tag{B.40}$$

Here $\left\{\Gamma_{\mathrm{i}}\left(\tau\right)\right\}$ refers to the space of all path alternating between $+\Lambda_i$ and $-\Lambda_i$ and $\mathrm{P}\left\{\Gamma_{\mathrm{i}}\left(\tau\right)\right\}$ is the probability of such a path, and we have introduced $\vartheta_k=\begin{cases}1, & k\leq n\\ -1, & k>n\end{cases}$. We will derive the second part of this equation separately below. The limit: $\lim_{\delta\to0}$ comes from the fact that some of the denominators may turn to zero without an extra factor of δ. Also we would like to note that there is a sum over the permutation group acting on $2n$ elements: P_{2n} which is there to count all the possible ordering of the times $\{\tau_1,...\tau_{2n}\}$. Now consider the formula in Equation (B.40) as a function of $\delta\in\mathbb{C}$. It is a meromorphic function, and it is not too hard to see that it has poles of order at most n (this comes directly from the structure of the denominators). On the other hand we know that for δ close to zero the value of $\left\langle\left|Z_i\left(\mathrm{T}\right)\right|^{2n}\right\rangle\leq2^{2n}\Lambda^{2n}\mathrm{T}^{2n}$. This is not obvious from Equation (B.40) but is obvious from the definition of $\left|Z_i\left(\mathrm{T}\right)\right|^{2n}$. As such all the poles in Equation (B.40) have to cancel. Now, schematically a typical term in Equation (B.40) may be written as $\alpha\frac{e^{A\delta\mathrm{T}}}{\delta^n}$ (with $A\in0\cup\mathbb{N}$). As all the poles in δ must cancel we may safely replace $\alpha\frac{e^{A\delta\mathrm{T}}}{\delta^n}\to\alpha\frac{(A\mathrm{T})^n}{n!}$. From this we see that for large T to leading order in T; $\left\langle\left|Z_i\left(\mathrm{T}\right)\right|^{2n}\right\rangle\sim\mathrm{T}^n$. The only terms which contribute to order T^n from Equation (B.40) are those $\sim\frac{1}{\delta^n}$, or ones where $\vartheta_{P_{2n}(2k)}=-\vartheta_{P_{2n}(2k-1)}$ for $k=1,\,2,...n$. From the fact that the correlation function $e^{-2\Omega_i|\tau_1-\tau_2|}$ is short ranged and from the fact that the phase factors in Equation (B.40) have to cancel pairwise we see that it is good enough to evaluate $\left\langle\left|Z_i\left(\mathrm{T}\right)\right|^{2n}\right\rangle$ in the dipole approximation. From this we see that

$\left\langle |Z_i(\mathrm{T})|^{2n} \right\rangle \cong n! \left\langle |Z_i(\mathrm{T})|^2 \right\rangle^n$. These are the moment functions of a complex Gaussian. Repeating the analysis of Section 3.6.1, we get a power law decay (for each mode i) for the coherence of Majorana qubit, and Equation (3.68) follows.

Equation. (B.40): We now wish to derive Equation (B.40). By considering the form of Equation (B.37) and the fact that Equation (B.40) has a sum over all permutations of $2n$ elements we see that its enough to derive that:

$$\begin{aligned}
&\int_0^{\mathrm{T}} d\tau_1 e^{\alpha_1\tau_1} \int_0^{\tau_1} d\tau_2 e^{\alpha_2\tau_2} ... \int_0^{\tau_{K-1}} d\tau_K e^{\alpha_K\tau_K} \\
&= \sum_{l=0}^{K} \left\{ \left\{ (-1)^{K-l} \exp\left(\sum_{j=1}^{l} \alpha_j \mathrm{T} \right) \right\} \times \left(\prod_{j=1}^{l} \frac{1}{\sum_{k=j}^{l} \alpha_k} \right) \times \left(\prod_{j=l+1}^{K} \frac{1}{\sum_{k=l+1}^{j} \alpha_k} \right) \right\}
\end{aligned} \tag{B.41}$$

To make this formula easier to understand we write it out explicitly in the case when $K = 4$.

$$\begin{aligned}
&\int_0^{\mathrm{T}} d\tau_1 e^{\alpha_1\tau_1} \int_0^{\tau_1} d\tau_2 e^{\alpha_2\tau_2} \int_0^{\tau_2} d\tau_3 e^{\alpha_3\tau_3} \int_0^{\tau_3} d\tau_4 e^{\alpha_4\tau_4} \\
&= \frac{1}{\alpha_1(\alpha_1+\alpha_2)(\alpha_1+\alpha_2+\alpha_3)(\alpha_1+\alpha_2+\alpha_3+\alpha_4)} - \frac{e^{\alpha_1\mathrm{T}}}{\alpha_1\alpha_2(\alpha_2+\alpha_3)(\alpha_2+\alpha_3+\alpha_4)} + \frac{e^{(\alpha_1+\alpha_2)\mathrm{T}}}{(\alpha_1+\alpha_2)\alpha_2\alpha_3(\alpha_3+\alpha_4)} \\
&- \frac{e^{(\alpha_1+\alpha_2+\alpha_3)\mathrm{T}}}{(\alpha_1+\alpha_2+\alpha_3)(\alpha_2+\alpha_3)\alpha_3\alpha_4} + \frac{e^{(\alpha_1+\alpha_2+\alpha_3+\alpha_4)\mathrm{T}}}{(\alpha_1+\alpha_2+\alpha_3+\alpha_4)(\alpha_2+\alpha_3+\alpha_4)(\alpha_3+\alpha_4)\alpha_4}
\end{aligned} \tag{B.42}$$

We shall derive Equation (B.41) by induction:

$$\begin{aligned}
\int_0^{\mathrm{T}} d\tau_1 e^{\alpha_1\tau_1} ... \int_0^{\tau_{K-1}} d\tau_K e^{\alpha_K\tau_K} &= \int_0^{\mathrm{T}} d\tau_1 e^{\alpha_1\tau_1} \sum_{l=1}^{K} \Big\{ -1^{K-l} e^{\sum_{j=2}^{l} \alpha_j \tau_1} \times \\
&\times \left(\prod_{j=2}^{l} \frac{1}{\sum_{k=j}^{l} \alpha_k} \right) \left(\prod_{j=l+1}^{K} \frac{1}{\sum_{k=l+1}^{j} \alpha_k} \right) \Big\} \\
&= \sum_{l=1}^{K} \left\{ -1^{K-l} \left(e^{\sum_{j=1}^{l} \alpha_j \mathrm{T}} - 1 \right) \left(\prod_{j=1}^{l} \frac{1}{\sum_{k=j}^{l} \alpha_k} \right) \right. \\
&\times \left. \left(\prod_{j=l+1}^{K} \frac{1}{\sum_{k=l+1}^{j} \alpha_k} \right) \right\}
\end{aligned} \tag{B.43}$$

All that remains now is to show that:

$$-1^K \prod_{i=1}^{K} \frac{1}{\sum_{j=1}^{i} \alpha_j} + \sum_{l=1}^{K} \left(-1^{K-l} \left(\prod_{j=1}^{l} \frac{1}{\sum_{k=j}^{l} \alpha_k} \right) \times \left(\prod_{j=l+1}^{K} \frac{1}{\sum_{k=l+1}^{j} \alpha_k} \right) \right) = 0 \quad \text{(B.44)}$$

To see this equality consider the left hand side of Equation (B.44) as a function of $\alpha_1 \in \mathbb{C}$. This expression is a meromorphic function $\mathbb{C} \to \mathbb{C}$ which goes to zero at infinity. By inspection, as a function of α_1, it has at most simple poles. It is straightforward to compute the residues at any of these poles and see that they are all zero, that is the expression is actually analytic. We can now apply Lioville's theorem [106] to conclude that the function on the left hand side of Equation (B.44) is identically zero.

Summation of Equation (B.7) for quadratic Hamiltonians

We will give an approximate calculation of the sum (B.7) for tunneling into a 2-D superconductor. To consider a simple example we will focus on the case where a p-wave superconductor is in close proximity to a 2-D s-wave superconductor with the chemical potential of the p-wave superconductor set inside the gap of the s-wave superconductor. This is a reasonable simplified model for say the surface sates formed when an STI is placed in proximity to an s-wave superconductor. Furthermore by taking the limit of a zero gap s-wave superconductor or by ignoring coherence factors we may model insulators or metals in contact with p-wave superconductors. We shall assume a constant point tunneling contact so that the relevant tunneling Hamiltonian may be written as:

$$\int d^2 r \mathbb{T} \left(\Psi^{\dagger}_{\mathrm{pw}}(r) \Psi_{\mathrm{sw}\uparrow}(r) + \Psi^{\dagger}_{\mathrm{sw}\uparrow}(r) \Psi_{\mathrm{pw}}(r) \right) \quad \text{(B.45)}$$

This form comes from the fact that for a p-wave superconductor the vortex is in one spin species only, say spin up.

We begin with a review of the relevant wavefunctions for zero modes of a p-wave superconductor. The eigenvalues of our Hamiltonian correspond to solutions of the following

BdG equation:

$$\begin{pmatrix} -\frac{\nabla^2}{2m} - \mu & \frac{1}{2}\left\{\Delta\left(\vec{r}\right), p_x - ip_y\right\} \\ \frac{1}{2}\left\{\Delta^*\left(\vec{r}\right), p_x + ip_y\right\} & \frac{\nabla^2}{2m} + \mu \end{pmatrix} \begin{pmatrix} u \\ v \end{pmatrix} = \epsilon \begin{pmatrix} u \\ v \end{pmatrix} \tag{B.46}$$

Here $\Delta\left(\vec{r}\right) = \exp\left(i\theta\right)\Delta\left(\left|\vec{r}\right|\right)$, with $\Delta\left(\left|\vec{r}\right|\right) = \frac{\left|\vec{r}\right|}{\xi}\Delta_\infty$ for $\left|\vec{r}\right| \leq \xi$ and $\Delta\left(\left|\vec{r}\right|\right) = \Delta_\infty$ for $\left|\vec{r}\right| \geq \xi$ (we have neglected an irrelevant overall phase factor). Here ξ is the penetration depth and Δ_∞ is the magnitude of the order parameter far from the vortex. From previous studies [126, 127], for rotationally symmetric type II superconducting vortices, we know that there is a zero mode for the Hamiltonian given in Equation (B.46). It is given by $\gamma = \int d^2r \left(u_0\left(r\right)\Psi\left(\overrightarrow{r}\right) + v_0(r)\Psi^\dagger\left(r\right)\right)$ with:

$$\begin{pmatrix} u_0\left(r\right) \\ v_0\left(r\right) \end{pmatrix} \cong \frac{N}{\sqrt{2}} J_0\left(k_F r\right)\exp\left(-\chi\left(r\right)\right) \begin{pmatrix} 1+i \\ 1-i \end{pmatrix} \tag{B.47}$$

Here $k_F = \sqrt{2m\mu}$ is the Fermi wavevector, $J_0\left(k_F r\right)$ is the l'th Bessel function and $\chi\left(r\right) = \frac{m}{k_F}\int_0^r \Delta\left(r\right)$. Where $\Delta\left(r\right)$ is the position dependent order parameter. Furthermore a good approximate value for the normalization constant is given by $N \cong 0.06\left(\frac{k_F}{\xi}\right)$ (see [126]).

Next we will recall the form of the wavefunctions for an s-wave superconductor. For s-wave superconductors we may write Bogolubov de Gennes equations in the form:

$$\begin{pmatrix} -\frac{\nabla^2}{2m} - \widetilde{\mu} & \widetilde{\Delta} \\ \widetilde{\Delta}^* & \frac{\nabla^2}{2m} + \widetilde{\mu} \end{pmatrix} \begin{pmatrix} f\left(r\right) \\ g\left(r\right) \end{pmatrix} = E \begin{pmatrix} f\left(r\right) \\ g\left(r\right) \end{pmatrix} \tag{B.48}$$

Here the top component represents creation operators for spin up while the bottom component represents annihilation operators for spin down fermions; $\widetilde{\mu}$ and $\widetilde{\Delta}$ are the chemical potential and the gap of the s-wave superconductor. Furthermore a similar equation may be written with the spins interchanged and $\widetilde{\Delta} \rightarrow -\widetilde{\Delta}$. We will place the

origin of co-ordinates at the center of the vortex in the p-wave superconductor. Solutions for this equation are of the form:

$$\begin{pmatrix} f^{(+,-)}(r) \\ g^{(+,-)}(r) \end{pmatrix} = \frac{1}{\mathcal{C}} \begin{pmatrix} A^{(+,-)} e^{il\theta} J_l(qr) \\ B^{(+,-)} e^{il\theta} J_l(qr) \end{pmatrix} \tag{B.49}$$

Here $\mathcal{C}$ is a size dependent normalization constant with $\frac{1}{\mathcal{C}} \cong \frac{\pi q}{R}$ (where R is the system radius). Eigenenergies and eigenfunctions are now given by:

$$\begin{cases} E^{(+,-)} = \pm\sqrt{\left(\frac{q^2}{2m} - \widetilde{\mu}\right)^2 + \widetilde{\Delta}^2} \\ (A^+,\, B^+) = (\cos(\theta/2)\exp(i\widetilde{\varphi}),\, \sin(\theta/2)) \\ (A^-,\, B^-) = (-\sin(\theta/2)\exp(i\widetilde{\varphi}),\, \cos(\theta/2)) \end{cases} \tag{B.50}$$

Here $\tan(\theta) = \frac{\frac{q^2}{2m} - \widetilde{\mu}}{\widetilde{\Delta}}$, $\frac{\widetilde{\Delta}}{\widetilde{\Delta}^*} = \exp(\mathrm{i}2\widetilde{\varphi})$ and J_l are the l'th Bessel functions. There are completely analogous equations for the opposite spin, with appropriate sign and phase changes. Using Equation (B.26) as well as the symmetry between the upper and lower component of the solution for the zero mode, see Equation (B.47) and various symmetries between the spin species we see that various trig functions (such as the sine, cosine and exponential appearing in the solution of Equation (B.49) above) cancel out. By taking the thermodynamic limit we can convert the sum (B.7) into an integral of the form: $\sum_{i=1}^{N} \frac{|\Gamma_i|^2}{\epsilon_i^2} \cong$

$$\begin{aligned} &8\pi \int_0^\infty dq \left(\frac{1}{\left((\widetilde{\mu}-\mu) + \sqrt{\left(\frac{q^2}{2m} - \widetilde{\mu}\right)^2 + \widetilde{\Delta}^2}\right)^2} + \frac{1}{\left((\widetilde{\mu}-\mu) - \sqrt{\left(\frac{q^2}{2m} - \widetilde{\mu}\right)^2 + \widetilde{\Delta}^2}\right)^2} \right) \times \\ &\times N^2 \left| \mathbb{T} \int_0^\infty dr r u_0(r) J_0(qr) \right|^2 \end{aligned} \tag{B.51}$$

We note that because of rotational invariance only $J_{l=0}$ terms contribute to the sum. Here u_0 is the upper component of the Majorana mode wavefunction (Equation (B.47)).

We wish to evaluate the integral given in Equation (B.51) above. We will begin by evaluating $\int_0^\infty drru_0(r) J_0(qr)$. As a first step we will use the approximate relation that: $u_0(r) \cong N \exp\left(-\frac{\Delta}{k_F\xi} r^2\right) J_0(k_F r)$ (see Equation (B.47) and discussion that immediately follows). Next we write that:

$$\begin{aligned}
\int_0^\infty drru_0(r) J_0(qr) &= \frac{N}{2\pi}\int_{-\infty}^{\infty} dx \int_{-\infty}^{\infty} dy \exp\left(-\frac{\Delta}{k_F\xi} r^2\right) J_0(k_F r) J_0(qr) \\
&= \frac{N}{(2\pi)^3}\int_{-\infty}^{\infty} dx \int_{-\infty}^{\infty} dy \exp\left(-\frac{\Delta}{k_F\xi} r^2\right) \\
&\times \int_0^{2\pi} d\theta_1 e^{-i\overrightarrow{k_F}(\theta_1)\cdot\vec{r}} \int_0^{2\pi} d\theta_2 e^{-i\vec{q}(\theta_2)\cdot\vec{r}} \\
&= \frac{N}{(2\pi)^3}\int_0^{2\pi} d\theta_1 \int_0^{2\pi} d\theta_2 \exp\left(-\frac{k_F\xi}{4\Delta}\left(\overrightarrow{k_F}(\theta_1) + \vec{q}(\theta_2)\right)^2\right) \\
&= \frac{N}{2\pi^2}\int_{-1}^{1} \frac{dx}{\sqrt{1-x^2}} \exp\left(-\frac{k_F\xi}{4\Delta}\left(k_F^2 + q^2 + 2qk_F x\right)\right) \\
&= \frac{N}{2\pi} \times I_0\left(\frac{q\xi}{2\Delta}\right) \exp\left(-\frac{k_F\xi}{4\Delta}\cdot\left(k_F^2 + q^2\right)\right) \\
&\cong \frac{N}{2\pi} \times \sqrt{\frac{\Delta}{\pi q\xi}} \times \exp\left(-\frac{k_F\xi}{4\Delta}(q-k_F)^2\right) \qquad \text{(B.52)}
\end{aligned}$$

Here $\overrightarrow{k_F}(\theta_1)$ is a vector with magnitude k_F and direction θ_1 along the x-axis and similarly for $\vec{q}(\theta_2)$. In the second line we have used a representation of the bessel function: $J_0(qr) = \frac{1}{2\pi}\int_0^{2\pi} d\theta e^{-i\vec{q}(\theta)\cdot\vec{r}}$ and $\vec{r}$ is along the y-axis. Here I_0 is a modified Bessel function of zeroth order and in the last step we have used an asymptotic form of the modified Bessel function $I_0\left(\frac{q\xi}{2\Delta}\right) \cong \sqrt{\frac{\Delta}{\pi q\xi}} \exp\left(-\left(\frac{q\xi}{2\Delta}\right)^2\right)$. This asymptotic form fails near $q = 0$ where it should be replaced by $I_0\left(\frac{q\xi}{2\Delta}\right) \cong 1 + \frac{1}{4}\left(\frac{q\xi}{2\Delta}\right)^2 + ...$ It is straight forward to check that this correction does not effect the final answer see Equation (B.53) below. Indeed because of the exponential decay we may safely approximate:

$$\int_0^\infty drru_0(r) J_0(qr) \cong \begin{cases} \frac{N}{2\pi}\sqrt{\frac{\Delta}{\pi q\xi}} & (q-k_F) \leq \frac{\Delta}{k_F\xi} \\ 0 & (q-k_F) \geq \frac{\Delta}{k_F\xi} \end{cases} \qquad \text{(B.53)}$$

From this we see that the integral given in Equation (B.51) above has effectively a finite range of definition and no singularities. As such it is clearly finite. Very similar arguments may be used to show that the sum (B.7) is bounded for tunneling contact with any gaped material such as an insulator with the chemical potential of the p-wave superconductor lying within the gap. Indeed quite generically for an itinerant system we may write the Hamiltonian as $H = -\frac{\nabla^2}{2\mathrm{m}^*} + ...$ which means that the eigenvectors of H are similar to those of an s-wave superconductor so the integrand in Equation (B.51) above also has exponential decay for large momentum as the solutions of $H|\Psi\rangle = E|\Psi\rangle$ would behave almost like Bessel functions. Because of the gap condition there will be no finite momentum divergences either, leading to a finite integral. This argument may be extended to models with band structure. By "folding out" appropriate bands from the first brillouin we may convert the sum $\sum_\delta \int\int_{BZ} \left(\frac{\Gamma_{k\delta}}{\epsilon_{k\delta}}\right)^2$ (where the integral is over the first Brillouin zone) into an integral over all of k-space $\rightarrow \int\int d^2k \left(\frac{\Gamma_{k\delta}}{\epsilon_{k\delta}}\right)^2$. As any possible divergence would come from high energy bands where the dispersion is essentially quadratic and the wavefunction is essentially of the continuum model, we may reduce the problem to a previously solved case.

Bibliography

[1] A. R. Akhmerov, Phys Rev B 82, 020509 (2010).

[2] W, Neuhauser, M. Hohenstatt, P. E. Toschek and H. Dehmelt, Phys. Rev. A **22**, 1137 (1980).

[3] N. Nagourney, J. Sandberg, and H. Dehmelt, Phys. Rev. Lett. **56**, 2797 (1986).

[4] T. Sauter, W. Neuhauser, R. Blatt and P. E. Toschek, Phys. Rev. Lett. **57**, 1696 (1986)

[5] J. J. Bollinger, J. D. Prestage, W. Itano and D. Wineland, Phys. Rev. Lett. **54**, 1000 (1985).

[6] S. A. Diddams, Th, Udem, J. C. Bergquist, E. A. Curtis, R. E. Drullinger, L. Hollberg, W. M. Itano, W. D. Lee, C. W. Oates, K. R. Vogel, and D. J. Wineland, Science **293**, 825 (2001).

[7] H. S. Margolis, G. P. Barwood, G. Huang, H. A. Klein, S. N. Lea, K. Szymaniec, and P. Gill, Science **306**, 1355 (2004).

[8] Th. Uden, S. A. Diddams, K. R. Vogel, C. W. Oates, E. A. Curtis, W. D. Lee, W. M. Itano, R. E. Drullinger, J. C. Bergquist, and L. Hollberg, Phys. Rev. Lett. **86**, 4996 (2001).

[9] E. Peik, B. Lipphardt, H. Scnatz, T. Schneider, Chr. Tamm and S. G. Karsheiboim, Phys. Rev. Lett. **93**, 170801 (2004).

[10] G. Rempe, R. J. Thompson, H. J. Kimble, and R. Lalezari, Opt. Lett. **17**, 363 (1992).

[11] P. W. H. Pinkse, T. Fischer, P. Maunz, and G. Rempe, Nature **404**, 365 (2000).

[12] C. J. Hood, T. W. Lynn, A. C. Doherty, A. S. Parkins, and H. J. Kimble, Science **287**, 1447 (2000).

[13] J. Ye, D. W. Vernooy, and H. J. Kimble, Phys. Rev. Lett **83**, 4987 (1999).

[14] J. McKeever, J. R. Buck, A. D. Boozer and H. J. Kimble, Phys. Rev. Lett. **93**, 143601 (2004).

[15] P. Maunz, T. Puppe, I. Schuster, N. Syassen, P. W. H. Pinkse, and G. Rempe, Nature **428**, 50 (2004).

[16] G. A. Prinz, Phys. Today **45** (4), 58 (1995).

[17] G. A. Prinz, Science **282**, 1660 (1998).

[18] J. M. Kikkawa, I. P. Smorchkova, N. Samarth and D. D. Awschalom, Science 277, 1284 (1997), J. M. Kikkawa and D. D. Awschalom, Phys. Rev. Lett. **80**, 4313 (1998).

[19] R. Fiederling, M. Keim, G. Reuscher, W. Ossau, G. Schmidt, A. Waag and L. W. Molenkamp, Nature **402**, 787 (1999).

[20] Y. Ohno, D. K. Young, B. Beschoten, F. Matsukura, H. Ohno and D. D. Awschalom, Nature **402**, 790 (1999).

[21] S. Tarucha, D. G. Austing, and T. Honda, Phys. Rev. Lett. **77**, 3613 (1996).

[22] C. Livermore, C. H. Crouch, R. M. Westervelt, K. L. Campman, and A. C. Gossard, Science **274**, 1332 (1996).

[23] T. H. Oosterkamp, S. F. Godijn, M. J. Uilenreef, Y. V. Nazarov, N. C. van der Vaart, and L. P. Kouwenhoven, Phys. Rev. Lett. **80**, 4951 (1998).

[24] Y. Makhlin, G. Schon, and A. Shnirman, Rev. Mod. Phys. **73**, 357 (2001).

[25] I. Chiorescu, Y. Nakamura, C. J. P. M. Harmans, and J. E. Mooij, Science **299**, 1869 (2003).

[26] R. Fazio, G. M. Palma, and J. Siewert, Phys. Rev. Lett. **83**, 5385 (1999).

[27] F. Meier and D. Loss, Phys. Rev. B **71**, 094519 (2005).

[28] D. Jacksch, H. Briegel, J. Cirac, C. Gardnier, and P. Zoller, Phys. Rev. Lett. **82**, 1975 (1999).

[29] G. K. Brennen, C. M. Caves, P. S. Jessen, and I. H. Deutsch, Phys. Rev. Lett. **82**, 1060 (1999).

[30] J. K. Pachos and P. L. Knight, Phys. Rev. Lett. **91**, 107902 (2003).

[31] P. O. Schmidt, T. Rosenband, C. Langer, W. M. Itano, J. C. Bergquist and D. J. Wineland Science **309**, 749 (2005).

[32] J. M. Taylor, P. Cappellaro, L. Childress, L. Jiang, D. Budker, P. R. Hemmer, A. Yacoby, R. Walsworth and M. D. Lukin, Nat. Phys. **4**, 810 (2008).

[33] J. R. Maze, P. L. Stanwix, J. S. Hodges, S. Hong, J. M. Taylor, P. Cappellaro, L. Jiang, M. V. G. Dutt, E. Togan, A. S. Zibrov, A. Yacoby, R. Walsworth and M. D. Lukin, Nature **455**, 644 (2008).

[34] G. Balasubramanian, I. Y. Chan, R. Kolesov, M. Al-Hmoud, J. Tisler, C, Shin, C, Kim, A. Wojcik, P. R. Hemmer, A. Krueger, T. Hanke, A. Leitenstorfer, R. Bratschitsch, F. Jelezko and J. Wrachtrup, Nature **455**, 648 (2008).

[35] W. S. Bakr, A. Peng, M. E. Tai, R. Ma, J. Simon, J. I. Gillen, S. Fölling, L. Pollet and M. Greiner, Science **329**, 547 (2010).

[36] J. Simon, W. S. Bakr, R. Ma, M. E. Tai, P. M. Preiss and M. Greiner, Nature **472**, 307 (2011).

[37] J. L. O'Brien, A. Furusawa and J. Vuckovic, Nature Photon. **3**, 687 (2009).

[38] M. H. Schleier-Smith, I. D. Laroux and V. Vulatic, Arxiv 0810.2582.

[39] S. L. Braunstein, C. M. Caves and G. J. Milburn, Ann. Phys. (San Diego) **247**, 135 (1996).

[40] P. Shor, Proceedings 35th Annual Symposium on Foundations of Computer Science, (1994).

[41] L. Grover, Phys. Rev. Lett. **79**, 325 (1997).

[42] D. P. DiVincenzo, Fortschr. Phys. **48**, 771 (2000).

[43] D. J. Wineland, J. J. Bollinger, W. M. Itano and D. J. Heinzen, Phys. Rev. A. **50**, 67 (1994).

[44] B. Yurke, S. L. McCall, and J. R. Klauder, Phys. Rev. A. **33**, 4033 (1986).

[45] For completeness we would like to note that $1-cos\,(\varphi) \geqq 0$ so every spin contributes positively.

[46] U. Haeberlen, *High Resolution NMR in Solids Selective Averaging* (Academic Press Inc., 1976).

[47] P. Neumann, N. Mizuochi, F. Rempp, P. Hemmer, H. Watanabe, S. Yamasaki, V. Jacques, T. Gaebel, F. Jelezko and J. Wrachtrup, Science **320**, 1326 (2008).

[48] S. M. Roy and S. L. Braunstein, Phys. Rev. Lett. **100**, 220501 (2008).

[49] We would like to note that the method presented in Chapter 2 scales favorably with Polarization (P) of the dark spins. For the method proposed here sensitivity scales $\backsim (P \cdot N)^{-1}$. For other methods say preparing a GHZ state out of N dark spins sensitivity scales $\backsim \left(P^N \cdot N\right)^{-1}$ while for spin squeezing methods for large N the sensitivity is limited by $\frac{1-P^2}{\sqrt{N}}$.

[50] J. J . Bollinger, Wayne M. Itano, and D. J. Wineland, Phys. Rev. A **54**, R4649 (1996).

[51] R. J. Epstein, F. M. Mendoza, Y. K. Kato and D. D. Awschalom, Nat. Phys. **1**, 94 (2005).

[52] M. V. G. Dutt, L. Childress, L. Jiang, E. Togan, J. Maze, F. Jelezko, A. S. Zibrov, P. R. Hemmer and M. D. Lukin, Science **316**, 1312 (2007).

[53] R. Hanson, F. M. Mendoza, R. J. Epstein, and D. D. Awschalom, Phys. Rev. Lett. **97**, 087601 (2006).

[54] T. Gaebel, M. Domhan, I. Popa, C. Wittmann, P. Neumann, F. Jelezko, J. R. Rabeau, N. Stavrias, A. D. Greentree, S. Prawer, J. Meijer, J. Twamley, P. R. Hemmer and J Wrachtrup, Nat. Phys. **2**, 408 (2006).

[55] D. Leibfried, M. D. Barrett, T. Schaetz, J. Britton, J. Chiaverini, W. M. Itano, J. D. Jost, C. Langer and D. J. Wineland, Science **304**, 1476 (2004)

[56] W. M. Witzel and S. D. Sarma, Phys. Rev. B **74**, 035322 (2006).

[57] M. Kitagawa and M. Ueda, Phys Rev A **47**, 5138 (1993).

[58] D. Leibfried, E. Knill, S. Seidelin, J. Britton, R. B. Blakestad, J. Chiaverini, D. B. Hume, W. M. Itano, J. D. Jost, C. Langer, R. Ozeri, R. Reichle and D. J. Wineland, Nature **438**, 638 (2005).

[59] D. Liebfried, B. DeMarco, V. Meyer, D. Lucas, M. Barrett, J. Britton, W. M. Itano, B. Jelenkovic, C. Langer, T. Rosenband, and D. J. Woneland, Nature **422**, 412 (2003).

[60] T. Rosenband, P. O. Schmidt, D. B. Hume, W. M. Itano, T. M. Fortier, J. E. Stalnaker, K. Kim, S. A. Diddams, J. C. J. Koelemeij, J. C. Bergquist, and D. J. Wineland, Phys. Rev. Lett. **98**, 220801 (2007).

[61] A. Sorensen, and K. Molmer, Phys. Rev. Lett. **82**, 1971 (1999).

[62] P. Mansfield Journal Physics C **4**, 1444 (1971).

[63] V. Jacques, P. Neumann, J. Beck, M. Markham, D. Twitchen, J. Meijer, F. Kaiser, G. Balasubramanian, F. Jelezko, and J. Wrachtrup, Phys. Rev. Lett. **102**, 0547403 (2009).

[64] I. P. Radu, J. B. Miller, C. M. Marcus, M. A. Kastner, L. N. Pfeiffer, and K. M. West, Science **320**, 899 (2008).

[65] R. L. Willet, L. N. Pfeiffer, and K. M. West, Proceedings of the National Academy of Sciences **106**, 8853 (2009).

[66] W. Bishara, P. Bonderson, C. Nayak, K. Shtengel, and J. K. Slingerland, Phys. Rev. B **80**, 155303 (2009).

[67] N. B. Kopnin and M. M. Saloma, Phys. Rev. B **44**, 9667 (1991).

[68] Y. Tsutsumi, T. Kawakami, T. Mizushima, M. Ichioka, and K. Machida, Phys. Rev. Lett. **97**, 167002 (2006).

[69] A. P. Mackenzie and Y. Maeno, Rev. Mod. Phys. **75**, 657 (2003).

[70] J. Xia, Y. Maeno, P. T. Beyersdorf, M. M. Fejer, and A. Kapitulnik, Phys. Rev. Lett. **97**, 167002 (2006).

[71] R. M. Lutchyn, P. Nagornykh, and V. M. Yakovenko, Phys. Rev. B **77**, 144516 (2008).

[72] R. M. Lutchyn, P. Nagornykh, and V. M. Yakovenko, Phys. Rev. B **80**, 104508 (2009).

[73] C. Kallin and A. J. Berlinsky, Journal of Physics: Condensed Matter **21**, 164210 (2009).

[74] T. M. Rice and M. Sigrist, J. Phys.: Condens. Matter **7**, L643 (1995).

[75] S. Das Sarma, C. Nayak, and S. Tewari, Phys. Rev. B **73**, 220502 (2006).

[76] S. Bravyi, Phys. Rev. A **73**, 042313 (2006).

[77] M. Sato, Y. Takahashi, and S. Fujimoto, Phys. Rev. Lett. **103**, 020401 (2009).

[78] C. Zhang, S. Tewari, R. M. Lutchyn, and S. Das Sarma, Phys. Rev. Lett. **101**, 160401 (2008).

[79] M. Sato and S. Fujimoto, Phys. Rev. B **79**, 094504 (2009).

[80] J. Linder, Y. Tanaka, T. Yokoyama, A. Sudbo, and N. Nagaosa, Phys. Rev. Lett. **104**, 067001 (2010).

[81] J. D. Sau, R. M. Lutchyn, S. Tewari, and S. Das Sarma, Phys. Rev. Lett. **104**, 040502 (2010).

[82] J. Alicea, Phys. Rev. B **81**, 125318 (2010).

[83] R. M. Lutchyn, T. Stanescu, S. Das Sarma, arXiv 1008.0629 (2010).

[84] J. D. Sau, S. Tewari, S. Das Sarma, Phys. Rev. A **82**, 052322 (2010).

[85] J. D. Sau, S. Tewari, R. Lutchyn, T. Stanescu, S. Das Sarma, Phys. Rev. B **82**, 214509 (2010).

[86] R. M. Lutchyn, J. D. Sau, S. Das Sarma, Phys. Rev. Lett. **105**, 077001 (2010).

[87] T. D. Stanescu, J. D. Sau, R. M. Lutchyn, S. Das Sarma, Phys. Rev. B **81**, 241310 (2010).

[88] J. D. Sau, R. M. Lutchyn, S. Tewari, S. Das Sarma, Phys. Rev. B **82**, 094522 (2010).

[89] S. Tewari, J. D. Sau, S. Das Sarma, Annals Phys. **325**, 219-231 (2010).

[90] J. D. Sau, D. J. Clarke, S. Tewari, arXiv 1012.0561 (2010).

[91] D. J Clarke, J. D. Sau, S. Tewari, arXiv 1012.0286 (2010).

[92] Y. Oreg, G. Refael, F. von Oppen, Phys. Rev. Lett. **105**, 177002 (2010).

[93] A. Cook, and M. Franz, arXiv 1105.1787.

[94] More generally we will ignore any spin structure of the Majorana modes from now on. Such a structure merely leads to a various matrix elements between the Majorana mode and surrounding states. These matrix elements may be absorbed into the definition of Γ_i (see Eq. (B.1)).

[95] D. A. Ivanov, Phys. Rev. Lett. **86**, 268 (2001).

[96] L. Fu, and C. L. Kane Phys. Rev. Lett. **100**, 096407 (2008).

[97] E. Akkremans and G. Montambaux, *Mesoscopic Physics of Electrons and Phonons*, Cambridge University Press (2007).

[98] H. Bruss and K. Flensberg, *Many-Body Quantum Theory in Condensed Matter Physics*, Oxford University Press (2004).

[99] M. V. Sadovskii, *Diagrammatics: Lectures on Selected Problems in Condensed Matter Theory*, World Scientific Publishing Co. (2006).

[100] Indeed all possible operators acting on the subspace spanned by the zero modes of the Hamiltonian may be written as sums and products of Majorana modes.

[101] A. M. Zagoskin, *Quantum Theory of Many-Body systems: Techniques and Applications*, Springer-Verlag, New York, 1998.

[102] J. Rammer and H. Smith, Rev. Mod. Phys. **58**, 323-359 (1986).

[103] A. Kamenev and A. Levchenko, Advances in Physics **58**, 197 (2009).

[104] J. W. Negele and H. Orland, *Quantum Many-Particle Physics*, Perseus Books Publishing, (1988).

[105] M. E. Peskin and D. V. Schroeder, *An Introduction to Quantum Field Theory*, Westerview Press, (1995).

[106] W. Rudin, *Real and Complex Analysis*, McGraw-Hill Book Company, (1966).

[107] S. B. Bravii and A. Y. Kitaev, Ann. Phys. **298**, 210 (2002).

[108] R. Jackiw and C. Rebbi, Phys. Rev. D **13**, 3398 (1976).

[109] C.-Y. Hou, C. Chamon, and C. Mudry, Phys. Rev. Lett. **98**, 186809 (2007).

[110] R. Jackiw and P. Rossi, Nucl. Phys. B **190**, 681 (1981).

[111] E. J. Weinberg, Phys. Rev. D **24**, 2669 (1981).

[112] L. Fu and C. L. Kane, *Phys. Rev. Lett.* **100**, 096407 (2008).

[113] G. Goldstein, and C. Chamon, Phys. Rev. B **84**, 205109 (2011).

[114] Spins are included in this formalism as a spin S system corresponds to a $2S+1$ dimensional bosonic subspace.

[115] S. Lang, *Linear Algebra*, Springer Science + Business Media Inc., (1987).

[116] C. Carroli, P. G. de Gennes, and J. Matricon, Phys. Lett. **9**, 307 (1964).

[117] J. E. Avron, R. Seiler and L. G. Yaffe, Commun. Math. Phys. **110**, 33 (1987)

[118] F. Wilczek and A. Zee, Phys. Rev. Lett. **52**, 2111 (1984).

[119] R. R. Aldinger, A. Bohm, M. Loewe, Found. of Phys. Lett. **4**, 219 (1991).

[120] For Bose modes the transformation is even simpler $\mathcal{O}_{1,m,\{\theta_j\}} \rightarrow \mathcal{O}_{2,m,\{\theta_j\}}$, $\mathcal{O}_{2,m,\{\theta_j\}} \rightarrow \mathcal{O}_{1,m,\{\theta_j\}}$.

[121] W. M. Witzel and S. Das Sarma, Phys. Rev. B **77**, 165319 (2008).

[122] R. A. Horn and C. R. Johnson, *Matrix Analysis*, Cambridge University Press, (1985).

[123] Some readout schemes do not make the distinction between states inside and outside the coding space.

[124] Though we do not use this result we note that a symmetry argument shows that $\left\langle \prod_{i=1}^{N} \Gamma\left(\tau_i\right) \right\rangle = 0$ for odd N.

[125] R. Loudon, *The Quantum Theory of Light*, Oxford University Press, (2000).

[126] E. Simanek, J. Low Temperature Physics **100**, 1 (1995).

[127] C. Carroli, P. G. de Gennes, and J. Matricon, Phys. Lett. **9**, 307 (1964).

[128] K. Khodjasteh and D. A. Lidar, Phys. Rev. A **75**, 062310 (2007).

[129] W.A. Coish and D. Loss, Phys. Rev. B **72**, 125337 (2005).

[130] S. Boixo and R. D. Somma, Phys. Rev. A **77**, 052320 (2008).

[131] S. F. Huelga, C. Macchiavello, T. Pellizzari, and A. K. Ekert, Phys. Rev. Lett. **79**, 3865 (1997)